DETERMINING BANANA RIPENESS USING MACHINE LEARNING CLASSIFIERS

BY
HONG CHEN

มหาวิทยาลัยรังสิต Rangsit University

A THESIS SUBMITTED IN PARTIAL FULFILLMENT
OF THE REQUIREMENTS FOR
THE DEGREE OF MASTER OF ENGINEERING
IN ELECTRICAL AND COMPUTER ENGINEERING
COLLEGE OF ENGINEERING

GRADUATE SCHOOL, RANGSIT UNIVERSITY
ACADEMIC YEAR 2024

Thesis enitled

DETERMINING BANANA RIPENESS USING MACHINE LEARNING CLASSIFIERS

by
HONG CHEN

was submitted in partial fulfillment of the requirements
for the degree of Master of Engineering in Electrical and Computer Engineering

Rangsit University
Academic Year 2024

Assoc.Prof. Opas Chutatape, Ph.D.
Examination Committee Chairperson

Asst.Prof. Supattana Nirukkanaporn, D.Eng.
Member

Assoc.Prof. Rong Phoophuangpairoj, Ph.D.
Member and Advisor

Approved by Graduate School

(Prof. Suejit Pechprasarn, Ph.D.)
Dean of Graduate School
March 14, 2025

มหาวิทยาลัยรังสิต Rangsit University

Acknowledgements

I would like to express my heartfelt gratitude to my advisor, Assoc. Prof. Rong Phoophuangpairoj, Ph.D., for his exceptional guidance, unwavering support, and invaluable insights throughout my research journey. His expertise and dedication have been pivotal in shaping the direction of my work, particularly in identifying and exploring a research topic that aligns with my academic interests and the broader significance of the field. His mentorship not only enhanced my understanding of complex concepts but also inspired me to approach challenges with curiosity and rigor. I am deeply grateful for his encouragement, constructive feedback, and patience, which have greatly enriched my academic and personal growth during this journey.

Hong Chen
Researcher

มหาวิทยาลัยรังสิต Rangsit University

6509457 : Hong Chen
Thesis Title : Determining Banana Ripeness Using Machine Learning Classifiers
Program : Master of Engineering in Electrical and Computer Engineering
Thesis Advisor : Assoc.Prof. Rong Phoophuangpairoj, Ph.D.

Abstract

This study explored the application of machine learning models for classifying banana ripeness and predicting internal fruit qualities such as Brix (sweetness) and pH. Recognizing the inefficiency and subjectivity of traditional fruit quality assessment methods, the research aimed to develop accurate, scalable systems using advanced classification and prediction techniques. The study comprised two main parts. In the first part, four classifiers—MobileNet, ResNet50, a simple CNN, and VGG16—were evaluated for banana ripeness classification. MobileNet achieved the highest accuracy (98.45%), surpassing VGG16 (96.82%), CNN (95.79%), and ResNet50 (92.43%), demonstrating its superior performance in ripeness classification tasks. The second part investigated various prediction models for Brix and pH values, including linear regression, support vector regression (SVR), and k-nearest neighbors (KNN). Softmax features extracted via MobileNet were utilized for predictions. KNN demonstrated superior performance, attaining R^2 values of 0.984 for Brix and 0.972 for pH, surpassing linear regression and SVR, which yielded R^2 values between 0.925 and 0.958. Additional experiments using RGB, L*a*b*, and combined RGB and L*a*b* color values showed KNN's superiority, with R^2 values of 0.947 for Brix and 0.896 for pH using RGB and L*a*b* color values.

(Total 95 pages)

Keywords: Machine Learning, Banana Ripeness Classification, Brix Prediction, pH prediction, RGB and L*a*b* colors

Student's Signature..Thesis Advisor's Signature..

มหาวิทยาลัยรังสิต Rangsit University

Table of Contents

Page

Acknowledgements **i**

Abstracts **ii**

Table of Contents **iii**

List of Tables **vii**

List of Figures **x**

Chapter 1 **Introduction** **1**

1.1 Background and Significance of the Problem 1

1.2 Research Objective 3

  1.2.1 Construct Machine Learning Models that Categorize Banana Ripeness Based on Images 3

  1.2.2 Finding the Relationship Between pH and Brix and the Ripening Properties of Bananas 3

  1.2.3 Create a Brix, pH, and Ripeness Prediction Model 3

1.3 Scope of the Study 3

1.4 Research Framework 4

Chapter 2 **Literature Review** **5**

2.1 Banana Ripeness 5

  2.1.1 Banana Ripeness Physiological and Biochemical Changes 6

2.2 Method for Detecting Banana Ripeness 7

  2.2.1 Traditional Methods 7

  2.2.2 Machine Learning for Detecting Banana Ripeness 7

2.3 CNN Architecture 8

2.4 MobileNet Architecture 9

2.5 ResNet50 Architecture 10

2.6 VGG16 Architecture 12

มหาวิทยาลัยรังสิต Rangsit University

Table of Contents (continued)

Page

2.7 Feature Extraction 13
    2.7.1 Feature Extraction in Image Processing 14
    2.7.2 RGB Features 14
2.8 Softmax Function 15
2.9 KNN, Support Vector Regression (SVR), and Linear Regression for Prediction **16**

Chapter 3 **Research Methodology** **18**
3.1 Research Materials 18
    3.1.1 Data for Creating Image Classification 18
    3.1.2 Data Used for Brix and pH Prediction 18
3.2 Research Instruments and Software 19
    3.2.1 Instruments Used in Data Collection 19
    3.2.2 Research Software and Algorithms 20
3.3 Data Collection 21
    3.3.1 Purchase Bananas 22
    3.3.2 Collect Banana Images 23
    3.3.3 RGB and L*a*b* Color Data Collection 24
    3.3.4 Collect Banana Juice 25
    3.3.5 Measure Brix Values 26
    3.3.6 pH Measurement 26
    3.3.7 Dataset 27
3.4 Data Analysis 27
    3.4.1 Using MobileNet, ResNet50, CNN Classifiers for Banana Image Classification 27
    3.4.2 Using Different Predictors to Predict Brix and pH Values Based on MobileNet Softmax 28

มหาวิทยาลัยรังสิต Rangsit University

Table of Contents (continued)

Page

3.4.3 Using Different Predictors to Predict Brix and pH Values Based on RGB and L*a*b* Values 29

3.4.4 Result Analysis Methodology 29

Chapter 4 Research Results 32

4.1 Image Classification Results 32

4.1.1 80% Images for Training and 20% Images for Testing 32

4.2 Predicting the Internal Properties of Bananas using Softmax Values 39

4.2.1 Use Linear Regression to Predict the Brix Values 39

4.2.2 Use Linear Regression to Predict pH 41

4.2.3 Use SVR to Predict Brix and pH Values 43

4.2.4 Use KNN to Predict Brix and pH values 50

4.2.5 Summarize the R^2 Results of Brix Values using Different Methods when using Softmax Values 53

4.3 Predicting the Internal Properties of Bananas Using RGB and L*a*b* Color Values Measured from One Point 54

4.3.1 Comparison of Different Methods for Predicting Brix Values Using RGB Color Features 54

4.3.2 Comparison of Different Methods for Predicting pH Values Using RGB Color Values Measured from One Point 59

4.3.3 Comparison of Different Methods for Predicting Brix Values Using L*a*b* Color Values Measured from One Point 65

4.3.4 Comparison of Different Methods for Predicting pH Values Using L*a*b* Color Values 70

มหาวิทยาลัยรังสิต Rangsit University

Table of Contents (continued)

Page

4.4 Predicting the Internal Properties of Bananas Using RGB and L*a*b* Color Values Measured from One Points 75
  4.4.1 Comparison of Different Methods for Predicting Brix Values Using RGB and L*a*b* Color Features 75
  4.4.2 Comparison of Different Methods for Predicting pH Values Using RGB and L*a*b* Color Features 80

Chapter 5 Conclusion and Recommendations 86
5.1 Conclusion 86
5.2 Recommendations 87
  5.2.1 Limitations 87
  5.2.2 Future Outlook 88

References 89

Biography 95

มหาวิทยาลัยรังสิต Rangsit University

List of Tables

Page

Tables

3.1 Instruments 19
3.2 Dataset 27
4.1 Precision, recall, and F1-score using MobileNet with 80% of images for training and 20% for testing. 33
4.2 Precision, recall, and F1-score using ResNet50 with 80% of images for training and 20% for testing. 35
4.3 Precision, recall, and F1-score using CNN with 80% of images for training and 20% for testing. 36
4.4 Precision, recall, and F1-score using VGG16 with 80% of images for training and 20% for testing. 38
4.5 Accuracy when using MobileNet, ResNet50, CNN, and VGG16 to classify banana ripeness 39
4.6 Brix prediction errors when using linear regression 40
4.7 pH prediction errors when using linear regression 42
4.8 Brix prediction errors when using SVR (polynomial kernel) 43
4.9 pH prediction errors when using SVR (polynomial kernel) 44
4.10 Brix prediction errors when using SVR with an RBF kernel 45
4.11 pH prediction errors when using SVR with an RBF kernel 47
4.12 Brix prediction errors when using SVR with a linear kernel 48
4.13 pH prediction errors when using SVR with a linear kernel 49
4.14 Brix values prediction errors when using KNN (k=3) 51
4.15 pH prediction errors when using KNN (k=3) 52
4.16 R^2 results when using different methods to predict Brix values 53
4.17 R^2 results when using different methods to predict pH values 54
4.18 R^2 Values of Different Methods for Predicting Brix Values Using RGB Color Features 55

มหาวิทยาลัยรังสิต Rangsit University

List of Tables (continued)

Page

Tables

4.19 Errors when using linear regression to predict Brix values from RGB color values 56

4.20 Errors when using SVR (linear kernel) to predict Brix values from RGB color values 57

4.21 Errors when using KNN (k=3) to predict Brix values from RGB color values 58

4.22 R^2 values of different methods for predicting pH values using RGB color values from one point 60

4.23 Errors when using linear regression to predict pH values from RGB color values measured from one point 60

4.24 Errors when using SVR (radial basis kernel) to predict pH values from RGB color values 62

4.25 Errors when using KNN (k=3) to predict pH values from RGB color values measured from one point 63

4.26 R^2 values of different methods for predicting brix values using L*a*b* color values measured from one point 65

4.27 Errors when using linear regression to predict Brix values from L*a*b* color values measured from one point 66

4.28 Errors when using SVR (rbf kernel) to predict Brix values from L*a*b* color values measured from one point 67

4.29 Errors when using KNN (k=3) to predict Brix values from L*a*b* color values measured from one point 69

4.30 R^2 values of different methods for predicting pH values using L*a*b* color values measured from one point 70

4.31 Errors when using linear regression to predict pH values from L*a*b* color values measured from one point 71

มหาวิทยาลัยรังสิต Rangsit University

List of Tables (continued)

Page

Tables

4.32 Errors when using SVR (radial basis kernel) to predict pH values from L*a*b* color values measured from one point 72
4.33 Errors when using KNN (k=3) to predict pH values from L*a*b* color values measured from one point 73
4.34 R^2 values of different methods for predicting Brix values using RGB and L*a*b* color features 75
4.35 Errors when using linear regression to predict Brix values from RGB and L*a*b* color values 76
4.36 Brix prediction errors when using SVR (radial basis kernel) 78
4.37 Errors when using KNN (k=3) to predict Brix values from RGB color values 79
4.38 R^2 values of different methods for predicting pH values using RGB and L*a*b* color features 81
4.39 pH prediction errors when using linear regression 82
4.40 pH prediction errors when using SVR (radial basis kernel) 83
4.41 pH prediction errors when using KNN (k=3) 84

มหาวิทยาลัยรังสิต Rangsit University

List of Figures

Page

Figures

1.1 Research Framework 4
2.1 Classification of ripeness stages of bananas 5
2.2 A simplified CNN architecture for dog classification 8
2.3 A residual block in a deep residual network 11
3.1 Instruments: (1) Photo Box, (2) iPhone 14 ProMax camera, (3) Centrifuge, (4) Colorimeter, (5) pH tester, (6) Brix refractometer 20
3.2 Data collection flow 22
3.3 Simummuang market selling bananas 23
3.4 Collecting banana image 23
3.5 Banana color measurement position 24
3.6 Using a colorimeter to measure RGB and L*a*b* color values 24
3.7 RGB and L*a*b* color data from 5 banana 25
3.8 Extracted banana juice 25
3.9 Brix measurement 26
3.10 pH measurement 27
3.11 Banana ripeness classification flow 28
3.12 Using different predictors to predict Brix and pH values 28
3.13 Using different predictors to predict Brix and pH values based on RGB and L*a*b* 29
4.1 Percentage of accurate and inaccurate banana image classification using MobileNet (80% of images used for training, 20% for testing) 33
4.2 Percentage of correct and incorrect banana image classification using ResNet50 (80% of images used for training, 20% for testing) 34
4.3 Percentage of correct and incorrect banana image classification using CNN (80% of images used for training, 20% for testing) 36

มหาวิทยาลัยรังสิต Rangsit University

List of Figures (continued)

Page

Figures

4.4 Percentage of correct and incorrect banana image classification using VGG16 (80% of images used for training, 20% for testing) 37

4.5 Graphs of measured and predicted Brix values when using linear regression 41

4.6 Measured and predicted pH values when using linear regression 42

4.7 Graphs measured and predicted Brix values when using SVR with a polynomial kernel 44

4.8 Graphs of measured and predicted pH values when using SVR with a polynomial kernel 45

4.9 Graphs of measured and predicted Brix values when using SVR with an RBF kernel 46

4.10 Graphs of measured and predicted pH values when using SVR with a radial kernel 47

4.11 Graphs of measured and predicted Brix values when using SVR with a linear kernel 49

4.12 Graphs of measured and predicted pH values when using SVR with a linear kernel 50

4.13 Graphs of measured and predicted Brix values when using KNN (k=3) 51

4.14 Graphs of measured and predicted pH values when using KNN (k=3) 53

4.15 Graphs of measured and predicted Brix values when using linear regression 56

4.16 Graphs of measured and predicted Brix values when using SVR (linear kernel) 58

4.17 Graphs of measured and predicted Brix values when using KNN (k=3) 59

มหาวิทยาลัยรังสิต Rangsit University

List of Figures (continued)

Page

Figures

4.18 Graphs of measured and predicted pH values from RGB color values when using linear regression 61

4.19 Graphs of measured and predicted pH values when using SVR (radial basis kernel) 63

4.20 Graphs of measured and predicted pH values when using KNN (k=3) 64

4.21 Graphs of measured and predicted Brix values when using linear regression 67

4.22 Graphs of measured and predicted pH values when using SVR (radial basis kernel) 68

4.23 Graphs of measured and predicted pH values when using KNN (k=3) 69

4.24 Graphs of measured and predicted Brix values from RGB and L*a*b* color values when using linear regression 71

4.25 Graphs of measured and predicted Brix values when using SVR (radial basis kernel) 73

4.26 Graphs of measured and predicted Brix values when using KNN (k=3) 74

4.27 Graphs of measured and predicted pH values from RGB and L*a*b* color values when using linear regression 77

4.28 Graphs of measured and predicted pH values when using SVR (RBF kernel) 79

4.29 Graphs of measured and predicted Brix values when using KNN (k=3) 80

4.30 Graphs of measured and predicted pH values from RGB and L*a*b* color values when using linear regression 82

4.31 Graphs of measured and predicted pH values when using SVR (RBF kernel) 84

4.32 Graphs of measured and predicted Brix values when using KNN (k=3) 85

มหาวิทยาลัยรังสิต Rangsit University

Chapter 1

Introduction

1.1 Background and Significance of the Problem

People have higher expectations for fruit quality as their living levels and quality of life have improved. Foreign trade is also impacted by quality, so it is critical to improve fruit quality testing and grading. Fruit quality plays a critical role in influencing international trade, especially as consumer expectations rise for high-quality, well-graded produce. Emphasis on improving testing and classification standards for fruit quality is becoming increasingly crucial in the agricultural sector (Moreno et al., 2021). One of the most commonly consumed fruits worldwide is the banana. After harvest, there is a respiratory peak of ripening, causing the fruits to become soft or even rot. This means that bananas have a very short shelf life. Customers who buy bananas in the market usually pay attention to the color of the peel first, as the color of bananas usually reflects the ripeness of the bananas (Saputro, Juansyah, & Handayani, 2018). Some people have particular preferences for the ripeness of their bananas. Due to their higher starch content compared to ripe bananas, unripe bananas contain less sugar. Ripe bananas taste better because they are sweeter, but studies of overripe bananas have shown that consumers are less likely to buy them because of their inferior quality, brown spots, and lower hardness (Symmank, Zahn, & Rohm, 2018).

Banana ripeness classification is crucial in agriculture as it determines the quality of bananas. The traditional use of a sensory assessment of fruit ripeness is costly, time-consuming, and skill-dependent. At present, the identification methods for fruit ripeness mainly rely on traditional manual discrimination and physicochemical analysis. The manual grading method wastes a lot of manpower and resources, and because people's senses differ, it can be challenging to test and grade fruits accurately. The subjectivity of grading is relatively strong, and prolonged observation can lead to eye

มหาวิทยาลัยรังสิต Rangsit University

fatigue. In addition to being inefficient, this method cannot guarantee the quality of grading (Sarkar, Das, Prakash, Mishra, & Singh, 2022). Therefore, non-destructive approaches such as image analysis are required for the recognition of various vegetables, fruits, and other agricultural products. Agricultural tasks such as fruit recognition, fruit freshness determination, and fruit defect detection employ computer vision and machine learning (Castro et al., 2019).

The advancement of computer vision and machine learning technology can be used to automatically classify fruit ripeness. Deep learning technology has evolved within machine learning, and one of the deep learning approaches that plays a crucial role is the convolutional neural network (CNN) (Saragih & Emanuel, 2021). CNNs were used to classify the ripeness level of a banana bunch and achieved an accuracy of 91.21% (Phoophuangpairoj, Ngoenrungrueang, & Audomsin, 2023). MobileNet is a variant of the CNN architecture designed to reduce the number of modeled parameters and computational complexity while maintaining good performance. Although MobileNet is lightweight, it can still provide good performance in tasks such as image classification and object detection. This makes it an ideal choice for image processing in environments with limited computing resources. MobileNet reduces the operation of standard convolution used in the standard convolutional neural network to a depth-wise separable convolution, which consists of depth-wise convolution and point-wise convolution (Howard et al., 2017). ResNet50 is a 50-layer convolutional neural organization. The residual network avoids the gradient disappearance and explosion issues that the conventional CNN model had by utilizing the skip connection concept, which adds the original input to the convolutional layer's output (Sharma & Singh, 2021).

The use of image processing technology has achieved high accuracy in the classification and detection of fruits. This study used professional equipment to collect the pH value, sweetness, hardness, and color changes, as well as images of seven stages of bananas. This study aims to find an efficient method for classifying the ripeness of bananas. Researchers looked into how to categorize fruit maturity using machine learning techniques. While the skin of a number of banana varieties can be used to

มหาวิทยาลัยรังสิต Rangsit University

evaluate their maturity, research needs to be done to forecast the characteristics within. This study will use various machine learning models for the classification of banana maturity, prediction of Brix (sweetness), and pH value.

1.2 Research Objectives

1.2.1 Construct Machine Learning Models that Categorize Banana Ripeness Based on Images

Develop an effective machine learning model capable of precisely classifying banana ripeness. This objective necessitates the acquisition of an adequate quantity and variety of banana image datasets, data preprocessing, the selection of suitable machine learning architectures, and the utilization of precision, recall, F1-score, macro average, and weighted average as metrics for assessing the performance of classification models.

1.2.2 Finding the Relationship Between pH and Brix and the Ripening Properties of Bananas

The association between banana qualities and pH, sweetness, and fundamental exterior factors will be investigated through statistical approaches and machine learning.

1.2.3 Create a Brix, pH, and Ripeness Prediction Model

Create predictive models that can determine a banana's pH and sweetness and its maturity based on machine learning approaches.

1.3 Scope of the Study

1.3.1 This study applied various machine learning models to classify banana maturity, and this study focused on the Musa acuminata bananas.

มหาวิทยาลัยรังสิต Rangsit University

1.3.2 This study applied various methods to predict Brix and pH values. The research focused on how to accurately classify the maturity of bananas and predict their Brix and pH levels from banana images and from the RGB and L*a*b* color values measured from a point on a banana.

1.4 Research Framework

This research framework focuses on classifying banana ripeness and predicting internal fruit qualities: Brix (sweetness) and pH values, using machine learning approaches. It consists of three main parts: 1) classifying banana ripeness from images, 2) predicting banana Brix and pH values using softmax features, and 3) predicting banana Brix and pH values using RGB and L*a*b* color values.

Figure 1.1 illustrated that the first part involved the classification of banana ripeness utilizing machine learning classifiers, including MobileNet, ResNet50, CNN, and VGG16. In the second part, the MobileNet is further used to extract features (seven softmax values) from the images, which are then used as inputs for linear regression, SVR, and KNN to predict Brix and pH values. In the third part, RGB and L*a*b* color values were obtained from bananas. Linear regression, SVR, and KNN utilized RGB values, L*a*b* values, and a mix of both to predict Brix and pH values.

มหาวิทยาลัยรังสิต Rangsit University

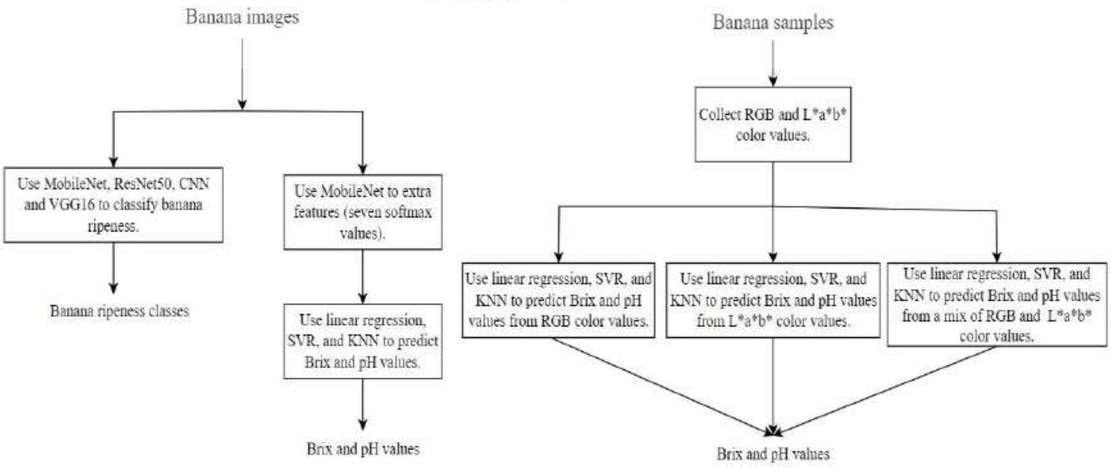
Banana images
Use MobileNet, ResNet50, CNN and VGG16 to classify banana ripeness.
Banana ripeness classes
Use MobileNet to extra features (seven softmax values).
Use linear regression, SVR, and KNN to predict Brix and pH values.
Brix and pH values
Banana samples
Collect RGB and L*a*b* color values.
Use linear regression, SVR, and KNN to predict Brix and pH values from RGB color values.
Use linear regression, SVR, and KNN to predict Brix and pH values from L*a*b* color values.
Use linear regression, SVR, and KNN to predict Brix and pH values from a mix of RGB and L*a*b* color values.
Brix and pH values

Figure 1.1 Research Framework

Chapter 2

Literature Review

2.1 Banana Ripeness

Banana ripeness refers to the physiological and biochemical changes that occur in the fruit during ripening. The ripening stage of bananas is usually classified into seven stages based on the peel color, firmness, and flavor of the fruit (Zhang, Lian, Fan, & Zheng, 2018), as shown in Table 2.1. The first stage of banana ripening is the full green stage; the fruit is not yet ripe. In the second stage, the peel of the banana begins to appear yellow, and the green color is greater than the yellow color, indicating that the fruit is not yet ripe. In the third stage, the fruit starts to mature as the yellow color intensifies and surpasses the green color. In the fourth stage, the peel is predominantly yellow, with some green areas visible at the top and bottom. The fifth stage is almost completely yellow, with fully ripe fruit, a soft texture, and a sweet taste. The sixth stage is the spotted stage, where the peel has brown spots, the fruit is overripe, the texture is softer, and the flavor is stronger. The seventh stage is the appearance of a black color, with a large amount of black, overripe, and pasty texture on the fruit peel (Zhang et al., 2018).

มหาวิทยาลัยรังสิต Rangsit University

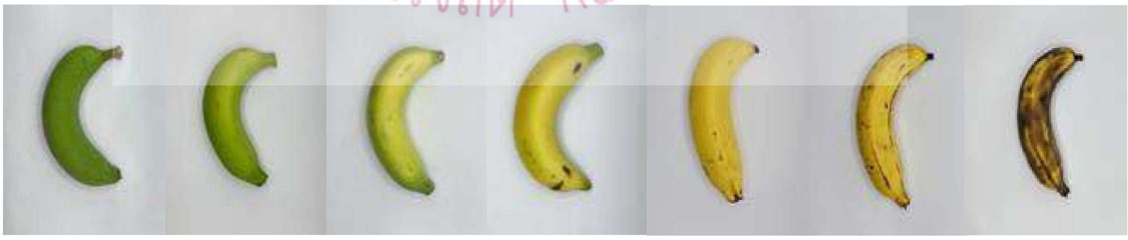

Class 0 Green and hard peels

Class 1 More green than yellow

Class 2 More yellow than green

Class 3 Yellow with green tip

Class 4 Full yellow

Class 5 Yellow with brown spots

Class 6 Overripe

Figure 2.1 Classification of ripeness stages of bananas

Source: Chen & Phoophuangpairoj, 2024

2.1.1 Banana Ripeness Physiological and Biochemical Changes

2.1.1.1 Physiological Changes

During the ripening process of bananas, several physiological changes occur in the fruit. The most significant change is fruit softening, which is due to cell wall degradation and loss of turgor pressure (El-Sharkawy, 2004). This results in a decrease in firmness and an increase in sweetness as the fruit ripens. Due to the breakdown of chlorophyll and the production of carotenoids, the color of the fruit also changes from green to yellow (Moreno et al., 2021).

2.1.1.2 Biochemical Changes

The ripening of bananas is also characterized by several biochemical changes. The most significant change is the production of ethylene gas, a natural plant hormone that regulates the ripening process (El-Sharkawy, 2004). As the fruit ripens, ethylene production increases, leading to the activation of various enzymes that break down complex molecules into simpler molecules, such as starch into sugar (El-Sharkawy, 2004). This leads to an increase in the sweetness and aroma of the fruit. The total soluble solids (TSS) content of the fruit also increases with increasing ripeness, while the titratable acidity (TA) and pH decrease (Moreno et al., 2021). Several studies explored how physiological and biochemical changes during the ripening of bananas affect their fruit quality and shelf life. For example, Jones (2018) and Imsabai, Ketsa, and van Doorn (2006) explored the mechanism of finger shedding during the ripening process of banana fruits, particularly the differences between the "Hom Thong" and "Namwa" varieties. Research has found that the shedding of fruit fingers mainly occurs at the junction of the stem and flesh, but the true delamination area has not been detected. Therefore, the shedding phenomenon is mainly related to the weakening of the fruit peel.

มหาวิทยาลัยรังสิต Rangsit University

2.2 Method for Detecting Banana Ripeness

2.2.1 Traditional Methods

Traditional methods mainly rely on observing the appearance characteristics of bananas, such as color, spots, flesh texture, and fruit shape. The operator visually determines the maturity of bananas and categorizes them into different levels, such as immature, mature, and overripe. These methods are influenced by the subjective judgment and experience of the operator, so there may be inconsistencies. Different people may produce different classification results for the same banana. Traditional methods rely on the experience and training of operators, thus requiring time to develop professional skills. This also limits the application of these methods in large-scale automation environments (Sarkar et al., 2022).

2.2.2 Machine Learning for Detecting Banana Ripeness

Automated fruit ripeness classification is possible with the help of emerging computer vision and machine learning technology. Among the many advancements in machine learning, the CNN stands out as a key component of deep learning (Saragih & Emanuel, 2021). Overall, traditional methods mainly rely on manual observation and subjective judgment, while machine learning methods utilize computer vision technology and data-driven methods to provide objective, automated, and highly accurate banana classification. The data sources include research literature and related academic research in the fields of agriculture and food science. This comparison highlights the potential of machine learning methods in improving classification efficiency and accuracy, especially in large-scale production and supply chain management.

มหาวิทยาลัยรังสิต Rangsit University

2.3 CNN Architecture

CNN, with its numerous variations, is one of the most widely used deep neural network designs. These are typical deep learning models for computer vision because of a number of features, including shift invariance, parameter sharing, and convolutional processes. The possible CNN architecture stacks three types of layers—convolutional, pooling, and fully connected, also known as dense layers—on top of each other (Albawi, Mohammed, & Al-Zawi, 2017). Figure 2.1 depicted the condensed CNN architecture for classifying dogs. Machine learning problems also make use of CNN. Deep learning has made significant progress in picture categorization over the last ten years, particularly in relation to CNN.

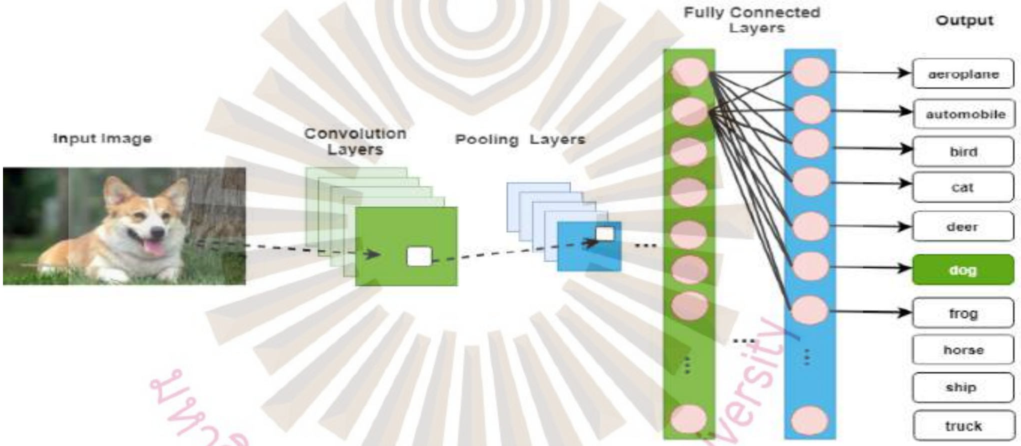

Figure 2.2 A simplified CNN architecture for dog classification
Source: Phiphiphatphaisit & Surinta, 2020

มหาวิทยาลัยรังสิต Rangsit University

Researchers developed a fruit grading control system using convolutional neural networks. They used CNN for tasks involving the detection and identification of fruits through parameter optimization. The test results for 971 images in 30 categories had a classification accuracy of about 94%. This implies that control applications that depend on visual subsystems can utilize the system and approach (Khaing, Naung, & Htut, 2018).

There are various types of Convolutional Neural Network (CNN) architectures in the fields of image classification, segmentation, and object detection. Most architectures primarily focus on accuracy as a key factor in model implementation. However, in practical applications, besides accuracy, other important factors such as memory usage and performance are equally critical. Although each CNN architecture has its own advantages and limitations, research comparing different architectures is not common, especially on how to choose the appropriate architecture based on actual application requirements and hardware capabilities (Darapaneni, Krishnamurthy, & Paduri, 2020).

The implementation of CNNs in automation systems and image classification jobs has received significant attention and validation in recent years. For instance, researchers used deep learning models, such as CNN, to categorize agricultural products. They were successful in obtaining effective distinction of several fruit types by analyzing the form, texture, and color characteristics of the fruits (Rahman et al., 2023). This suggested that the use of CNN models in precision agriculture could potentially improve classification effectiveness.

2.4 MobileNet Architecture

Howard et al. (2017) introduced the depthwise separable convolution-based MobileNet architecture, aiming to build a lightweight deep CNN that reduces computation time and generates excessively tiny models. MobileNet utilizes depthwise separable convolution to minimize computational complexity and parameters in conventional convolution operations. The fundamental concept is to partition the ordinary convolution into two phases: depthwise convolution and pointwise convolution. Deep convolution performs convolution operations on each input channel, while point convolution combines data from multiple channels using 1x1 convolution, which makes computing much simpler. Every layer of the MobileNet architecture incorporates batch normalization and the ReLU activation function, enhancing the network's training performance. MobileNet markedly decreases processing demands and model dimensions, rendering it appropriate for deployment on mobile devices.

มหาวิทยาลัยรังสิต Rangsit University

Phiphiphatphaisit and Surinta (2020) investigated food classification with the MobileNet architecture, which includes batch normalization, dropout layers, rectified linear units, global average pooling layers to mitigate overfitting, and a softmax layer at the last layer. The outcomes of the experiments indicated that the suggested iteration of the MobileNet architecture attains significantly more accuracy compared to the first MobileNet architecture.

Gulzar (2023) developed a fruit recognition system that used the MobileNet architecture as its foundation. They constructed this system to classify fruits. This was accomplished by the use of batch normalization and global average pooling layers. In addition, the generalization capability of the model was further improved by the combination of data augmentation and transfer learning.

The MobileNet model is widely used in computer vision tasks for mobile and embedded devices due to its excellent balance between accuracy and speed. Howard et al. (2017) first proposed MobileNet V1, which significantly reduced the model's parameters and computational complexity by introducing depthwise separable convolutions. It demonstrated high accuracy and significant speed advantages in classification tasks on the ImageNet dataset.

มหาวิทยาลัยรังสิต Rangsit University

2.5 ResNet50 Architecture

ResNet50 is a 50-layer convolutional neural network. This network solves the gradient disappearance and explosion problem with the traditional CNN model by using the skip connection idea to add the original input to the output of the convolutional layer (Sharma & Singh, 2021). Figure 2.2 illustrated the residual network, or ResNet, as its acronym. Deep convolutional neural networks have advanced significantly in the area of image detection and classification throughout time. It became popular to solve more difficult problems and increase the accuracy of categorization or recognition. Over recent years, deep convolutional neural networks have achieved significant advancements in image detection and classification tasks. They have become essential for addressing complex problems and improving accuracy in various domains, such as object recognition and medical image analysis. The training of deeper networks remains challenging due to problems such as vanishing gradients and overfitting, particularly as network depth increases (Burt, Thigpen, Keil, & Principe, 2021). Residual learning frameworks were designed to address these issues by facilitating more efficient training of deeper networks.

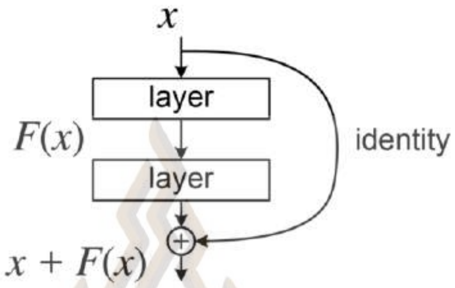

Figure 2.3 A residual block in a deep residual network

Source: Researcher

In terms of network structure improvement, scholars proposed HS ResNet (Hierarchical Split ResNet), which improves the performance of the model by introducing multi-level segmentation and connections in a single residual block. This improved ResNet-50 achieved a Top-1 accuracy of 81.28% on the ImageNet-1k dataset, demonstrating its advantages in image classification tasks (Yuan et al., 2020).

ResNet50 is often used as a backbone network for feature extraction, providing powerful feature representation capabilities for object detection and semantic segmentation tasks. For example, frameworks such as Mask R-CNN used ResNet50 as the infrastructure to achieve high-precision detection and segmentation of targets on the COCO dataset (He, Gkioxari, Dollár, & Girshick, 2017). Cell image classification based on deep learning can prevent erroneous diagnostic decisions. This study mainly investigated the implementation of transfer learning to improve the diagnostic accuracy based on the classification of malaria-infected cells. The total number of infected and uninfected cell images in the dataset was 27,558. 70%, 15%, and 15% were used for training, testing, and validation, respectively. The model's inputs were RGB (red, green, blue) images.

The ResNet50 using pre-trained weights, with the final layer being a fully connected dense layer with sigmoid activation, was applied. The proposed model consists of two layers: a pre-trained ResNet layer and a dense layer. Reddy and Juliet (2019) recommended against freezing some layers, such as batch normalization (BN) layers, due to the difficulty in matching the dataset's average and variance with the pre-trained weights.

2.6 VGG16 Architecture

A deep CNN architecture called VGG16 was proposed by Simonyan and Zisserman (2015) in the ImageNet Large Scale Visual Recognition Challenge (ILSVRC). Its goal was to make image classification tasks more accurate. Simonyan and Zisserman (2015) named the architecture VGG16 due to its 16 trainable layers of weights, which included 13 convolutional layers and 3 fully connected layers. VGG16 reduced the number of parameters while ensuring feature extraction depth by stacking multiple 3x3 convolution kernels instead of larger ones (such as 7x7 or 5x5). This design concept effectively improved the recognition ability of the model while reducing computational complexity. The network structure of VGG16 adopts a fixed max pooling layer, which down samples images after each convolutional layer to gradually reduce the size of the feature map while preserving key information. The last three fully connected layers classify the high-level features extracted by convolution (Simonyan & Zisserman, 2015).

มหาวิทยาลัยรังสิต Rangsit University

VGG16 was widely used in image classification tasks as one of the classic convolutional neural network (CNN) architectures. VGG16's deep structure and small-sized convolution kernels have made it a foundational architecture in image classification applications in recent years. These properties enable VGG16 to capture rich feature information, resulting in high accuracy on huge datasets like ImageNet (Kumar, S. & Kumar, H., 2024). Despite these developments, VGG16 remains a baseline model for comparing newer architectures in tasks like object detection and medical picture categorization. Although the earliest proposed VGG16 was computationally intensive, researchers optimized its performance in various ways to meet the needs of efficient classification. For example, some studies use transfer learning to accelerate the model training process while improving the accuracy of few sample tasks. VGG16 and VGG19 were proposed using CNN architectures for processing medical images to classify brain tumors and pneumonia. Transfer learning strategies and data augmentation techniques reduced overfitting by fine-tuning and freezing models, enhancing classification reliability (Al-Azzwi, 2024). A hybrid pre-trained VGG16 convolutional neural network (CNN) and support vector machine (SVM) classifier model was also proposed. VGG16 was used to extract features from input remote sensing data, while the SVM classifier performed classification output based on the feature map output by CNN (Tun, N. L., Gavrilov, Tun, N. M., Trieu, & Aung, 2021). In addition, VGG16 is integrated into multiple model structures and combined with other networks such as ResNet and Inception to improve classification accuracy. For example, the publicly available chest X-ray image dataset obtained from the Kaggle platform was used for pneumonia recognition, and an improved VGG16 model was employed to improve the classification accuracy of pneumonia X-ray images (Jiang, Liu, Shao, & Huang, 2021). In order to further improve the classification performance of remote sensing images, many researchers have explored hybrid models that combine traditional machine learning methods with deep learning techniques. A pre-trained VGG16 network was combined with a support vector machine (SVM) classifier to form a hybrid classification model. In this type of model, VGG16 was responsible for extracting features from the input remote sensing image, while SVM makes classification decisions based on the feature map output by CNN (Tun et al., 2021).

2.7 Feature Extraction

Feature extraction refers to the process of extracting useful information from raw data. Typically, it simplifies the data's complexity while preserving pertinent information for the task. Many fields, particularly image processing, natural language processing, and biomedical data analysis, have widely applied and developed feature extraction in recent years.

2.7.1 Feature Extraction in Image Processing

Research on low-level feature extraction (such as color, texture, and shape features) in image processing continues to advance, especially in content-based image retrieval (CBIR), where it has found widespread application. These methods could effectively capture the physical features of images, helping the system to better classify and retrieve images. Wang, Han, and Jin (2019) applied sparse representation to extract global and local features, thereby improving retrieval efficiency and accuracy.

2.7.2 RGB Features

The RGB color model is crucial in various fields, especially in digital imaging and computer graphics. It signifies colors as combinations of three fundamental hues: red, green, and blue. Each color channel can take values typically ranging from 0 to 255, enabling the depiction of more than 16 million unique colors. Recent research works have investigated multiple aspects of the RGB color model. A study examined the impact of color space selections on deep learning image colorization, revealing that different color representations can significantly affect model performance in image restoration and classification tasks (Kong, Tian, Duan, & Long, 2021). Another study investigated the reassessment of RGB representation to enhance image restoration models, suggesting that improvements in RGB processing could produce better results in real-world applications. The effectiveness and applicability of the RGB color model in various contexts have prompted ongoing investigation into other color spaces that may offer advantages in specific scenarios, particularly in machine learning and computer vision (Ballester et al., 2022). Each channel's value typically ranges from 0 to 255, indicating the intensity levels of red, green, and blue, respectively (Poynton, 2012). In contrast, the L*a*b* color model is grounded in human visual perception and is composed of three components: L (lightness), a (from green to red), and b (from blue to yellow) (Sharma, 2017).

The L*a*b* color space is a color representation grounded in human visual perception, designed to offer a model that more accurately reflects actual colors. L*a*b* color space is a color representation model based on human visual perception, which has been widely used in image processing and color management fields for its accurate description of colors and uniform color distribution characteristics. This space consists of three components: L represents brightness, a represents the red green axis, and b * represents the yellow blue axis. This structural design enabled it to accurately characterize color changes (Luo, Cui, & Rigg, 2001). Utilizing the L*a*b* color space enabled users to exert more precise control over colors, thereby improving the visual effects of digital photographs (Borenstain, Bar-Haim, Goldshtein, & Cohen-Taguri, 2020).

RGB and L*a*b* color measurements were utilized to classify the ripeness of Banganapalli mangoes during their ripening process. The significance level for RGB and L* a* b* data concerning ripening days was analyzed using ANOVA. During the ripening phase, the L*a*b* values and RGB values were statistically significant ($P < 0.01$). Compared to L*a*b* color measurement, RGB color measurement would be more appropriate because it only requires a straightforward image processing technique and inexpensive equipment. The red ratio (R/B), the green ratio (G/B), and both blue ratios accurately predicted mango ripening (EyNambi, Thangavel, Shahir, & Geetha, 2015).

2.8 Softmax Function

Softmax is a mathematical function used to convert a set of values (such as logits output by a model) into a probability distribution. It is commonly used in the final layer of classification problems, mapping the scores (logits) of each class to values within the [0, 1] interval and ensuring that the sum of probabilities for all classes is 1 (Goodfellow, Bengio, & Courville, 2016). The last layer in the MobileNet architecture is usually a fully connected layer. A softmax function changes the output from this layer to a normalized probability distribution, which ends the classification task. The extraction of softmax values not only yields the model's prediction outcomes but also assesses the model's confidence via these probability values. In image classification tasks, the highest value produced by softmax typically indicates the model's most confident predicted category (Sandler, Howard, Zhu, Zhmoginov, & Chen, 2018).

2.9 KNN, Support Vector Regression (SVR), and Linear Regression for Prediction

In recent years, various fields have widely applied KNN, an instance-based nonparametric algorithm, to prediction tasks. Its simplicity and ease of implementation make it perform well on small datasets (Zhan, Zhang, & Liu, 2021). However, KNN is sensitive to data noise and parameter K values, and researchers have proposed various optimization methods to improve its predictive performance. For example, some studies combined particle swarm optimization (PSO) algorithms to automatically tune K values, thereby reducing prediction errors (Xie et al., 2024). The KNN algorithm is widely used in classification analysis, but it is susceptible to interference from noisy samples, which can affect classification performance and prediction accuracy (Ukey et al., 2023).

SVR is an extension of SVM aimed at solving nonlinear relationships in regression problems. SVR maps data to high-dimensional space through kernel functions, enabling accurate prediction on complex nonlinear datasets. In the past few years, SVR has performed well in multiple fields, especially in meteorology, hydrology, energy load forecasting, and other areas (Zhan et al., 2021). Researchers have come up with better ways to choose kernel functions and optimize parameters, like combining Bayesian optimization or grid search, to make SVR better at making predictions and applying its findings to more situations (Sahoo, Hoi, & Li, 2019). In the fields of energy consumption and environmental pollutant concentration prediction, the combination of SVR with other algorithms, such as genetic algorithms and neural networks, has shown good prediction performance (Li, 2020). SVR performs well in handling time series data with strong nonlinear relationships and has strong application value.

The linear regression model is still widely used in predictive analysis due to its advantages in interpretability and ease of implementation. Demand forecasting, socio-economic analysis, and market trend research commonly employ linear regression. Its modeling simplicity and ease of explanation make it effective on structured datasets (Braun, Altan, & Beck, 2014). Some researchers use linear regression along with multivariate statistical analysis (like factor analysis and principal component analysis) to lessen the effect of multicollinearity on how well predictions work (Hirose, H., Soejima, & Hirose, K., 2012). Recently, researchers have gradually combined linear regression with machine learning methods to enhance the applicability and accuracy of predictions. Linear regression is one of the most interpretable prediction models (Munkhdalai, Munkhdalai, & Ryu, 2022).

มหาวิทยาลัยรังสิต Rangsit University

Chapter 3

Research Methodology

The chapter outlined the materials, methods, and instruments used in the study, detailing the data collection processes for banana image classification, Brix, and pH prediction. It also explains the preparation of banana samples, acquisition of image and color data, and the methodologies for data analysis.

3.1 Research Materials

3.1.1 Data for Creating Image Classification

The experiments used 1307 images of a banana (Musa acuminata). For the training and testing, the images were divided into 80% and 20%. Using 80% of the images for training and 20% of the images for testing, a total of 1047 images of a banana, consisting of 205, 212, 155, 120, 106, 103, and 146 images of class 0, class 1, class 2, class 3, class 4, class 5, and class 6, were used for training. For the test, a total of 260 images of a banana consisting of 51, 53, 39, 30, 26, 25, and 36 images of classes 0 through 6 were classified. The standards used to categorize bananas were clear, allowing even non-experts to classify them reasonably correctly (Chen & Phoophuangpairoj, 2024).

มหาวิทยาลัยรังสิต Rangsit University

3.1.2 Data Used for Brix and pH Prediction

The MobileNet was constructed from 80 images of bananas for the purpose of feature extraction, as determined by the findings of Hong and Phoophuangpairoj (2024). The Brix and pH prediction was examined using the softmax derived from a MobileNet and RGB, L*a*b*, Brix, and pH values measured from 12, 11, 13, 11, 13, 10, and 10 bananas of class 0 to class 6, respectively. Linear regression, SVR regression, and KNN regression were used to analyze the data, which included three spots of RGB values, three spots of L*a*b*, Brix, and pH values, and softmax outputs from MobileNet. R2 and the discrepancies between actual and predicted values served as the basis for the evaluation.

3.2 Research Instruments and Software

3.2.1 Instruments Used in Data Collection

Table 3.1 Instruments

No.	Instruments
1.	Photo Box (PULUZ) 40 x 40 x 40 cm
2.	iPhone 14 proMax camera
3.	Colorimeter (Linshang LS171)
4.	Centrifuge (SURYQ 800D)
5.	Brix Refractometer (ATAGO PAL-1)
6.	pH Tester (YIERYI BLE-C66)

A photo box (PULUZ 40 x 40 x 40 cm) and an iPhone 14 camera were used in this work to take pictures of bananas, and a Linshang LS171 colorimeter was used to measure each banana's color. To extract juice, the banana was blended and put into a tube. Then the juice was separated from the pulp using a centrifuge (SURYQ 800D) to extract the banana juice. The pH and Brix values were measured using a BLE-C66 pH tester and an ATAGO PAL-1 Brix refractometer. The tools utilized to gather pictures, color values, Brix, and pH readings of banana juice were displayed in Figure 3.1.

มหาวิทยาลัยรังสิต Rangsit University

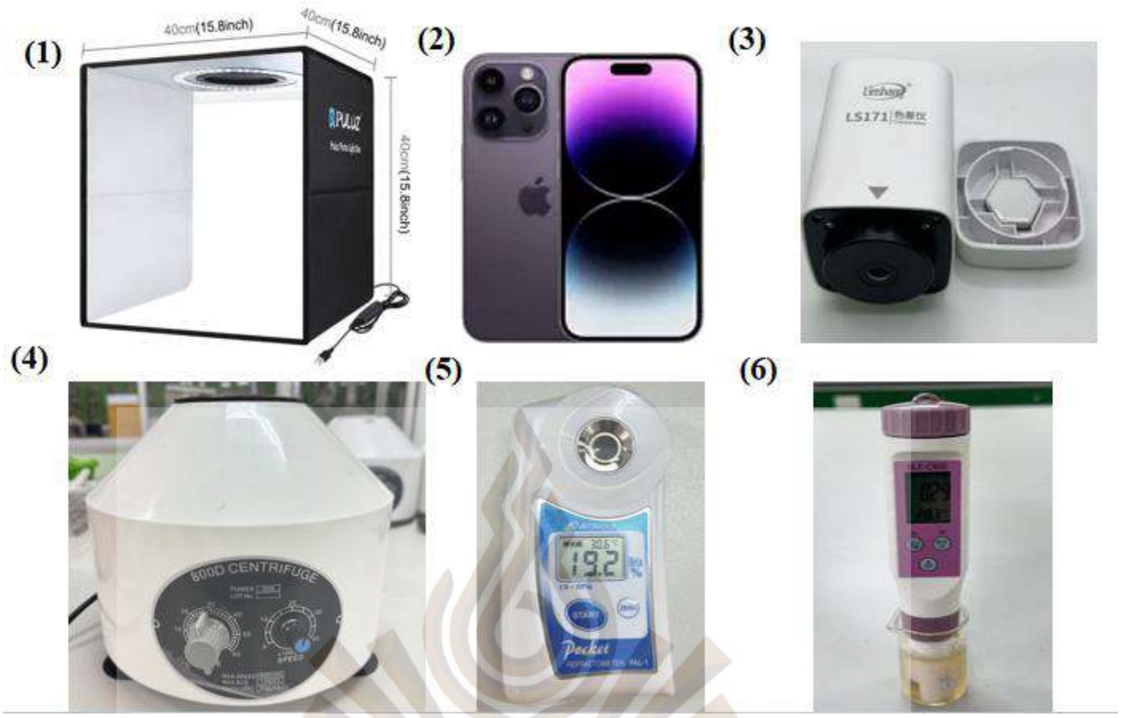

Figure 3.1 Instruments: (1) Photo Box, (2) iPhone 14 ProMax camera, (3) Centrifuge, (4) Colorimeter, (5) pH tester, (6) Brix refractometer

Source: Researcher

3.2.2 Research Software and Algorithms

Python and machine learning packages, namely TensorFlow, Keras, and scikit-learn, were used to create the MobileNet, CNN, ResNet50, and VGG16 classifiers. Additionally, linear regression, SVR, and KNN were used to predict Brix and pH values from RGB and L*a*b* colors.

Python served as the core programming language, integrating various machine learning frameworks and algorithms. It was used to implement classification models (MobileNet, CNN, ResNet50, and VGG16) and regression models (linear regression, SVR, and KNN) for predicting Brix and pH values.

TensorFlow and Keras were employed to construct deep learning models such as MobileNet, CNN, ResNet50, and VGG16. They provided the tools for defining,

มหาวิทยาลัยรังสิต Rangsit University

training, and fine-tuning these architectures, enabling accurate classification of banana ripeness into seven levels.

Scikit-learn was used to implement machine learning algorithms like linear regression, SVR, and KNN. These models predicted the Brix and pH values using the softmax outputs of MobileNet as input features.

MobileNet, a lightweight convolutional neural network architecture, was optimized for mobile and embedded vision applications. It was applied to classify banana ripeness into seven levels, with its softmax layer outputs further utilized as inputs to regression models for predicting Brix and pH values.

Linear regression was employed to establish a linear relationship between the softmax outputs of MobileNet and the target values (Brix and pH). By fitting a straight line to the data, it provided a simple and interpretable model for predicting sweetness and acidity levels of bananas.

SVR was utilized to capture more complex, non-linear relationships between the MobileNet softmax outputs and the target values. By employing kernel functions, SVR offered a flexible approach for improving the accuracy of Brix and pH predictions.

KNN predicted Brix and pH values by finding the k most similar data points (neighbors) in the feature space of MobileNet softmax outputs. It calculated the average of the neighbors' target values, allowing for a robust and non-parametric approach to regression.

3.3 Data Collection

Figure 3.2 illustrates the steps involved in data collection: 1) Purchase bananas, 2) Collect banana sample images, 3) Collect banana color data, 4) Collect banana juice, 5) Measure Brix values, and 6) Measure pH values.

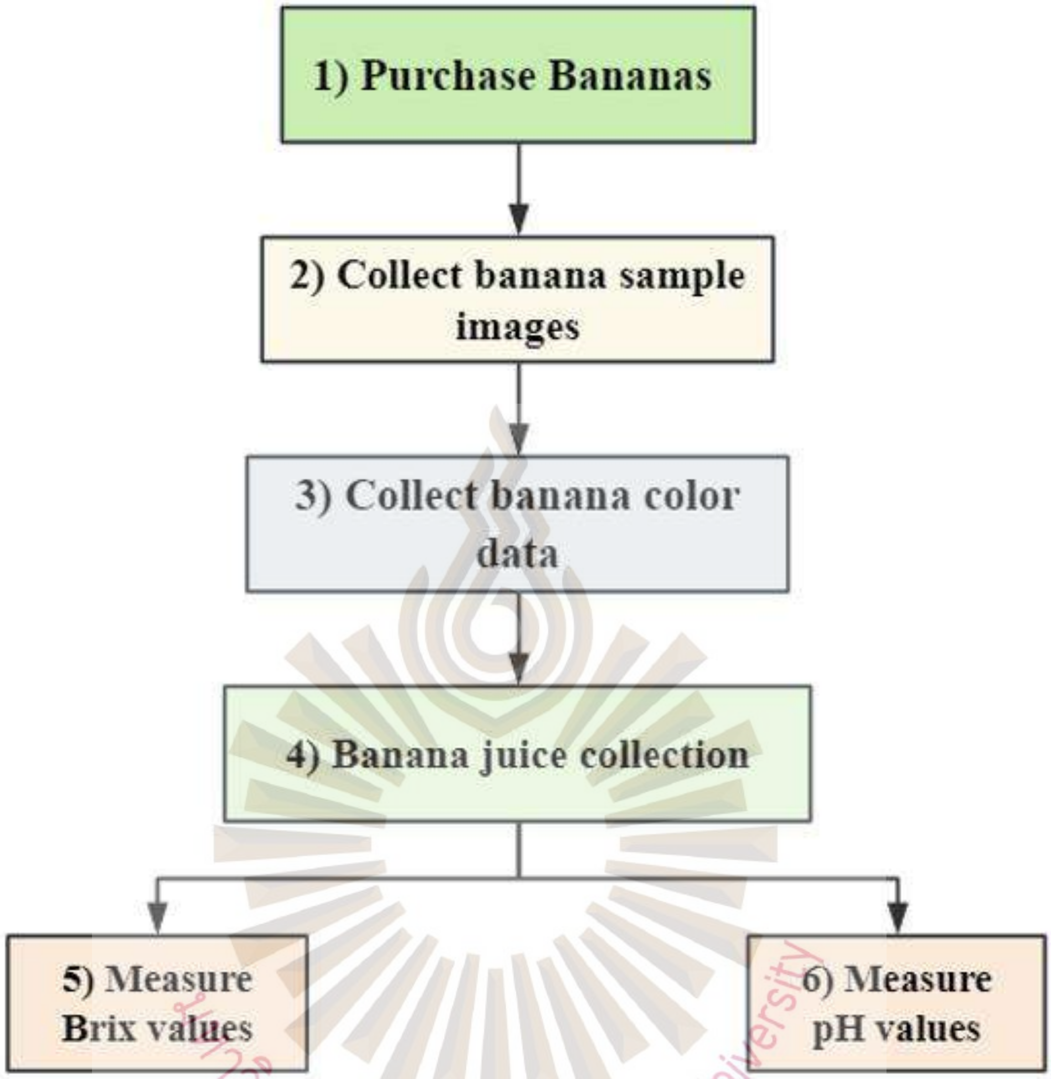
1) Purchase Bananas
2) Collect banana sample images
3) Collect banana color data
4) Banana juice collection
5) Measure Brix values
6) Measure pH values

Figure 3.2 Data collection flow

มหาวิทยาลัยรังสิต Rangsit University

3.3.1 Purchase Bananas

The bananas used in the study were all purchased from the Simummuang market, with only immature bananas from the first stage being purchased. The remaining banana grades were left at home to wait and observe changes in banana ripeness.

Figure 3.3 Simummuang market selling bananas

Source: Researcher

3.3.2 Collect Banana Images

As shown in Figure 3.4, the photographs of bananas were taken using an iPhone 14 Pro Max camera and a PULUZ lighting studio shooting tent box measuring 40 x 40 x 40 cm, which provided 24-26 lumen LED brightness and a color temperature of 5500 kelvins.

มหาวิทยาลัยรังสิต Rangsit University

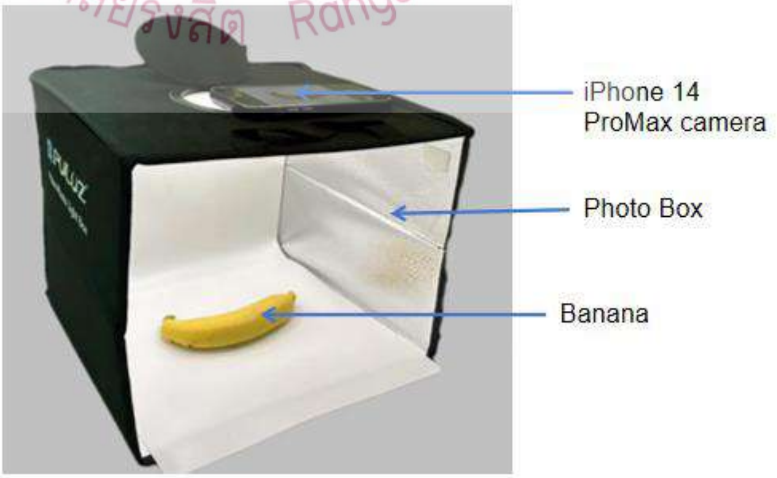

Figure 3.4 Collecting banana image

Source: Researcher

3.3.3 RGB and L*a*b* Color Data Collection

A colorimeter was used to measure the RGB and L*a*b* color values. RGB and L*a*b* color values were measured from one parts of a banana middle position, as shown in Figure 3.5.

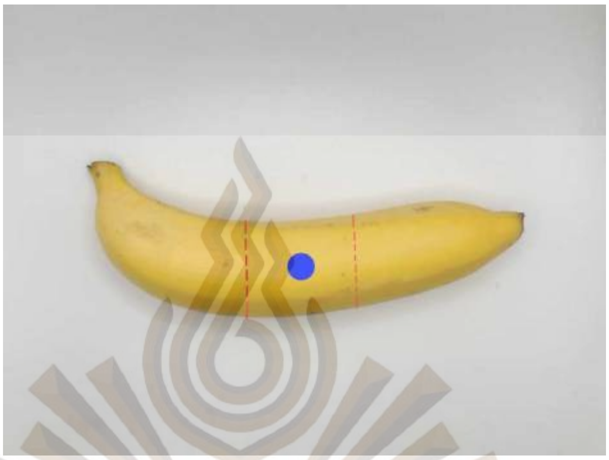

Figure 3.5 Banana color measurement positions

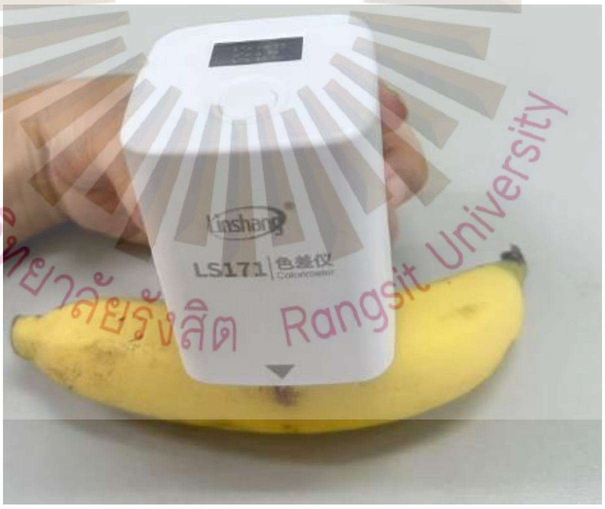

Figure 3.6 Using a colorimeter to measure RGB and L*a*b* color values

Figure 3.6 shows the RGB and L*a*b* color values of bananas measured using a colorimeter. After collecting all color values, RGB and L*a*b* values were saved in an Excel table file.

มหาวิทยาลัยรังสิต Rangsit University

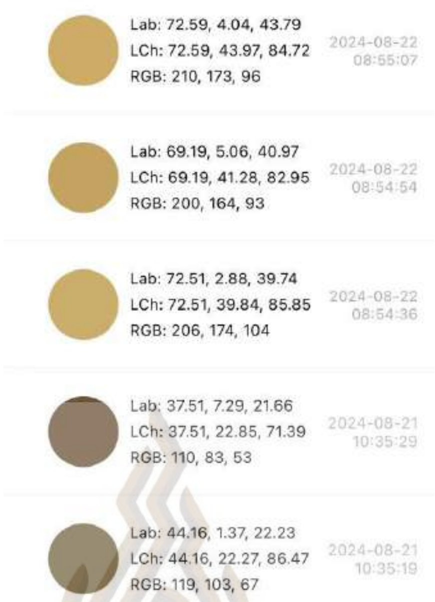

Lab: 72.59, 4.04, 43.79
LCh: 72.59, 43.97, 84.72
RGB: 210, 173, 96
2024-08-22 08:55:07

Lab: 69.19, 5.06, 40.97
LCh: 69.19, 41.28, 82.95
RGB: 200, 164, 93
2024-08-22 08:54:54

Lab: 72.51, 2.88, 39.74
LCh: 72.51, 39.84, 85.85
RGB: 206, 174, 104
2024-08-22 08:54:36

Lab: 37.51, 7.29, 21.66
LCh: 37.51, 22.85, 71.39
RGB: 110, 83, 53
2024-08-21 10:35:29

Lab: 44.16, 1.37, 22.23
LCh: 44.16, 22.27, 86.47
RGB: 119, 103, 67
2024-08-21 10:35:19

Figure 3.7 RGB and L*a*b* color data from 5 banana

Source: Researcher

3.3.4 Collect Banana Juice

The juice extraction started with putting each banana into a blender and then putting the blended flesh of the banana into a tube. Next, put the tube containing the banana pulp into the centrifuge. For grade 1-3 banana pulp, the centrifuge time was set to 45 minutes, and the speed was 3000 r/min. For grade 4-7 banana pulp, the centrifuge time was set to 20 minutes, and the speed was 2000 r/min. Figure 3.6 showed examples of extracted banana juices.

มหาวิทยาลัยรังสิต Rangsit University

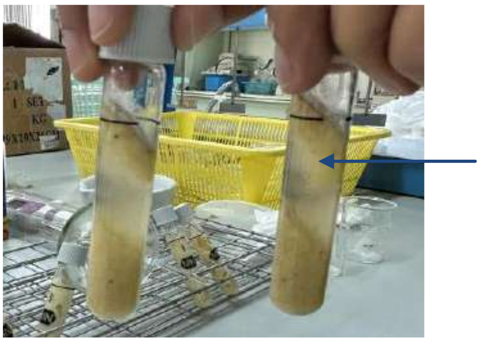

Extracted
banana juice

Figure 3.8 Extracted banana juice

3.3.5 Measure Brix Values

When measuring banana juice with a Brix refractometer, take 1-2 drops of the extracted juice and drop them onto the detection lens of the Brix refractometer. The Brix values of all banana samples were measured and recorded. Figure 3.7 showed the Brix measurement.

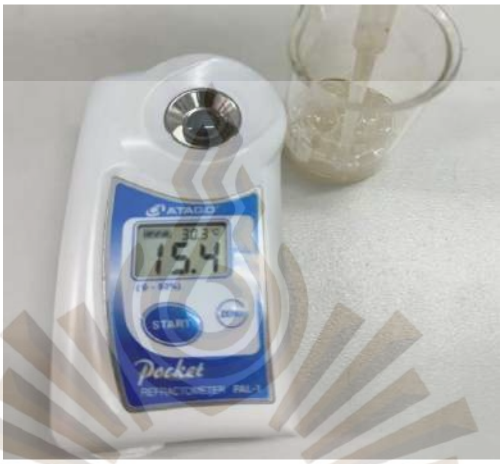

Figure 3.9 Brix measurement

3.3.6 pH Measurement

To measure the pH value, submerge the meter in banana juice, then wait 30 seconds for the reading to be stable before recording the data.

มหาวิทยาลัยรังสิต Rangsit University

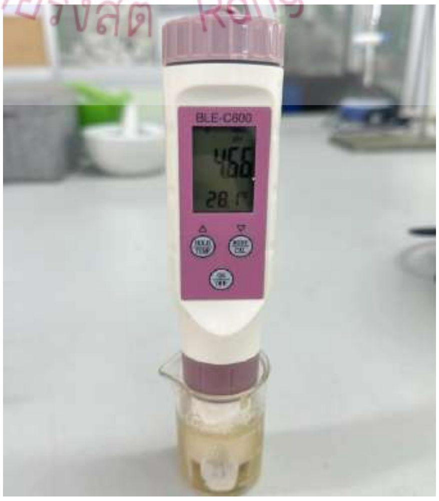

Figure 3.10 pH measurement

3.3.7 Dataset

Table 3.2 displayed the data used in the experiments for classifying banana ripeness and predicting Brix and pH values.

Table 3.2 Dataset

No.	Dataset Name	Description	Number of Data
1.	Image Data	Total images	1307 images
		For training	1047 images
		For testing	260 images
2.	RGB values	For prediction	240 values measured using a colorimeter from 80 bananas
3.	L*a*b* values	For prediction	240 values measured using a colorimeter from 80 bananas
4.	Brix values	For prediction	80 values
5.	pH values	For prediction	80 values

3.4 Data Analysis

3.4.1 Using MobileNet, ResNet50, CNN Classifiers for Banana Image Classification

Figure 3.11 showed the image classification flow of the first part of the study. After collecting banana images, resize banana images. The images were resized to 224 x 224 pixels. Subsequently, MobileNet, CNN, and ResNet50 were trained and employed to classify the banana images.

มหาวิทยาลัยรังสิต Rangsit University

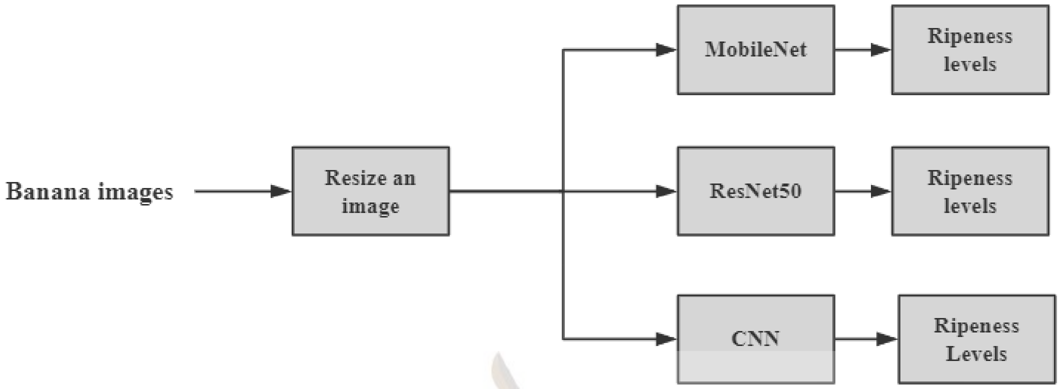

Figure 3.11 Banana ripeness classification flow

3.4.2 Using Different Predictors to Predict Brix and pH Values Based on MobileNet Softmax

As shown in Tabl 3.12, the seven outputs from a softmax layer were extracted and used as features to predict Brix and pH values. The features were extracted using MobileNet. The second part of this study was to use different prediction methods to predict Brix and pH values based on softmax values as input features. The prediction models utilized in this study include linear regression and SVR, which employs linear, polynomial, and radial basis kernel functions, and KNN. The experiment aimed to compare the performance of these models in predicting Brix and pH values.

มหาวิทยาลัยรังสิต Rangsit University

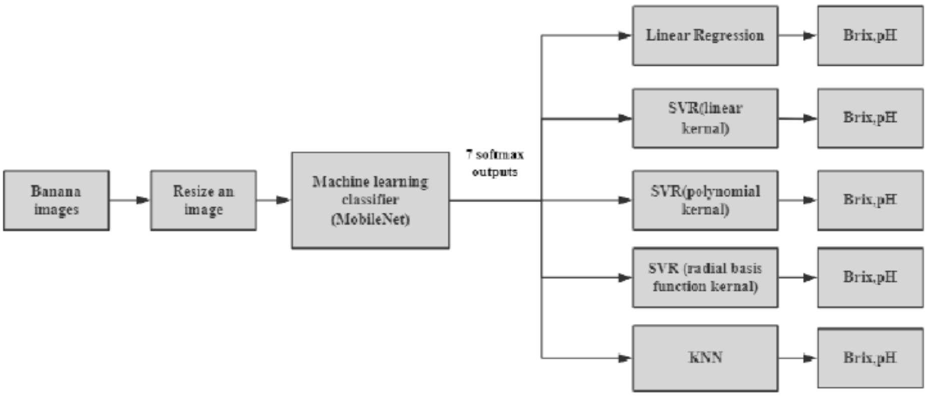

Figure 3.12 Using different predictors to predict Brix and pH values

3.4.3 Using Different Predictors to Predict Brix and pH Values Based on RGB and L*a*b* Values

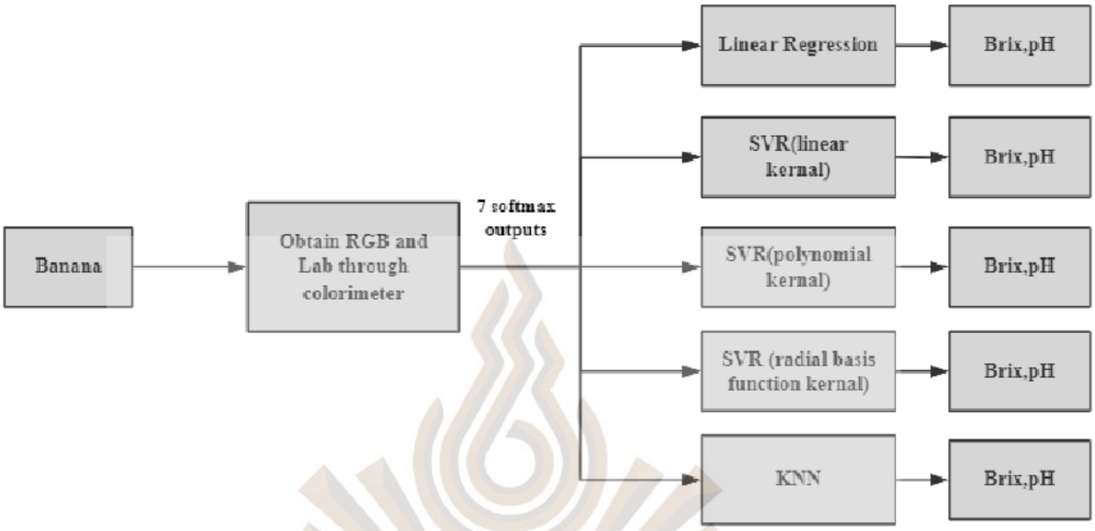

Figure 3.13 Using different predictors to predict Brix and pH values based on RGB and L*a*b*

มหาวิทยาลัยรังสิต Rangsit University

The second part used different prediction methods to predict Brix and pH values based on RGB and L*a*b* color values as input features. The prediction models utilized in this study include linear regression and SVR, which employs linear, polynomial, and radial basis kernel functions, as well as KNN. The experiments aimed to compare the performance of these models in predicting Brix and pH values.

3.4.4 Result Analysis Methodology

Accuracy, the overall proportion used to measure the correctness of a model

TP : True Positive

TN : True Negative

FP: False Positive

FN : False Negative

$$Accuracy = \frac{TP + TN}{TP + TN + FP + FN} \tag{3-1}$$

Precision formula refers to the proportion of samples predicted as belonging to a certain category that actually belongs to that category, calculated using the following formula:

$$Precision = \frac{TP}{TP + FP} \tag{3-2}$$

Recall refers to the proportion of samples that are correctly predicted as belonging to a certain category, calculated using the following formula:

$$Recall = \frac{TP}{TP + FN} \tag{3-3}$$

The F1 Score formula balances the relationship between the harmonic mean of precision and recall, calculated using the following formula:

$$F1\ Score = 2 * \frac{Precision * Recall}{Precision + Recall} \tag{3-4}$$

Absolute error is the difference between the predicted value and the true value, calculated using the following formula:

$$Absolute\ error = |Predict\ value - Actual\ value| \tag{3-5}$$

Relative error is the ratio of absolute error to the true value, calculated using the following formula:

$$Relative\ error = \frac{|Predict\ value - Actual\ value|}{|Actual\ value|} \tag{3-6}$$

The percentage error is the percentage form of relative error, and the calculation formula is:

$$Percentage\ error = \frac{|Predict\ value - Actual\ value|}{|Actual\ value|} * 100 \tag{3-7}$$

R^2 : The coefficient of determination measures the goodness of fit of a regression model to data, with values ranging from 0 to 1. The closer R^2 is to 1, the better the model fits and can explain more variance.

SS res: The formula for calculating the difference between the predicted and actual values of the model is:

$$SS_{res} = \sum_{i=1}^{n} (y1_i - y2_i)^2 \tag{3-8}$$

มหาวิทยาลัยรังสิต Rangsit University

SS tot: The formula for calculating the difference between the actual value and the average value is:

$$SS_{tot} = \sum_{i=2}^{n} (y_i - \bar{y})^2 \tag{3-9}$$

R^2 formula is as follows:

$$R^2 = 1 - \frac{SS_{res}}{SS_{tot}} \tag{3-10}$$

มหาวิทยาลัยรังสิต Rangsit University

Chapter 4

Research Results

4.1 Image Classification Results

This section employed CNN, ResNet50, MobileNet, and VGG16 models for the classification and analysis of banana ripeness. Firstly, the percentages of these four models in correctly and incorrectly classifying banana ripeness images were illustrated. The classification performance of each model was compared. Then, based on the classification results, generate a table containing accuracy, recall, and F1-scores to quantitatively analyze the performance of different models in banana ripeness classification. In the experiment, 20% of the images were used for testing and 80% for training. A total of 1047 banana images were used for training, including 205, 212, 155, 120, 106, 103, and 146 images of classes 0, 1, 2, 3, 4, 5, and 6, respectively. In the test, a total of 260 banana images were classified, consisting of 51, 53, 39, 30, 26, 25, and 36 images from 0 to 6 classes. The dataset included more images of immature bananas in classes 0, 1, 2, and 3, as they were easier to collect from wholesale markets.

4.1.1 80% Images for Training and 20% Images for Testing

Figure 4.1 displays the stacked graph of the MobileNet. Class 1 achieved an accuracy of 98.11%, while a minority (1.89%) misclassified class 1 bananas as class 0 bananas. Class 2 achieved an accuracy of 94.87%, with 5.13% of the images incorrectly predicted as class 1. The accuracy attained in class 3 and 4 were 100% and the accuracy of class 5 was 96%. The model incorrectly classified 4% of the class 5 images as class 6. Overall, the model performed well in the banana ripeness classification, especially class 0, 3, 4, and 6.

มหาวิทยาลัยรังสิต Rangsit University

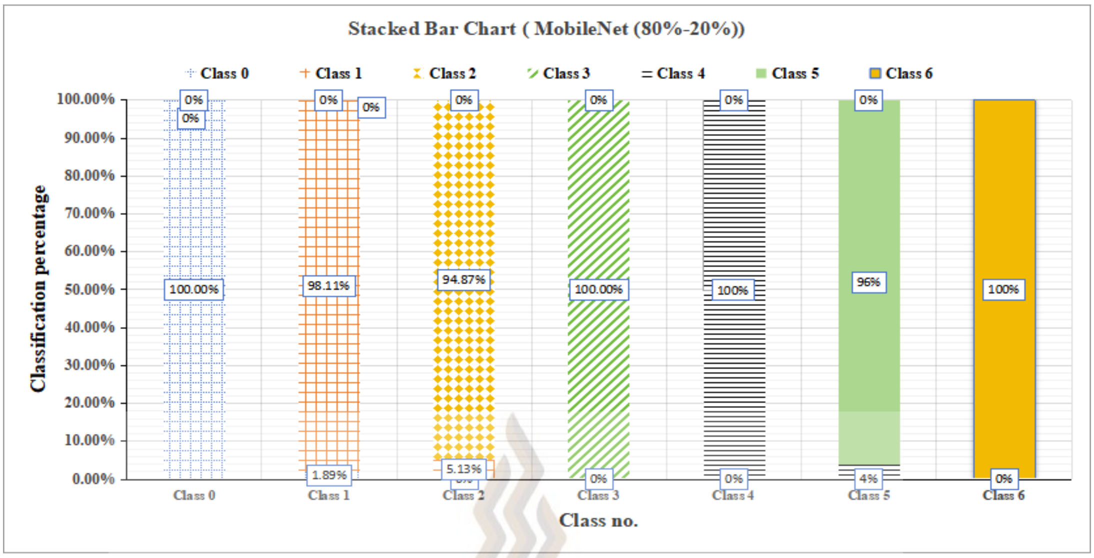

Figure 4.1 Percentage of accurate and inaccurate banana image classification using MobileNet (80% of images used for training, 20% for testing)

Table 4.1 shows that the MobileNet model performed very well in classifying banana ripeness, with accuracy, recall, and F1-score all approaching or equal to 1.00, especially in Class 0, Class 3, and Class 4, where accuracy and recall are both 1.00. The overall accuracy was 98%, indicating that the model could accurately distinguish bananas of different ripeness levels and was a very effective classifier.

มหาวิทยาลัยรังสิต Rangsit University

Table 4.1 Precision, recall, and F1-score using MobileNet with 80% of images for training and 20% for testing

Result / Real class	precision	recall	F1-score	support
Class 0	1.00	1.00	1.00	49
Class 1	0.98	0.98	0.98	53
Class 2	0.95	0.97	0.96	39
Class 3	1.00	1.00	1.00	30
Class 4	1.00	1.00	1.00	26
Class 5	0.96	0.96	0.96	25
Class 6	0.97	1.00	0.99	36

Table 4.1 Precision, recall, and F1-score using MobileNet with 80% of images for training and 20% for testing (continued)

Result Real class	precision	recall	F1-score	support
Macro avg	0.98	0.984	0.984	258
Weight avg	0.982	0.984	0.983	258

Figure 4.2 displays a stacked graph of prediction results of the ResNet50 model in different classes. The accuracy of class 1 is 96.23%, with a small number of images (1.89%) being incorrectly predicted as class 0 and class 2. The accuracy of class 2 is 97.37%, with only 2.63% of the images being incorrectly predicted as class 1. The accuracy of category 3 is 96.67%, and 3.33% of the images were misclassified as class 4. The classification performance of class 4 is poor, with an accuracy rate of 65.38%. 23.08% of the images were incorrectly predicted as class 5, and 11.54% of the images were misclassified as class 3. The accuracy of class 5 is 88%, but 12% of the images were incorrectly predicted as class 6.

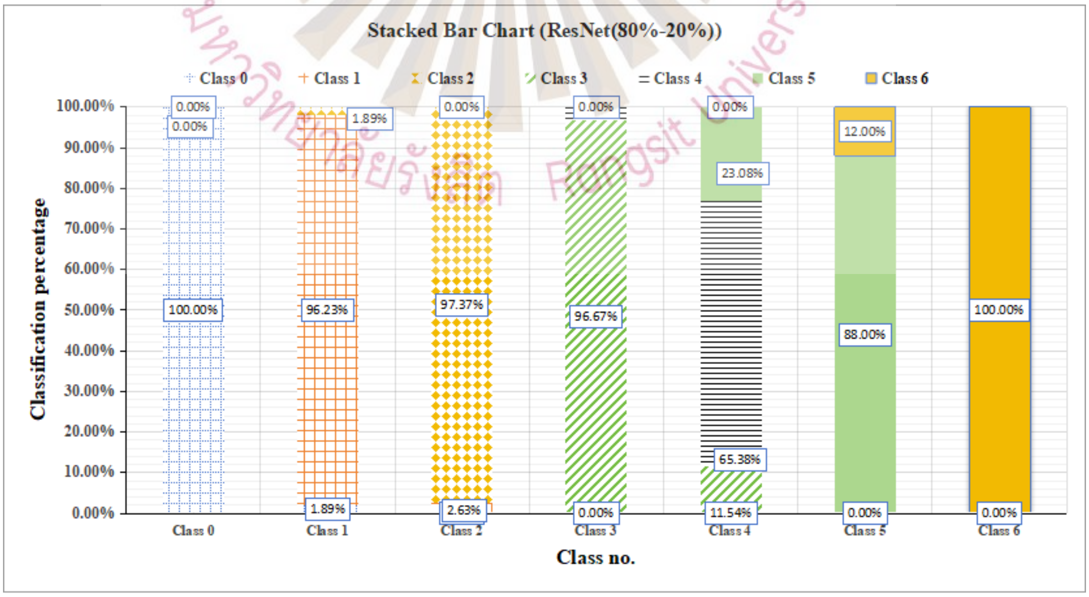

Figure 4.2 Percentage of correct and incorrect banana image classification using ResNet50 (80% of images used for training, 20% for testing)

มหาวิทยาลัยรังสิต Rangsit University

Table 4.2 summarizes the precision, recall, and F1-score for the ResNet50 model, using 80% of the images for training and 20% for testing. Class 0 and Class 6 showed excellent performance, with high F1-scores of 0.95 and 0.96, respectively, indicating effective classification for these classes in terms of both precision and recall. However, Class 4 and Class 5 had relatively lower F1-scores of 0.82 and 0.87, respectively.

Table 4.2 Precision, recall, and F1-score using ResNet50 with 80% of images for training and 20% for testing

Result Real class	precision	recall	F1-score	support
Class 0	0.98	0.92	0.95	49
Class 1	0.94	0.91	0.93	53
Class 2	0.93	0.97	0.95	39
Class 3	0.96	0.83	0.89	30
Class 4	0.84	0.81	0.82	26
Class 5	0.80	0.96	0.87	25
Class 6	0.92	1.00	0.96	36
Macro avg	0.90	0.91	0.91	258
Weight avg	0.92	0.92	0.92	258

มหาวิทยาลัยรังสิต Rangsit University

Figure 4.3 shows a stacked graph based on the CNN for banana ripeness classification. The accuracy of class 0 was 96.08%. The accuracy of class 1 was 90.57%, but 9.43% of the images were misclassified as class 0. The accuracy of class 2 was 94.87%, with only a few images (5.13%) misclassified as class 1. The accuracy of class 3 was 96.67%, with 3.33% of the images misclassified as class 4. The accuracy of class 4 was 92.31%, and 7.69% of the images were misclassified as class 5. Classes 5 and 6 had excellent classification performance, with no misclassifications.

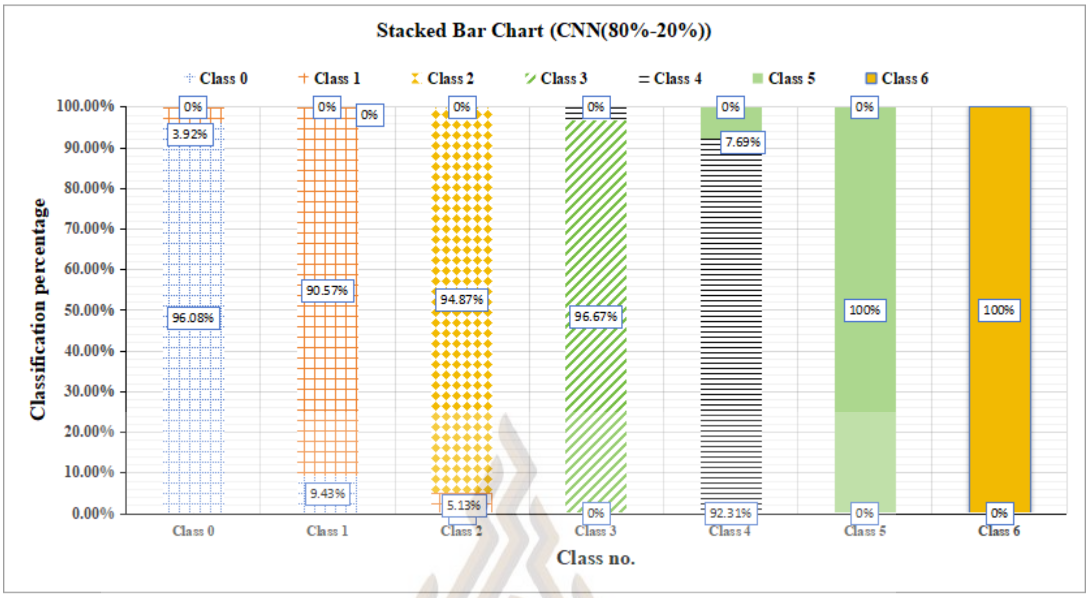

Figure 4.3 Percentage of correct and incorrect banana image classification using CNN (80% of images used for training, 20% for testing)

Table 4.3 displays the precision, recall, and F1-score of CNN, using 80% of images for training and 20% for testing. The CNN achieved 1.00 accuracy, recall, and F1-score in classifying banana ripeness images for Class 5 and Class 6, but its classification accuracy was lower than MobileNet in other classes, with Class 1 only achieving an accuracy of 0.90.

Table 4.3 Precision, recall, and F1-score using CNN with 80% of images for training and 20% for testing

Result / Real class	precision	recall	F1-score	support
Class 0	0.96	0.93	0.96	49
Class 1	0.90	0.91	0.91	53
Class 2	0.93	0.95	0.95	39
Class 3	0.96	0.96	0.97	30
Class 4	0.92	0.91	0.92	26
Class 5	1.00	1.00	1.00	25

มหาวิทยาลัยรังสิต Rangsit University

Table 4.3 Precision, recall, and F1-score using CNN with 80% of images for training and 20% for testing (continued)

Result Real class	precision	recall	F1-score	support
Class 6	1.00	1.00	0.99	36
Macro avg	0.952	0.952	0.957	258

Figure 4.4 shows a stacked chart based on the VGG16 model for banana ripeness classification. The chart primarily correctly classified Class 0 as Class 0, with an accuracy rate of 95.92%, but misclassifies Class 1 as Class 1 by 4.08%. The classification performance of Class 1 was good, with an accuracy of 94.34%. However, 1.89% of the samples were misclassified as Class 0, and 3.77% were misclassified as Class 2. Class 2 was almost completely correctly classified with an accuracy rate of 97.43%, with only 2.56% misclassified as Class 1. The accuracy of Class 4 was 96.15%, but 3.85% was misclassified as Class 5. The accuracy of Class 5 was 96%, with 4% of samples misclassified as Class 6. This indicates that the VGG16 model had good classification accuracy in most categories, but there were some misclassifications in some similar categories.

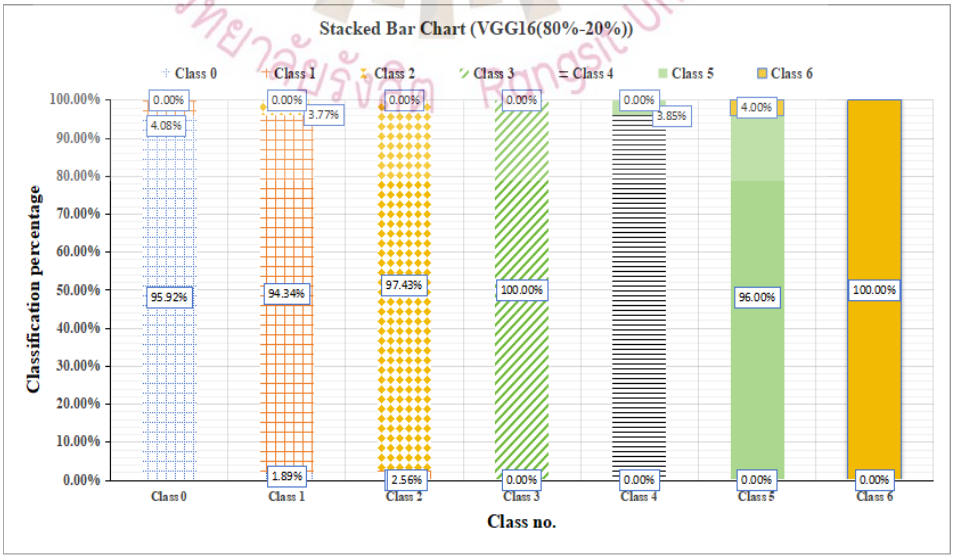

มหาวิทยาลัยรังสิต Rangsit University

Figure 4.4 Percentage of correct and incorrect banana image classification using VGG16 (80% of images used for training, 20% for testing)

Table 4.4 presents the precision, recall, and F1-score for the VGG16 model, using 80% of the images for training and 20% for testing. The results showed that Class 3 and Class 6 had excellent performance, with F1-scores of 1.00, indicating that the model correctly classified these classes in terms of precision and recall. Class 1 performed somewhat worse than the other classes and had precision and recall at 0.94.

Table 4.4 Precision, recall, and F1-score using VGG16 with 80% of images for training and 20% for testing

Result Real class	precision	recall	F1-score	support
Class 0	0.98	0.96	0.97	49
Class 1	0.94	0.94	0.94	53
Class 2	0.95	0.97	0.96	39
Class 3	1.00	1.00	1.0	30
Class 4	1.00	0.96	0.98	26
Class 5	0.96	0.96	0.96	25
Class 6	0.97	1.00	0.99	36
Macro avg	0.971	0.971	0.971	258
Weight avg	0.92	0.971	0.972	258

มหาวิทยาลัยรังสิต Rangsit University

The results showed that MobileNet stands out with the highest accuracy of 98.45%, making it the best-performing model and particularly suitable for classifying banana ripeness. The accuracy of VGG16 and CNN is 96.82% and 95.79%, respectively, both showing strong classification ability, but their efficiency was slightly lower than MobileNet. Despite ResNet50's power, its performance was relatively low at 92.43%, suggesting that it may not have received the same optimization for this specific task as other models. Table 4.5 compares the performance of MobileNet, ResNet50, CNN, and VGG16 classifiers with 80% of images for training.

Table 4.5 Accuracy when using MobileNet, ResNet50, CNN, and VGG16 to classify banana ripeness

Classification Method	Accuracy
MobileNet	98.45%
ResNet50	92.43%
CNN	95.79%
VGG16	97.10%

When 70% of the images were used for training and 30% for testing, MobileNet achieved an accuracy of 93.90%, which still outperformed ResNet50 and CNN. However, when the training data was increased to 80% and the testing data reduced to 20%, the accuracy of MobileNet significantly improved to 98.45% (Chen & Phoophuangpairoj, 2024). Future research will necessitate more training and testing photos to gain a better understanding of the accuracy obtainable with each method.

4.2 Predicting the Internal Properties of Bananas Using Softmax Values

This section of the chapter discussed in detail the use of classification results obtained from the Softmax layer to determine the internal characteristics of bananas. The Brix and pH values were measured from 12, 11, 13, 11, 13, 10, and 10 bananas of class 0 to class 6, respectively, for the Brix and pH prediction. In the prediction process, the output values of the Softmax layer were used as features to predict the Brix and pH values of bananas using linear regression, SVR, and KNN, respectively.

4.2.1 Use Linear Regression to Predict the Brix Values

The following equation was the equation obtained from applying the linear regression to predict Brix values:

มหาวิทยาลัยรังสิต Rangsit University

$$\text{PredictedBrixvalue}=(\text{Softmax0}*-16.99)+(\text{Softmax1}*-14.49)+(\text{Softmax2}*-8.148)+(\text{Softmax3}*-3.196)+(\text{Softmax4}*-0.2)+(\text{Softmax5}*2.592)+(\text{Softmax6}*-0.867)+20.264 \tag{4-1}$$

According to literature, if the R^2 value is between 0.3 and 0.5, it usually indicates a weak or low effect size. If the R^2 value is between 0.5 and 0.7, it is considered to have a moderate effect size and display considerable explanatory power. A value of R^2 higher than 0.7 is usually considered a strong effect size, indicating that a significant portion of the variability in the dependent variable can be explained by the model (Minitab Blog Editor, 2013). Linear regression was conducted with softmax and Brix values, yielding an R^2 of 0.958, signifying that the equation could reliably forecast the outcomes.

Table 4.6 displays the absolute error, standard deviation, relative error, and percentage error for each banana class when using the linear regression model for Brix prediction. In terms of absolute, relative, and percentage errors, the model had relatively good prediction performance, as indicated by the minimum errors between Class 0 and class 6. However, class 2 showed a high error rate, indicating that the Brix values were still relatively difficult to predict using linear regression.

Table 4.6 Brix prediction errors when using linear regression

	class 0	class 1	class 2	class 3	class 4	class 5	class 6	All classes
Absolute error	0.1679	0.7340	2.1577	1.0635	0.7462	0.9246	0.5078	0.9113
Standard deviation	0.1112	0.3971	2.1491	0.9728	0.5430	0.6538	0.0205	1.1258
Relative error	0.0502	0.1516	0.2105	0.0641	0.0358	0.0418	0.0418	0.0842
Standard deviation	0.0328	0.0912	0.2278	0.0626	0.0246	0.0299	0.0205	0.1165
Percentage error	5.0200	15.1634	21.0536	6.4111	3.5787	4.1797	2.6290	8.4182
Standard deviation	3.2808	9.1199	22.7832	6.2596	2.4558	2.9908	2.0487	11.6491

มหาวิทยาลัยรังสิต Rangsit University

Figure 4.5 shows the results of using linear regression to predict the Brix value based on softmax values. The obtained R^2 value was 0.958, indicating a correlation between the measured and predicted values. But there were obvious errors found in the bananas numbered 23, 24, 25, 28, and 41.

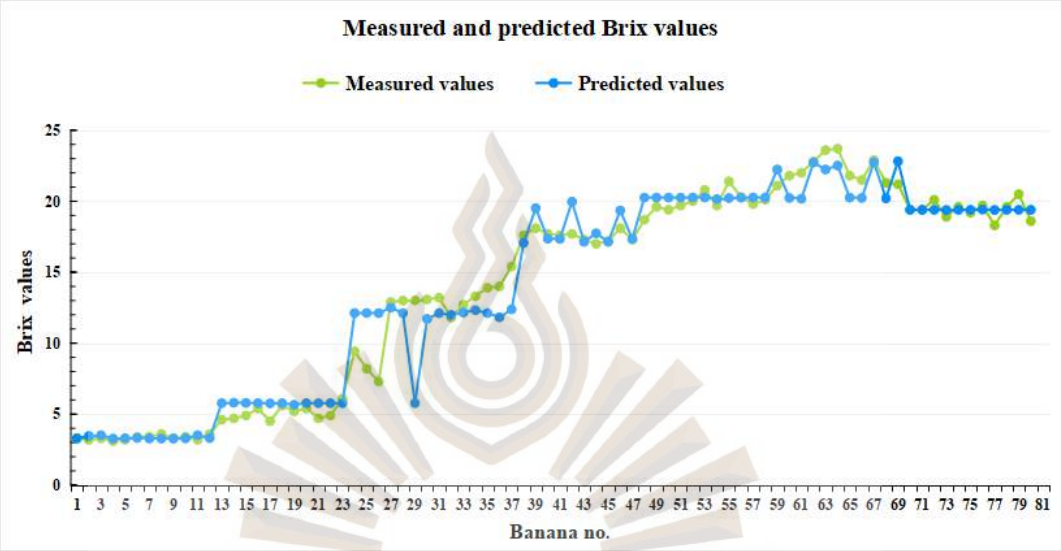

Figure 4.5 Graphs of measured and predicted Brix values when using linear regression

4.2.2 Use Linear Regression to Predict pH

The following equation was the equation obtained from applying the linear regression to predict pH values:

$$\text{PredictedpHvalue}=(\text{Softmax0}*-0.723)+(\text{Softmax1}*-0.418)+(\text{Softmax2}*-0.261)+(\text{Softmax3}*-0.190)+(\text{Softmax4}*-0.002)+(\text{Softmax5}*0.194)+(\text{Softmax6}*-0.562)+4.771 \qquad (4\text{-}2)$$

Linear regression was performed using softmax and pH values, with an R^2 of 0.929, indicating that the equation can accurately predict the results.

Table 4.7 shows the pH prediction errors when using linear regression. The absolute error, relative error, and percentage error of all classes were 0.0861, 0.0189, and 1.8868, respectively. The results revealed that certain classes, including class 0 and

มหาวิทยาลัยรังสิต Rangsit University

class 6, exhibited high errors, suggesting that the model was still unable to provide accurate predictions.

Table 4.7 pH prediction errors when using linear regression

	class 0	class 1	class 2	class 3	class 4	class 5	class 6	All classes
Absolute error	0.1501	0.0589	0.0511	0.0935	0.0618	0.0865	0.1031	0.0861
Standard deviation	0.0692	0.0431	0.0467	0.0549	0.0515	0.0718	0.0144	0.0661
Relative error	0.0370	0.0135	0.0113	0.0204	0.0128	0.0175	0.0175	0.0189
Standard deviation	0.0172	0.0097	0.0103	0.0122	0.0103	0.0145	0.0144	0.0148
Percentage error	3.6995	1.3530	1.1332	2.0416	1.2768	1.7496	1.9186	1.8868
Standard deviation	1.7154	0.9745	1.0275	1.2168	1.0307	1.4531	1.4377	1.4849

Figure 4.6 shows the measured and predicted pH values under the linear regression model, with red diamonds representing measured values and blue dots representing predicted values. There was a significant deviation between the predicted values and the measured values, such as the values numbered 6 through 11, where the errors were high.

มหาวิทยาลัยรังสิต Rangsit University

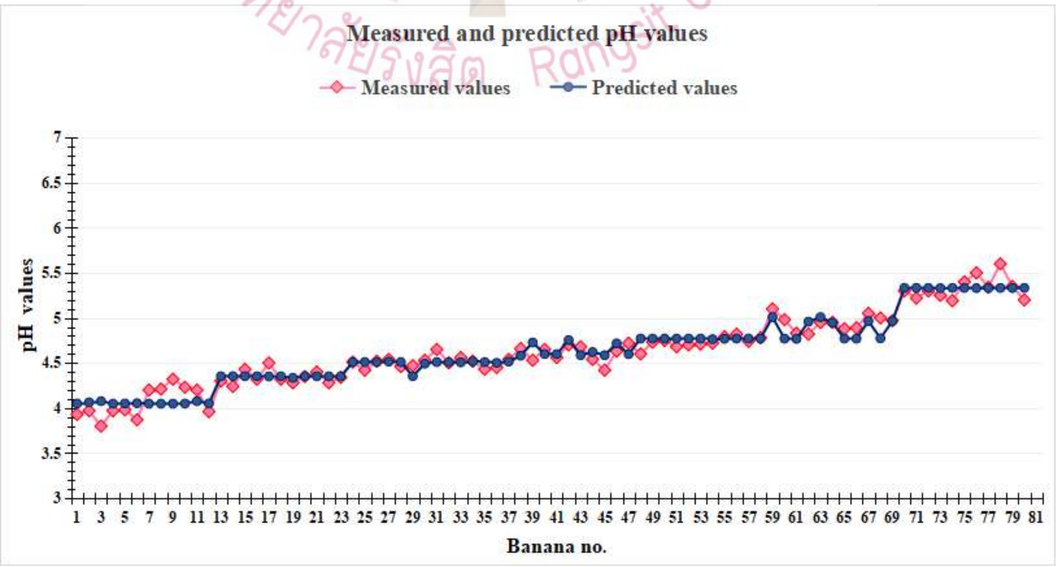

Figure 4.6 Measured and predicted pH values when using linear regression

4.2.3 Use SVR to Predict Brix and pH Values

The study applied support vector regression (SVR) models to predict the Brix and pH values of bananas using the MobileNet Softmax values. To make predictions more accurate, the researcher compared the performance of three SVR kernel functions: the polynomial kernel function, the radial basis kernel function, and the linear kernel function.

4.2.3.1 Use SVR (polynomial kernel) to Predict Brix Values

Table 4.8 displays the errors in predicting Brix values using the SVR (polynomial kernel). An interesting finding was that the SVR (polynomial kernel) was not very good at predicting Brix values. This was especially true for some classes of bananas, like class 1, class 2, class 4, and class 5.

Table 4.8 Brix prediction errors when using SVR (polynomial kernel)

	class 0	class 1	class 2	class 3	class 4	class 5	class 6	All classes
Absolute error	1.0734	1.5962	1.9812	0.6373	1.5467	1.8926	0.5986	1.3203
Standard deviation	1.2485	0.9649	2.3929	0.6863	1.0435	1.3898	0.0180	1.3614
Relative error	0.3172	0.2903	0.2003	0.0368	0.0740	0.0856	0.0856	0.1491
Standard deviation	0.3817	0.1480	0.2716	0.0411	0.0469	0.0626	0.0180	0.2169
Percentage error	31.7249	29.0282	20.0314	3.6774	7.4021	8.5563	3.0993	14.9052
Standard deviation	38.1668	14.8023	27.1575	4.1147	4.6904	6.2618	1.8003	21.6909

Figure 4.7 illustrates the results of employing SVR with a polynomial kernel to predict the Brix values of bananas. The R^2 value of the model was 0.925, signifying that the SVR model could elucidate about 92.5% of the Brix value. Nevertheless, there were considerable variations and discrepancies between the predicted and measured values.

มหาวิทยาลัยรังสิต Rangsit University

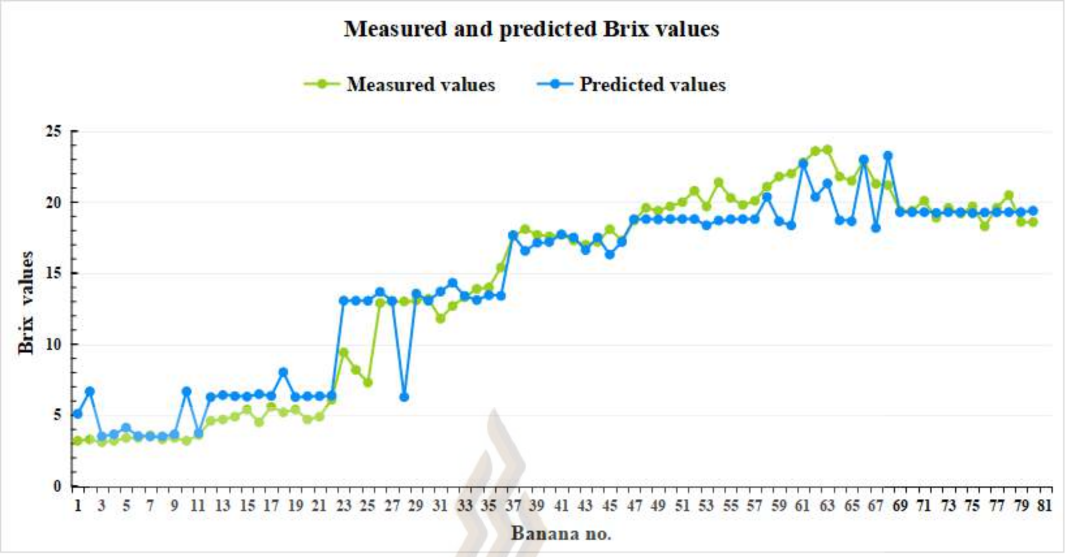

Figure 4.7 Graphs measured and predicted Brix values when using SVR with a polynomial kernel

4.2.3.2 Use SVR (polynomial) to Predict pH Values

Table 4.9 presents a summary of the errors associated with the use of the SVR (polynomial kernel) model for pH prediction. Although the relative error and percentage error are generally low, specific classes, such as class 0 and class 6, still exhibited rather large error values. This indicates that the model had difficulty capturing changes in the pH values.

Table 4.9 pH prediction errors when using SVR (polynomial kernel)

	class 0	class 1	class 2	class 3	class 4	class 5	class 6	All classes
Absolute error	0.1538	0.0677	0.0605	0.0772	0.0715	0.0853	0.1089	0.0888
Standard deviation	0.0993	0.0455	0.0432	0.0580	0.0553	0.0723	0.0160	0.0725
Relative error	0.0382	0.0156	0.0135	0.0168	0.0148	0.0171	0.0171	0.0195
Standard deviation	0.0259	0.0106	0.0096	0.0128	0.0111	0.0145	0.0160	0.0167
Percentage error	3.8177	1.5602	1.3476	1.6802	1.4754	1.7092	2.0196	1.9468
Standard deviation	2.5896	1.0571	0.9617	1.2767	1.1076	1.4498	1.5964	1.6744

มหาวิทยาลัยรังสิต Rangsit University

Figure 4.8 illustrates the results of using SVR (polynomial kernel) to predict banana pH values. Although the overall trend was consistent, there were some deviations between the predicted values and the measured values at certain data points (such as the values numbered 6 through 9). The R^2 value is 0.914, indicating that the SVR polynomial kernel model could explain 91.4% of pH changes.

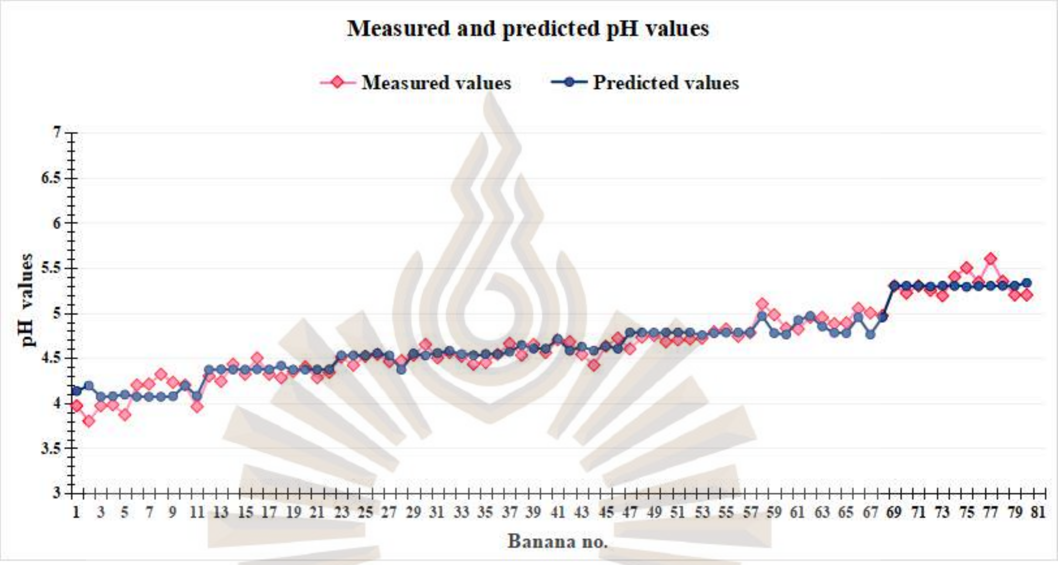

Figure 4.8 Graphs of measured and predicted pH values when using SVR with a polynomial kernel

4.2.3.3 Use SVR with RBF Kernel to Predict Brix Values

Table 4.10 shows the prediction error for Brix values using the SVR with an RBF kernel. Although the average error is within an acceptable range, some classes, such as class 2 and class 5, had poor prediction performance.

Table 4.10 Brix prediction errors when using SVR with an RBF kernel

	class 0	class 1	class 2	class 3	class 4	class 5	class 6	All classes
Absolute error	0.8231	1.1310	1.8004	0.5300	0.9920	1.9357	0.6667	1.0975
Standard deviation	0.2414	0.9482	2.5407	0.7044	0.9411	1.2025	0.0200	1.2811
Relative error	0.2395	0.1984	0.1857	0.0312	0.0460	0.0863	0.0863	0.1176

Table 4.10 Brix prediction errors when using SVR with an RBF kernel (continued)

	class 0	class 1	class 2	class 3	class 4	class 5	class 6	All classes
Standard deviation	0.0608	0.1166	0.2834	0.0439	0.0420	0.0495	0.0200	0.1456
Percentage error	23.9511	19.8419	18.5736	3.1178	4.6018	8.6262	3.4149	11.7587
Standard deviation	6.0790	11.6611	28.3384	4.3870	4.2002	4.9497	1.9973	14.5635

Figure 4.9 shows the results of using the SVR with a radial basis kernel to predict banana Brix values. This figure shows the comparison between the actual measured Brix values and the predicted Brix values. Although the overall trend is consistent, there is still a certain degree of fluctuation and error at certain data points (such as the values numbered 22 through 24 and those numbered 56 through 66). The R² value was 0.941, indicating that the model could explain 94.1% of the Brix value variation.

มหาวิทยาลัยรังสิต Rangsit University

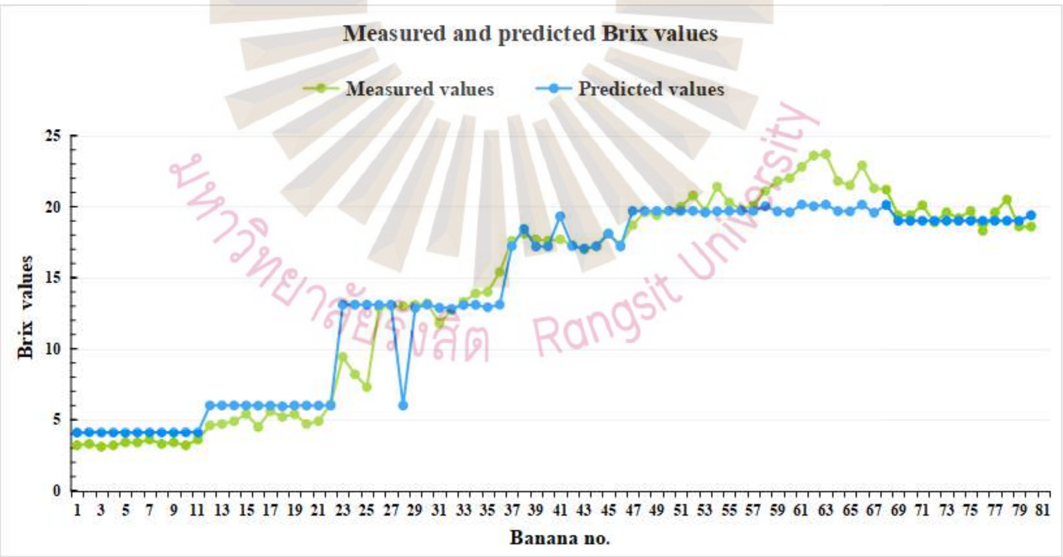

Figure 4.9 Graphs of measured and predicted Brix values when using SVR with an RBF kernel

4.2.3.4 Use SVR with RBF kernel to predict pH values

Table 4.11 displays the prediction errors of pH values using an RBF-kernel SVR. The average absolute error of all classes was 0.0860, indicating rather low errors. However, the error of class 0 was relatively high, suggesting that enhancements in its prediction are necessary.

Table 4.11 pH prediction errors when using SVR with an RBF kernel

	class 0	class 1	class 2	class 3	class 4	class 5	class 6	All classes
Absolute error	0.1468	0.0666	0.0565	0.0786	0.0722	0.0736	0.1084	0.0860
Standard deviation	0.0601	0.0410	0.0422	0.0579	0.0525	0.0630	0.0157	0.0635
Relative error	0.0362	0.0154	0.0126	0.0171	0.0150	0.0147	0.0147	0.0188
Standard deviation	0.0156	0.0095	0.0094	0.0127	0.0107	0.0126	0.0157	0.0142
Percentage error	3.6177	1.5359	1.2572	1.7068	1.4963	1.4730	2.0091	1.8798
Standard deviation	1.5593	0.9539	0.9377	1.2695	1.0665	1.2604	1.5677	1.4209

The results of predicting banana pH using SVR with a radial basis kernel were displayed in Figure 4.10. The overall error was low, although there were some deviations between the predicted and measured values at certain data points (such as the values numbered 2, 9, 74, and 76). The R² value is 0.926, indicating that the SVR polynomial kernel model can explain approximately 92.6% of pH variation.

มหาวิทยาลัยรังสิต Rangsit University

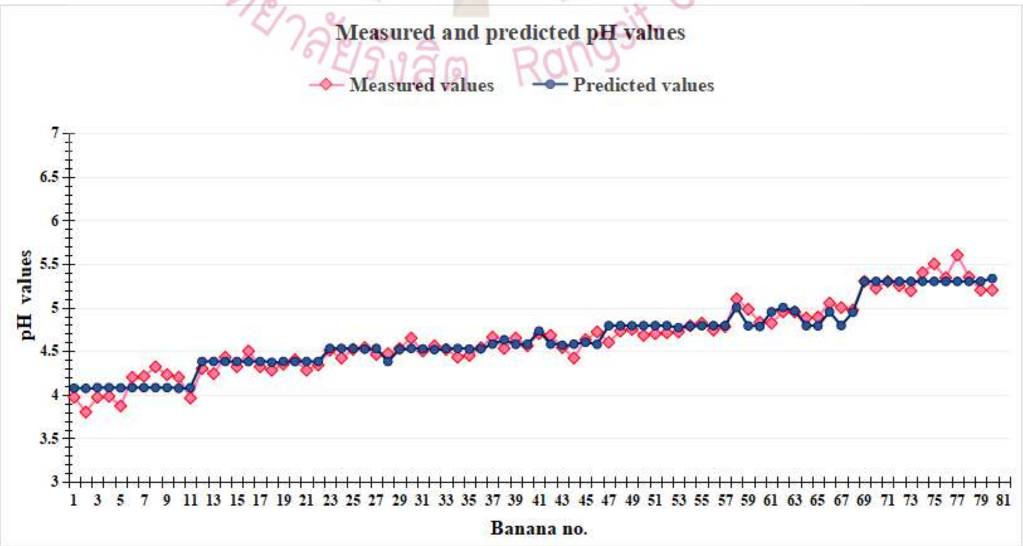

Figure 4.10 Graphs of measured and predicted pH values when using SVR with a radial kernel

4.2.3.5 Use SVR with a Linear Kernel to Predict Brix values

Table 4.12 shows the prediction error of Brix values using the SVR with a linear kernel. The prediction of Brix values when using SVR linear regression performed quite well in some classes (such as class 0), with small errors. However, the error in Class 2 was significantly high. The absolute error of all classes was 0.8413. The relative and percentage errors of all classes were 0.0741 and 7.4115, respectively.

Table 4.12 Brix prediction errors when using SVR with a linear kernel

	class 0	class 1	class 2	class 3	class 4	class 5	class 6	All classes
Absolute error	0.2048	0.7045	1.9172	0.7372	0.7206	1.0420	0.5764	0.8413
Standard deviation	0.1504	0.9971	2.6583	0.7181	0.7551	0.7408	0.0209	1.2683
Relative error	0.0573	0.1082	0.1940	0.0426	0.0339	0.0475	0.0475	0.0741
Standard deviation	0.0348	0.1016	0.2864	0.0435	0.0344	0.0341	0.0209	0.1291
Percentage error	5.7268	10.8177	19.4040	4.2605	3.3936	4.7455	3.0144	7.4115
Standard deviation	3.4774	10.1582	28.6419	4.3479	3.4441	3.4099	2.0945	12.9137

Figure 4.11 shows the comparison of measured and predicted Brix values for bananas using the SVR with a linear kernel. The R^2 value was 0.952, which was higher than using the polynomial kernel and the RBF kernel. The measured values (green dots) and predicted values (blue dots) were close to each other but had high errors in some areas, especially around banana samples 22-24.

มหาวิทยาลัยรังสิต Rangsit University

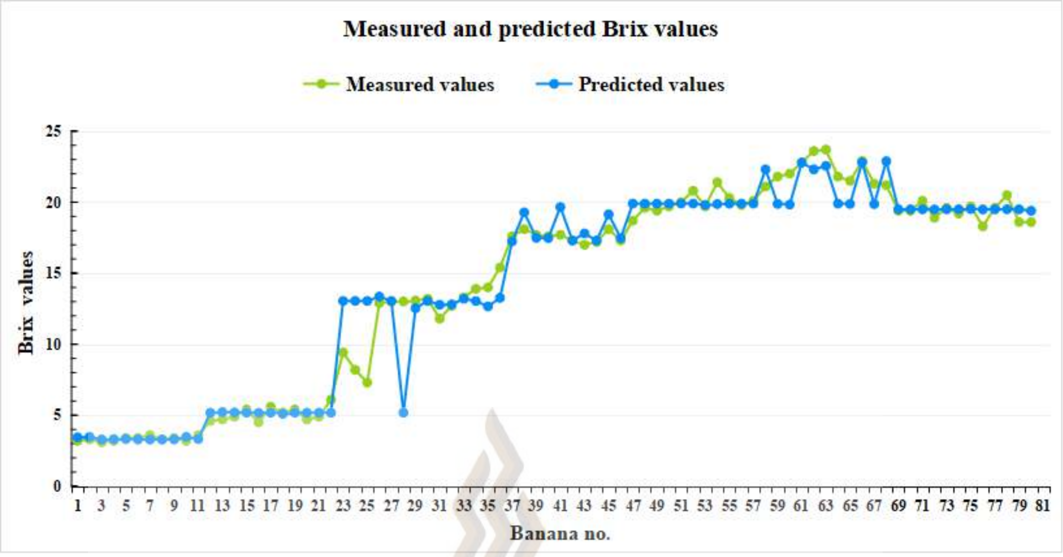

Figure 4.11 Graphs of measured and predicted Brix values when using SVR with a linear kernel

4.2.3.6 Use SVR with a Linear Regression to Predict pH Values

Table 4.13 shows the prediction error for pH values using the SVR with a linear kernel. The overall absolute error of the SVR for pH value was 0.0891. The relative and percentage errors were 0.0195 and 1.9490, respectively.

Table 4.13 pH prediction errors when using SVR with a linear kernel

	class 0	class 1	class 2	class 3	class 4	class 5	class 6	All classes
Absolute error	0.1480	0.0623	0.0571	0.0984	0.0725	0.0778	0.1063	0.0891
Standard deviation	0.0690	0.0405	0.0428	0.0600	0.0522	0.0614	0.0147	0.0642
Relative error	0.0365	0.0143	0.0127	0.0214	0.0150	0.0155	0.0155	0.0195
Standard deviation	0.0179	0.0093	0.0095	0.0133	0.0106	0.0123	0.0147	0.0146
Percentage error	3.6516	1.4328	1.2702	2.1401	1.5016	1.5529	1.9776	1.9490
Standard deviation	1.7907	0.9320	0.9522	1.3282	1.0587	1.2282	1.4682	1.4573

The results of using SVR with a linear kernel to predict the pH values from the softmax values are displayed in Figure 4.12, where the horizontal axis displays the banana sample numbers and the vertical axis displays the pH values. The red diamonds represented the measured values, and the blue dots represented the predicted values. The R^2 value was 0.922, which is lower than the RBF kernel.

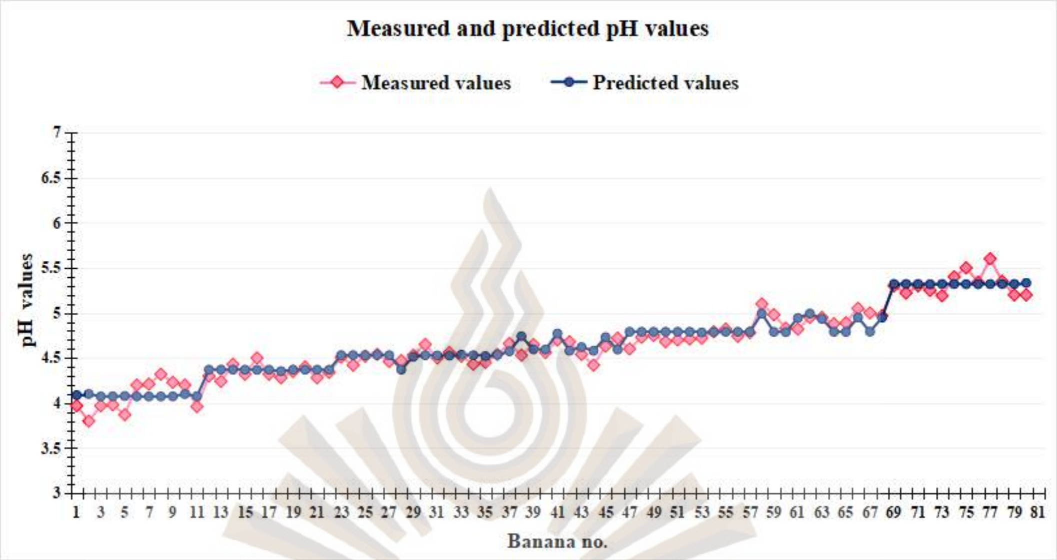

Figure 4.12. Graphs of measured and predicted pH values when using SVR with a linear kernel

4.2.4 Use KNN to Predict Brix and pH Values

In this section, the KNN algorithm was used to predict the Brix and pH values of bananas from the seven softmax features.

4.2.4.1 Use KNN (k=3) to Predict Brix Values

Table 4.14 summarizes the Brix value prediction errors for KNN with k=3, with an overall percentage error of 3.4084%, reflecting reliable performance. Most classes, especially Class 4, exhibit high accuracy with minimal percentage errors (as low as 0.9372%) and consistent predicted, as indicated by small standard deviations in absolute and percentage errors.

มหาวิทยาลัยรังสิต Rangsit University

Table 4.14 Brix values prediction errors when using KNN (k=3)

	class 0	class 1	class 2	class 3	class 4	class 5	class 6	All classes
Absolute error	0.0850	0.2040	1.1263	0.4431	0.1958	0.3756	0.3036	0.3938
Standard deviation	0.0645	0.1876	1.7052	0.4496	0.3692	0.4362	0.0138	0.7728
Relative error	0.0252	0.0342	0.1068	0.0258	0.0094	0.0168	0.0168	0.0341
Standard deviation	0.0200	0.0257	0.1540	0.0277	0.0175	0.0196	0.0138	0.0683
Percentage error	2.5161	3.4183	10.678	2.5805	0.9372	1.6804	1.5880	3.4084
Standard deviation	1.9986	2.5655	15.396	2.7660	1.7505	1.9562	1.3826	6.8306

Figure 4.13 shows the prediction of the Brix values from banana images using the KNN (k=3), where green dots represented the measured values and blue dots represented the predicted values. The trend of the two curves was basically consistent. The R^2 value of the model was 0.984, indicating a high correlation between the measured and predicted values. This revealed that the KNN (k=3) predictor exhibited high accuracy in predicting Brix values with small errors.

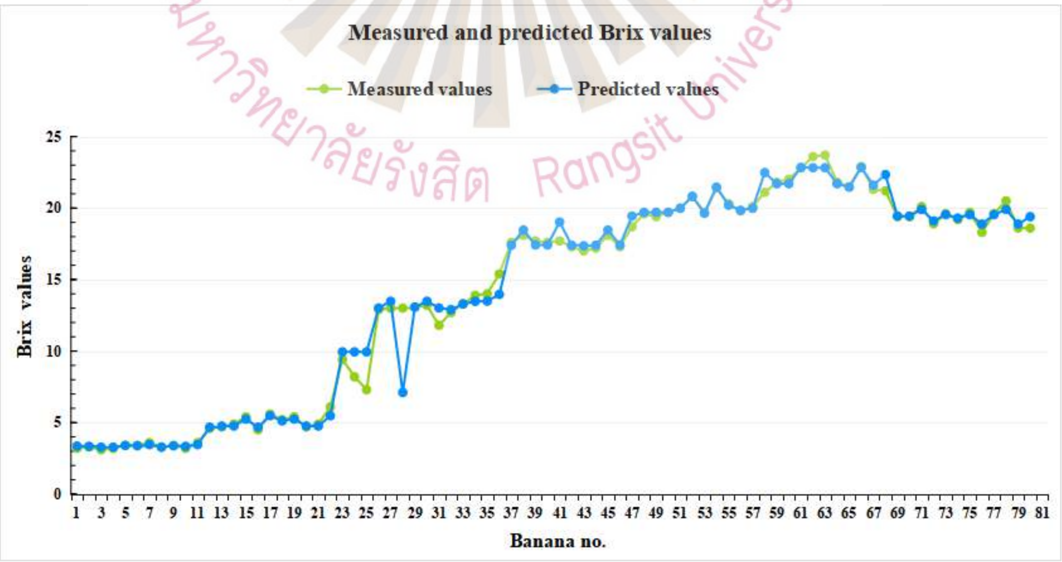

Figure 4.13 Graphs of measured and predicted Brix values when using KNN (k=3)

มหาวิทยาลัยรังสิต Rangsit University

4.2.4.2 Use KNN (k=3) to Predict pH Values

Table 4.15 shows the error in predicting pH values using KNN (k=3). The prediction error at class 0 was highest. The absolute, relative, and percentage errors of all classes were 0.0335, 0.0072, and 0.721, respectively. Overall, the model performs the best in predicting pH values using the softmax values.

Table 4.15 pH prediction errors when using KNN (k=3)

	class 0	class 1	class 2	class 3	class 4	class 5	class 6	All classes
Absolute error	0.0385	0.0173	0.0277	0.0445	0.0286	0.0256	0.0519	0.0335
Standard deviation	0.0355	0.0231	0.0264	0.0515	0.0414	0.0265	0.0102	0.0393
Relative error	0.0096	0.0040	0.0061	0.0098	0.0058	0.0051	0.0051	0.0072
Standard deviation	0.0091	0.0052	0.0057	0.0115	0.0084	0.0053	0.0102	0.0084
Percentage error	0.9576	0.3958	0.6106	0.9789	0.5845	0.5111	0.9637	0.7217
Standard deviation	0.9082	0.5232	0.5691	1.1549	0.8419	0.5302	1.0172	0.8383

The graphs in Figure 4.14 show the measured and predicted values when using the KNN (k=3) to predict the pH values of bananas. The R^2 value of the model was 0.972, which was higher than the R^2 values of SVR and linear regression. This indicated that the KNN (k=3) performed better than SVR and linear regression in predicting pH values, with the errors smaller than SVR and linear regression.

มหาวิทยาลัยรังสิต Rangsit University

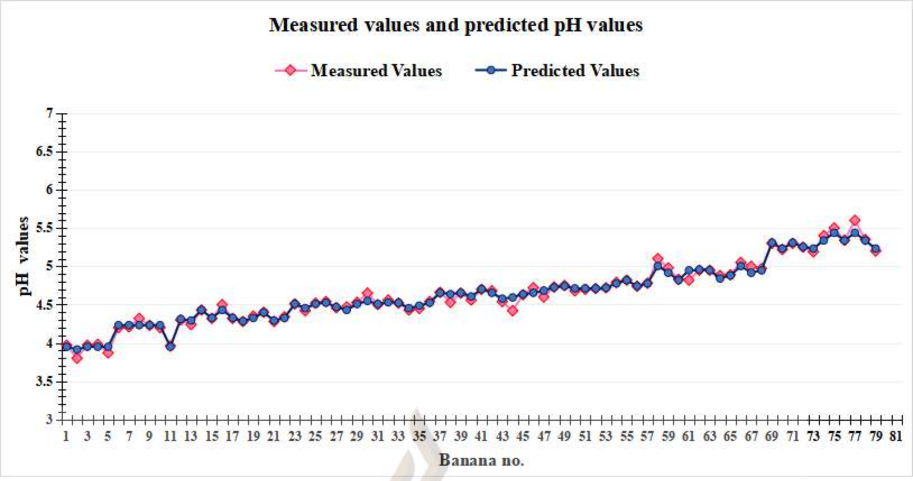

Figure 4.14 Graphs of measured and predicted pH values when using KNN (k=3)

4.2.5 Summarize the R^2 results of Brix Values using Different Methods when using Softmax Values

Table 4.16 compares the predictive performance of different models for Brix values using softmax features. Linear regression showed an R^2 value of 0.958. SVR models demonstrated varying performance, with the linear kernel performing best ($R^2 = 0.952$), followed by the radial basis kernel ($R^2 = 0.941$) and the polynomial kernel ($R^2 = 0.925$). KNN had the highest predictive accuracy, with k=3 achieving the best R^2 value of 0.984, followed by k=5 ($R^2 = 0.966$) and k=7 ($R^2 = 0.952$). KNN outperformed other methods overall.

มหาวิทยาลัยรังสิต Rangsit University

Table 4.16 R^2 results when using different methods to predict Brix values

Features	Methods	R^2
Softmax values	**Linear regression**	**0.958**
Softmax values	**SVR (linear)**	**0.952**
Softmax values	SVR (polynomial)	0.925
Softmax values	SVR (radial basis function)	0.941
Softmax values	**KNN (k=3)**	**0.984**
Softmax values	KNN (k=5)	0.966
Softmax values	KNN (k=7)	0.952

When predicting pH values using different methods, Table 4.17 shows the R^2 values. It also compares how well different models did with the softmax features. KNN showed the best performance, with R² values of 0.972 (k=3), 0.9412 (k=5), and 0.921 (k=7). Linear regression ranked second, with an R² value of 0.925. Among SVR models, the radial basis kernel performed best (R² = 0.926), slightly surpassing linear regression, while the linear and polynomial kernels achieved R² values of 0.921 and 0.914, respectively. Overall, KNN demonstrated the highest accuracy, making it the most effective model for predicting pH values.

Table 4.17 R^2 results when using different methods to predict pH values

Features	Methods	R^2
Softmax values	**Linear regression**	**0.925**
Softmax values	SVR (linear)	0.922
Softmax values	SVR (polynomial)	0.914
Softmax values	**SVR (radial basis function)**	**0.926**
Softmax values	**KNN (k=3)**	**0.972**
Softmax values	KNN (k=5)	0.941
Softmax values	KNN (k=7)	0.921

4.3 Predicting the Internal Properties of Bananas using RGB and L*a*b* Color Values Measured from One Point

This section further examined the relationships between the RGB and L*a*b* color values of bananas and their Brix and pH measurements. RGB and L*a*b* color values served as feature variables to predict Brix and pH values utilizing linear regression, SVR, and KNN models. The Brix and pH values were measured for 12, 11, 13, 11, 13, 10, and 10 bananas of class 0 to class 6, respectively, for the Brix and pH prediction.

4.3.1 Comparison of Different Methods for Predicting Brix Values Using RGB Color Features

Table 4.18 compares the R² squared values of different methods for predicting Brix values using RGB color features. Among these methods, KNN (k=3) had the highest R² value (0.943), indicating that its predictive performance was superior to other

มหาวิทยาลัยรังสิต Rangsit University

methods. Linear regression and SVR (linear kernel) also showed relatively good performance, with R^2 values of 0.853 and 0.778, respectively. In contrast, the prediction accuracy of SVR (polynomial kernel) and SVR (radial basis kernel) were lower, with R^2 values of 0.475 and 0.585, respectively.

Based on these results, subsequent analysis will focus on errors related to linear regression, SVR (linear kernel), and KNN (k=3), as well as their corresponding measurements and predictions of Brix values.

Table 4.18 R2 values of different methods for predicting Brix values using RGB color features

Features	Methods	R^2
RGB values	**Linear regression**	**0.853**
RGB values	**SVR (linear)**	**0.778**
RGB values	SVR (polynomial)	0.475
RGB values	SVR (radial basis function)	0.585
RGB values	**KNN (k=3)**	**0.943**
RGB values	KNN (k=5)	0.892
RGB values	KNN (k=7)	0.826

4.3.1.1 Use Linear Regression to Predict Brix Based on RGB Values

The equation to predict Brix values derived from the linear regression analysis was as follows:

$$\text{PredictedBrixvalue}=(R*0.422)+(G*-0.425)+(B*0.002)+6.542 \qquad (4\text{-}3)$$

Table 4.19 shows the errors in predicting Brix value from RGB color values using the linear regression method. The absolute error, standard deviation, relative error, and percentage error for each banana class were reported. The overall absolute error, relative error, and percentage error were 2.1130, 0.2412, and 24.121, respectively. The percentage errors were relatively high in class 0 and class 1.

มหาวิทยาลัยรังสิต Rangsit University

Table 4.19 Errors when using linear regression to predict Brix values from RGB color values

	class 0	class 1	class 2	class 3	class 4	class 5	class 6	All classes
Absolute error	1.6610	2.5439	3.1418	2.4058	1.2216	1.6570	2.1353	2.1130
Standard deviation	1.8442	2.2830	1.5834	1.3231	0.9690	1.4066	0.0836	1.6720
Relative error	0.4859	0.5225	0.2787	0.1431	0.0588	0.0736	0.0736	0.2412
Standard deviation	0.5330	0.4885	0.1768	0.0862	0.0452	0.0593	0.0836	0.3309
Percentage error	48.588	52.245	27.867	14.314	5.8755	7.3641	10.880	24.121
Standard deviation	53.304	48.851	17.684	8.6217	4.5204	5.9324	8.3595	33.093

Figure 4.15 shows the comparison between the measured Brix values (green dots) of banana samples and the Brix values predicted using a linear regression model (blue dots). The figure reveals significant fluctuations in the predicted values, highlighting the limitations of the linear regression model's prediction capabilities.

มหาวิทยาลัยรังสิต Rangsit University

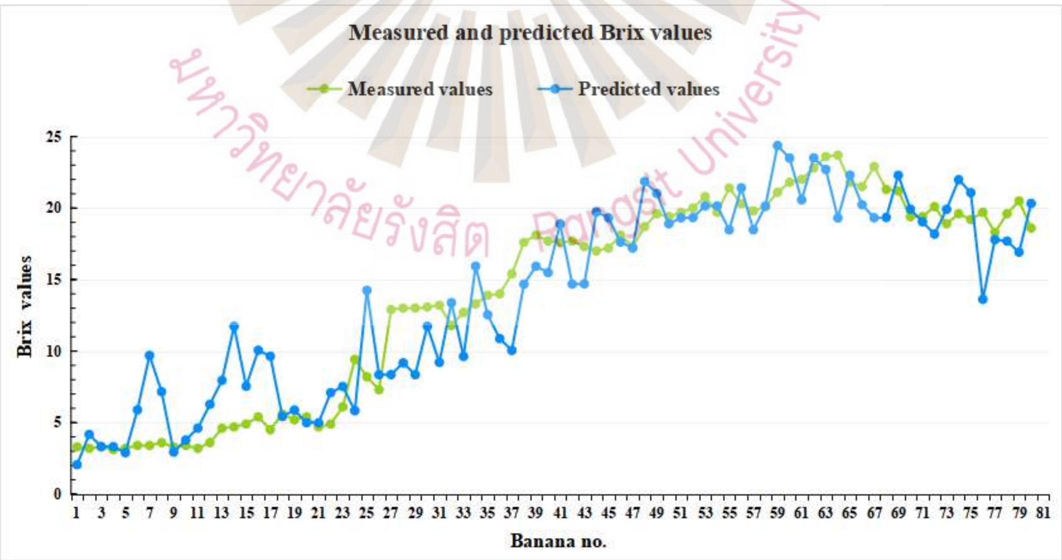

Figure 4.15 Graphs of measured and predicted Brix values when using linear regression

4.3.1.2 Use SVR (linear kernel) to Predict Brix Based on RGB Values

The errors of using SVR (linear kernel) to predict Brix values from RGB color values were displayed in Table 4.20. The overall absolute error, relative error, and percentage error were 2.5509, 0.3871, and 38.713, respectively. The high average percentage error indicated significant errors in the prediction. Its performance was inferior to that of alternative approaches such as KNN.

Table 4.20 Errors when using SVR (linear kernel) to predict Brix values from RGB color values

	class 0	class 1	class 2	class 3	class 4	class 5	class 6	All classes
Absolute error	4.2031	4.4611	2.3536	1.6375	0.7566	2.1883	2.5501	2.5509
Standard deviation	1.3982	2.5289	1.9818	1.0046	0.7665	1.2388	0.1136	2.0545
Relative error	1.2137	0.8876	0.2287	0.0945	0.0358	0.1001	0.1001	0.3871
Standard deviation	0.3598	0.5614	0.2541	0.0621	0.0353	0.0530	0.1136	0.5138
Percentage error	121.36	88.762	22.868	9.4521	3.5816	10.007	13.040	38.713
Standard deviation	35.984	56.135	25.412	6.2055	3.5323	5.3034	11.357	51.384

The predicted Brix values from the SVR (linear kernel) model were very different from the measured Brix values in a number of ranges, as shown in Figure 4.16. These ranges included the bananas numbered 1–22 and 74–77.

มหาวิทยาลัยรังสิต Rangsit University

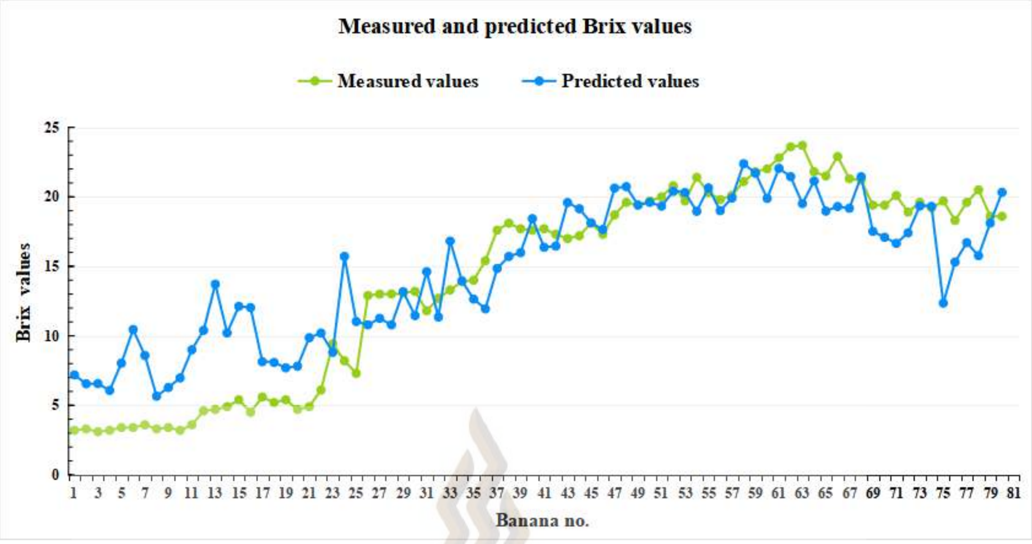

Figure 4.16 Graphs of measured and predicted Brix values when using SVR (linear kernel)

4.3.1.3 Use KNN (k=3) to Predict Brix Based on RGB Values

Table 4.21 shows the error of using the KNN (k=3) model to predict Brix values based on RGB color values. The overall absolute error was 1.1894, and the standard deviation was 1.1661, indicating that the model has a small prediction error. The KNN (k=3) model exhibited lower prediction errors in all categories, and its performance was superior to the linear regression and SVR methods.

มหาวิทยาลัยรังสิต Rangsit University

Table 4.21 Errors when using KNN (k=3) to predict Brix values from RGB color values

	class 0	class 1	class 2	class 3	class 4	class 5	class 6	All classes
Absolute error	0.4506	2.0133	1.4731	1.1236	0.9544	1.2959	1.1246	1.1894
Standard deviation	0.7006	1.5123	1.5051	0.4744	0.5942	1.2873	0.0727	1.1661
Relative error	0.1280	0.3707	0.1400	0.0644	0.0459	0.0579	0.0579	0.1229
Standard deviation	0.2002	0.3105	0.1709	0.0284	0.0280	0.0579	0.0727	0.1849
Percentage error	12.801	37.070	13.997	6.4431	4.5857	5.7919	5.8363	12.290
Standard deviation	20.016	31.045	17.088	2.8419	2.8044	5.7920	7.2668	18.486

Figure 4.17 shows the comparison between the predicted Brix value and the measured value of the KNN (k=3) model. The graphs revealed a relatively high degree of matching between the predicted and measured values.

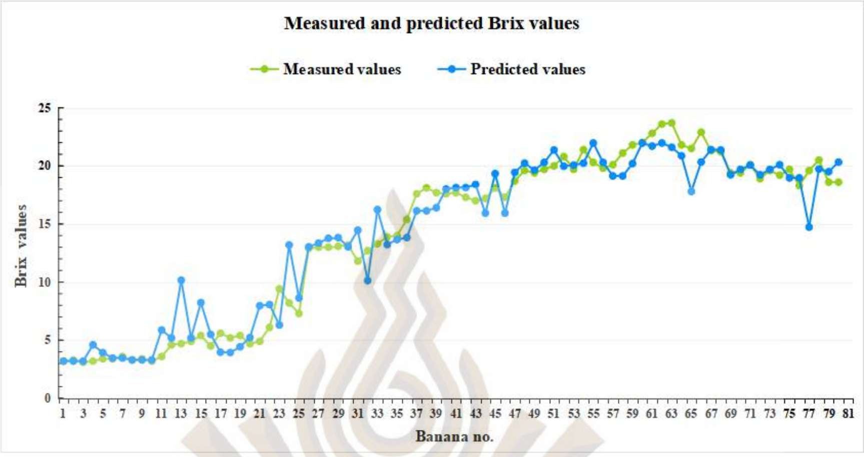

Figure 4.17 Graphs of measured and predicted Brix values when using KNN (k=3)

4.3.2 Comparison of Different Methods for Predicting pH Values Using RGB Color Values Measured from One Point

Table 4.22 compares the R^2 values of different methods for predicting pH values using RGB color values measured from one point. Among linear regression, SVR, and KNN, KNN (k=3) achieved the highest R^2 value (0.896), demonstrating its superior pH predictive performance compared to other methods. SVR (radial basis kernel) and KNN (k=5) also showed relatively high performance, with R^2 values of 0.829 and 0.823, respectively. Linear regression and SVR (linear kernel) had moderate performance, with R^2 values of 0.761 and 0.750, respectively. In contrast, the prediction accuracies of SVR (polynomial kernel) and KNN (k=7) were lower, with R^2 values of 0.571 and 0.706, respectively.

Based on these results, subsequent analysis will focus on the prediction errors related to linear regression, KNN (k=3), and SVR (radial basis function kernel).

มหาวิทยาลัยรังสิต Rangsit University

Table 4.22 R2 Values of Different Methods for Predicting pH Values Using RGB Color Values from One Point

Features	Methods	R^2
RGB values	**Linear regression**	**0.761**
RGB values	SVR (linear)	0.750
RGB values	SVR (polynomial)	0.571
RGB values	**SVR (radial basis function)**	**0.829**
RGB values	**KNN (k=3)**	**0.896**
RGB values	KNN (k=5)	0.823
RGB values	KNN (k=7)	0.706

4.3.2.1 Use Linear Regression to Predict pH Based on RGB Values Measured from One Point

The equation to predict a pH value derived from the linear regression was as follows:

$$\text{pH value}=(R*0.021)+(G*-0.029)+(B*0.004)+5.166 \qquad (4\text{-}4)$$

Table 4.23 shows the errors when using linear regression to predict pH values from RGB color features. The overall absolute error across all classes was 0.158, with the lowest absolute error for class 1 (0.0954) and the highest for class 0 (0.2705). Overall, the prediction accuracy of linear regression was moderate.

มหาวิทยาลัยรังสิต Rangsit University

Table 4.23 Errors when using linear regression to predict pH values from RGB color values measured from one point

	class 0	class 1	class 2	class 3	class 4	class 5	class 6	All classes
Absolute error	0.2705	0.0954	0.1344	0.1568	0.0977	0.1444	0.2127	0.1580
Standard deviation	0.1537	0.0760	0.0823	0.1577	0.0708	0.0577	0.0290	0.1282
Relative error	0.0677	0.0221	0.0297	0.0345	0.0206	0.0292	0.0292	0.0348

Table 4.23 Errors when using linear regression to predict pH values from RGB color values measured from one point (continued)

	class 0	class 1	class 2	class 3	class 4	class 5	class 6	All classes
Standard deviation	0.0395	0.0178	0.0181	0.0351	0.0151	0.0121	0.0290	0.0294
Percentage error	6.7682	2.2057	2.9730	3.4511	2.0625	2.9164	3.9333	3.4802
Standard deviation	3.9517	1.7828	1.8050	3.5064	1.5066	1.2066	2.8966	2.9405

The graphs of measured and predicted pH values based on RGB color values when employing linear regression were displayed in Figure 4.18. The R^2 value was 0.761, indicating that the predicted pH values were rather different from those that were measured.

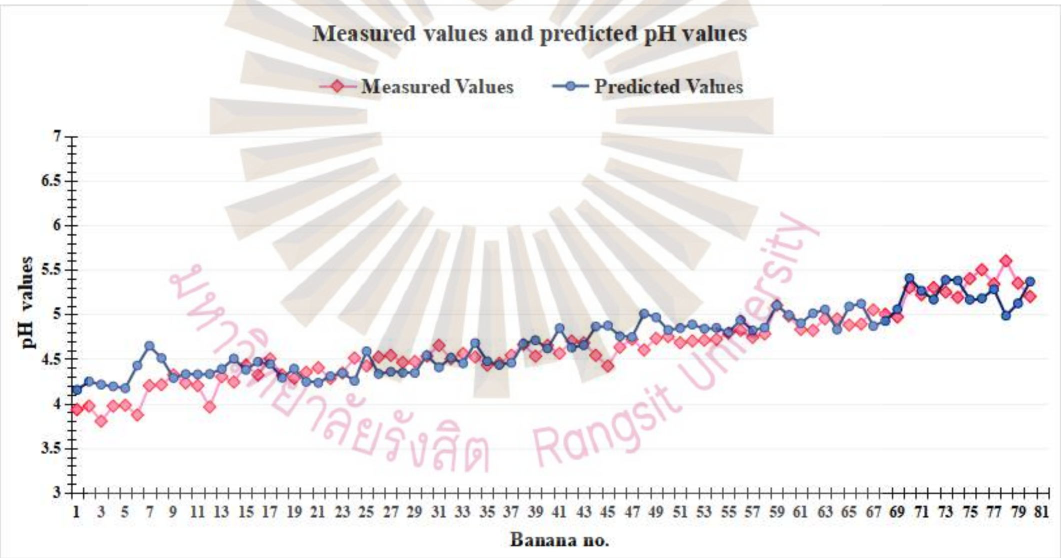

มหาวิทยาลัยรังสิต Rangsit University

Figure 4.18 Graphs of measured and predicted pH values from RGB color values when using linear regression

4.3.2.2 Use SVR (Radial Basis Kernel) to Predict pH Based on RGB Values Measured from One Point

Table 4.24 summarizes the errors when using SVR with an radial basis kernel to predict pH values. The overall absolute error was 0.1237, which was lower compared to that of linear regression. Class 2 had the lowest absolute error (0.0850) among all classes, while class 0 had a slightly higher error (0.1711). The results suggested that the SVR (radial basis kernel) provided a better prediction than the linear regression.

Table 4.24 Errors when using SVR (radial basis kernel) to predict pH values from RGB color values

	class 0	class 1	class 2	class 3	class 4	class 5	class 6	All classes
Absolute error	0.1711	0.1131	0.0850	0.1208	0.0738	0.1349	0.1832	0.1237
Standard deviation	0.1244	0.0754	0.0574	0.0941	0.0512	0.0992	0.0294	0.1032
Relative error	0.0426	0.0260	0.0188	0.0265	0.0152	0.0270	0.0270	0.0268
Standard deviation	0.0316	0.0176	0.0125	0.0210	0.0101	0.0198	0.0294	0.0223
Percentage error	4.2583	2.6035	1.8837	2.6491	1.5225	2.6989	3.3854	2.6840
Standard deviation	3.1600	1.7566	1.2543	2.1035	1.0109	1.9773	2.9429	2.2292

Figure 4.19 shows measured and predicted pH values based on RGB color values when using the SVR (radial basis kernel). The R^2 value was 0.829, better than the linear regression performance.

มหาวิทยาลัยรังสิต Rangsit University

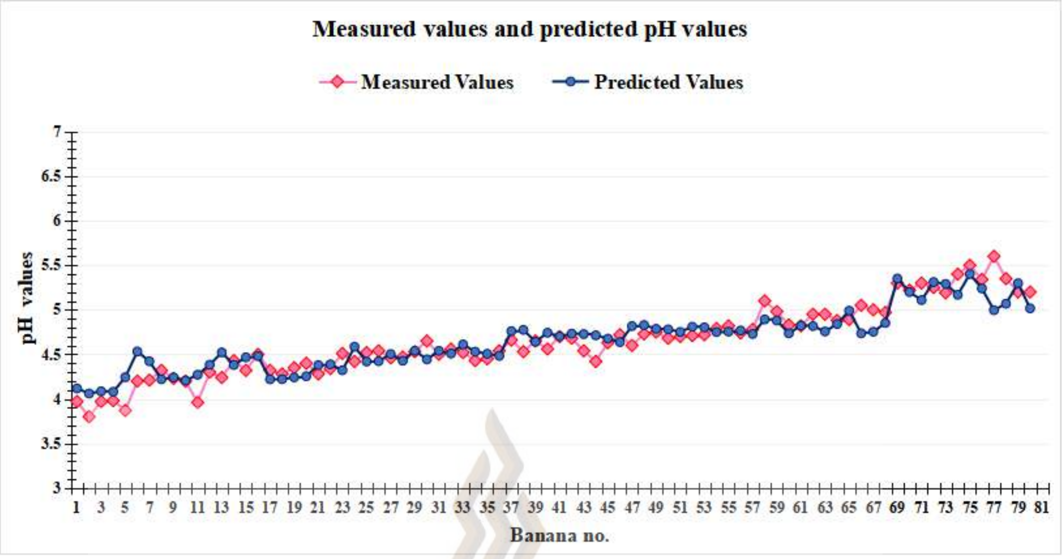

Figure 4.19 Graphs of measured and predicted pH values when using SVR (radial basis kernel)

4.3.2.3 Use KNN (k=3) to Predict pH Based on RGB Values Measured from One Point

Table 4.25 presents the errors when using KNN (k=3) to predict pH values. The overall absolute error was the lowest among the three methods at 0.0885, with a standard deviation of 0.0895. This method significantly outperformed both linear regression and SVR (radial basis kernel). This demonstrated that KNN (k=3) was the most accurate method for predicting pH values based on RGB color values measured from one point.

Table 4.25 Errors when using KNN (k=3) to predict pH values from RGB color values measured from one point

	class 0	class 1	class 2	class 3	class 4	class 5	class 6	All classes
Absolute error	0.0964	0.1424	0.0489	0.0715	0.0733	0.0978	0.1008	0.0885
Standard deviation	0.1020	0.0902	0.0371	0.0502	0.0973	0.0715	0.0249	0.0895
Relative error	0.0243	0.0329	0.0108	0.0156	0.0150	0.0196	0.0196	0.0193

มหาวิทยาลัยรังสิต Rangsit University

Table 4.25 Errors when using KNN (k=3) to predict pH values from RGB color values measured from one point (continued)

	class 0	class 1	class 2	class 3	class 4	class 5	class 6	All classes
Standard deviation	0.0261	0.0214	0.0082	0.0109	0.0194	0.0143	0.0249	0.0193
Percentage error	2.4291	3.2895	1.0827	1.5561	1.5018	1.9589	1.8449	1.9270
Standard deviation	2.6076	2.1371	0.8174	1.0893	1.9385	1.4269	2.4886	1.9337

Figure 4.20 shows measured and predicted pH values based on RGB color values when using KNN (k=3). The R^2 value was 0.896, better than linear regression and SVR performance. Overall, the predicted values and measured values were very similar, although there were some small errors.

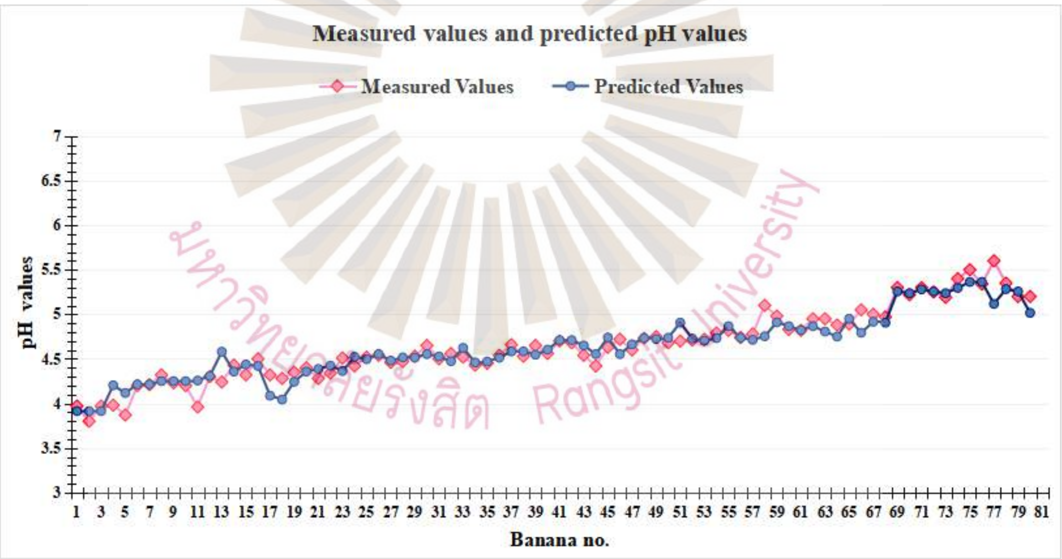

Figure 4.20 Graphs of measured and predicted pH values when using KNN (k=3)

มหาวิทยาลัยรังสิต Rangsit University

4.3.3 Comparison of Different Methods for Predicting Brix Values Using L*a*b* Color Values Measured from One Point

Table 4.26 compares the R^2 values of different methods for predicting Brix values using L*a*b* color features. Among these methods, KNN (k=3) achieved the highest R^2 value (0.941), demonstrating its superior predictive performance compared to other methods. KNN (k=5) and KNN (k=7) also showed relatively good performance, with R^2 values of 0.864 and 0.844, respectively. SVR (radial basis function) performed moderately well, achieving an R^2 value of 0.775. In contrast, the performance of linear regression and SVR (linear kernel) was lower, with R^2 values of 0.668 and 0.641, respectively. SVR (polynomial kernel) showed the lowest prediction performance, with an R^2 value of 0.461.

Based on these results, subsequent analysis will focus on errors related to linear regression, KNN (k=3), and SVR (radial basis kernel).

Table.4.26 R2 values of different methods for predicting Brix values using L*a*b* color values measured from one point

Features	Methods	R^2
L*a*b* values	**Linear regression**	**0.668**
L*a*b* values	SVR (linear)	0.641
L*a*b* values	SVR (polynomial)	0.461
L*a*b* values	SVR (radial basis function)	0.775
L*a*b* values	KNN (k=3)	0.941
L*a*b* values	KNN (k=5)	0.864
L*a*b* values	KNN (k=7)	0.844

4.3.3.1 Use Linear Regression to Predict Brix Based on L*a*b* Values

The equation to predict a Brix value derived from the application of linear regression was as follows:

มหาวิทยาลัยรังสิต Rangsit University

$$\text{Brix value}=(L^{*}0.112)+(a^{*}0.84)+(b^{*}0.16)+2.038 \quad (4\text{-}5)$$

Table 4.27 shows the error of linear regression in predicting the Brix values of different banana classes. The average absolute error for all categories was 3.3178, with a standard deviation of 3.0969, indicating relatively high variability. The very high relative error of 0.3676 and the percentage errors of 36.764 indicated the poor performance of the linear regression in predicting Brix values.

Table 4.27 Errors when using linear regression to predict Brix values from L*a*b* color values measured from one point

	class 0	class 1	class 2	class 3	class 4	class 5	class 6	All classes
Absolute error	3.8610	1.5588	2.7171	3.3790	3.2013	4.2360	4.5675	3.3178
Standard deviation	6.5831	1.5934	1.5155	2.1011	1.4735	1.9026	0.1246	3.0969
Relative error	1.2004	0.3181	0.2344	0.2003	0.1569	0.1902	0.1902	0.3676
Standard deviation	2.0683	0.3408	0.1261	0.1323	0.0693	0.0809	0.1246	0.8629
Percentage error	120.03	31.810	23.444	20.032	15.690	19.017	23.391	36.764
Standard deviation	206.83	34.080	12.607	13.228	6.9271	8.0946	12.456	86.286

Figure 4.21 shows the comparison between the predicted Brix values and the measured values of the linear regression model. The graphs showed a relatively low degree of matching between predicted and measured values, with an R^2 value of 0.668.

มหาวิทยาลัยรังสิต Rangsit University

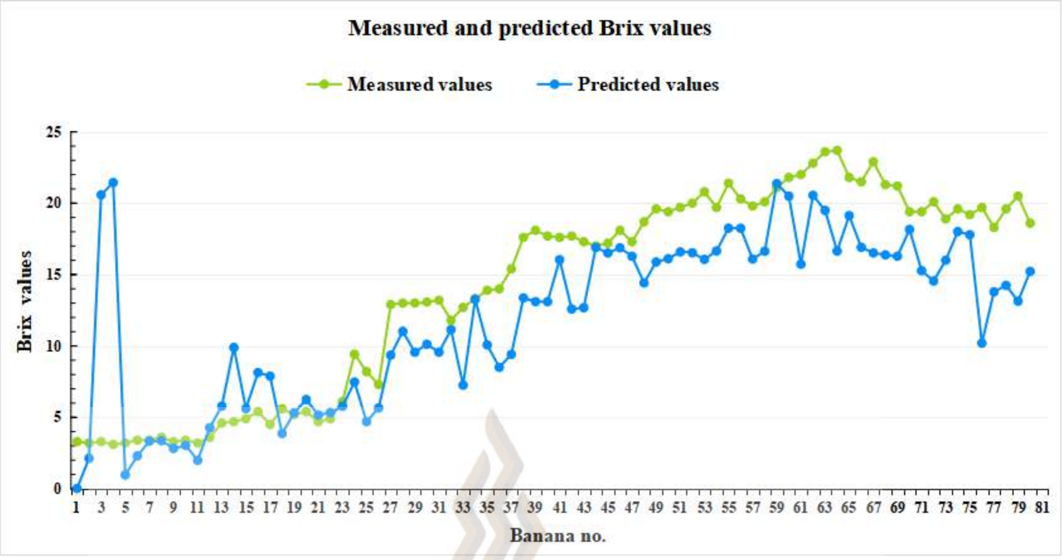

Figure 4.21 Graphs of measured and predicted Brix values when using linear regression

4.3.3.2 Use SVR (radial basis kernel) to Predict Brix Based on L*a*b* Values

Table 4.28 shows that compared to linear regression, SVR with an RBF kernel exhibited a lower overall error but still had a high absolute error in certain classes, like class 0 (4.5763) and class 1 (2.8650).

Table 4.28 Errors when using SVR(rbf kernel) to predict Brix values from L*a*b* color values measured from one point

	class 0	class 1	class 2	class 3	class 4	class 5	class 6	All classes
Absolute error	4.5763	2.8650	1.7674	1.4482	0.7751	1.8000	0.9705	2.0306
Standard deviation	5.0583	2.4167	1.4167	1.3364	0.8492	1.2283	0.0460	2.6004
Relative error	1.3858	0.5763	0.1413	0.0852	0.0359	0.0802	0.0802	0.3432
Standard deviation	1.6049	0.5221	0.1098	0.0814	0.0379	0.0516	0.0460	0.7878
Percentage error	138.57	57.630	14.130	8.5157	3.5874	8.0212	4.9617	34.319
Standard deviation	160.48	52.213	10.982	8.1396	3.7896	5.1634	4.6015	78.784

มหาวิทยาลัยรังสิต Rangsit University

Figure 4.22 shows the comparison between the predicted Brix value and the measured value of the SVR (radial basis kernel) model. The degree of matching between the predicted and measured values was higher than in linear regression, with an R-squared of 0.775 compared to an R^2 of 0.668. The predicted and measured values exhibit significant errors prior to reaching the bananas numbered 45.

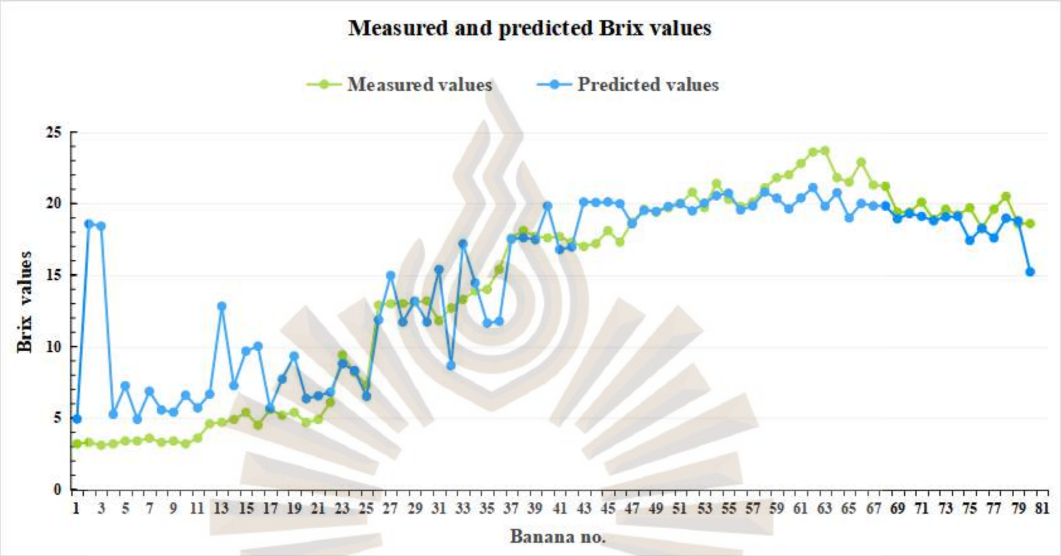

Figure 4.22 Graphs of measured and predicted Brix values when using SVR (radial basis kernel)

มหาวิทยาลัยรังสิต Rangsit University

4.3.3.3 Use KNN (k=3) to Predict Brix Based on L*a*b* Values

Table 4.29 shows the error in predicting Brix values from L*a*b* values using KNN (k=3). KNN (k=3) achieved the lowest error and best performance among all methods. The average absolute error for all categories was 1.2296, with a standard deviation of 1.1671, reflecting low error variability. The relative error and percentage error were 0.1416 and 14.163, respectively.

Table 4.29 Errors when using KNN (k=3) to predict Brix values from L*a*b* color values measured from one point

	class 0	class 1	class 2	class 3	class 4	class 5	class 6	All classes
Absolute error	1.2806	1.2909	1.6117	1.2569	0.7979	1.8222	0.6346	1.2296
Standard deviation	1.9671	0.9795	1.0726	0.6358	0.7063	1.5184	0.0287	1.1671
Relative error	0.3845	0.2306	0.1377	0.0726	0.0380	0.0843	0.0843	0.1416
Standard deviation	0.6188	0.1608	0.0892	0.0376	0.0326	0.0740	0.0287	0.2705
Percentage error	38.445	23.060	13.766	7.2550	3.8031	8.4304	3.3244	14.163
Standard deviation	61.880	16.077	8.9191	3.7604	3.2587	7.3979	2.8730	27.054

Figure 4.23 shows the comparison between the predicted Brix values and the measured values when using KNN (k=3) and L*a*b* values. The graphs showed that the degree of matching between predicted and measured values was higher than that of linear regression and SVR, but there were significant deviations in data numbered 2, 3, and 68.

มหาวิทยาลัยรังสิต Rangsit University

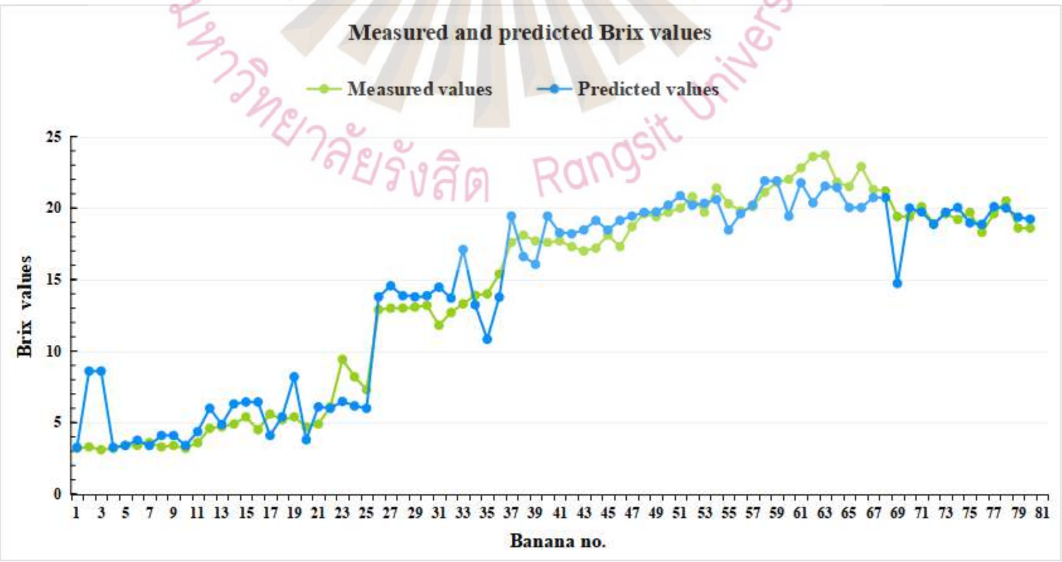

Figure 4.23 Graphs of measured and predicted Brix values when using KNN (k=3)

4.3.4 Comparison of Different Methods for Predicting pH Values Using L*a*b* Color Values

Table 4.30 compares the R^2 values of different methods of predicting pH values using L*a*b* color features. Among these methods, KNN (k=3) achieved the highest R^2 value (0.844), demonstrating its superior predictive performance compared to other methods. In contrast, linear regression, SVR (linear kernel), and SVR (polynomial kernel) showed lower performance, with R^2 values of 0.529, 0.495, and 0.482, respectively.

Based on these results, subsequent analysis will focus on errors related to KNN (k=3), SVR (radial basis kernel), and linear regression, as they provided a range of performance levels suitable for understanding predictive performance.

Table 4.30 R2 values of different methods for predicting pH Values Using L*a*b* color values measured from one point

Features	Methods	R^2
L*a*b* values	**Linear regression**	**0.529**
L*a*b* values	SVR (linear)	0.495
L*a*b* values	SVR (polynomial)	0.482
L*a*b* values	**SVR (radial basis function)**	**0.819**
L*a*b* values	**KNN (k=3)**	**0.844**
L*a*b* values	KNN (k=5)	0.754
L*a*b* values	KNN (k=7)	0.667

4.3.4.1 Use Linear Regression to Predict pH Based on L*a*b* Values

The equation to predict pH values derived from the linear regression was as follows:

$$\text{pH value} = (R^*-0.007)+(G^*0.041)+(B^*-0.001)+5.154 \qquad (4\text{-}6)$$

Table 4.31 shows the errors in predicting pH values based on L*a*b* color values using linear regression. The average absolute error of all banana classes was 0.1564, with the lowest error found in class 4 (0.0565) and the highest error found in class 6 (0.2520). This indicated that it was difficult to accurately predict using the linear regression.

Table 4.31 Errors when using linear regression to predict pH values from L*a*b* color values measured from one point

	class 0	class 1	class 2	class 3	class 4	class 5	class 6	All classes
Absolute error	0.3913	0.0671	0.0855	0.1090	0.0565	0.1529	0.2520	0.1564
Standard deviation	0.4455	0.0656	0.0639	0.0808	0.0462	0.1010	0.0389	0.2234
Relative error	0.0996	0.0155	0.0190	0.0239	0.0116	0.0304	0.0304	0.0349
Standard deviation	0.1158	0.0154	0.0142	0.0183	0.0092	0.0199	0.0389	0.0553
Percentage error	9.9593	1.5525	1.8954	2.3905	1.1643	3.0419	4.6452	3.4922
Standard deviation	11.5783	1.5447	1.4227	1.8256	0.9158	1.9855	3.8927	5.5278

Figure 4.24 illustrates the measured and predicted pH values, derived from L*a*b* color values, through the use of linear regression. The R^2 value was 0.529. The graphs clearly showed significant errors between the predicted and measured values for the bananas numbered 1-6 and 74-79.

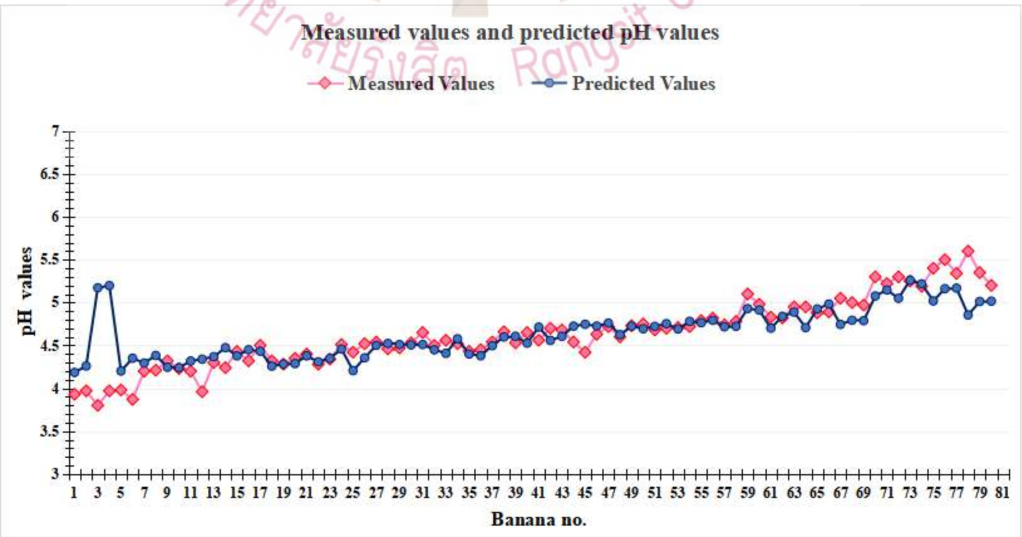

Figure 4.24 Graphs of measured and predicted pH values from L*a*b* color values when using linear regression

มหาวิทยาลัยรังสิต Rangsit University

4.3.4.2 Use SVR (radial basis kernel) to Predict pH Based on L*a*b* Values

Table 4.32 shows the error in predicting pH values based on L*a*b* color values using SVR (radial basis kernel). Compared with linear regression, SVR with an RBF kernel achieved better prediction accuracy. The average absolute error for all banana classes was 0.1071, with the lowest error found in class 4 (0.0541) and the highest error found in class 0 (0.1942). The standard deviation of absolute errors was 0.1265, indicating that the prediction was more consistent compared to the linear regression.

Table 4.32 Errors when using SVR (radial basis kernel) to predict pH values from L*a*b* color values measured from one point

	class 0	class 1	class 2	class 3	class 4	class 5	class 6	All classes
Absolute error	0.1942	0.0796	0.0715	0.1054	0.0541	0.1503	0.1080	0.1071
Standard deviation	0.2552	0.0529	0.0596	0.0902	0.0511	0.1203	0.0157	0.1265
Relative error	0.0495	0.0183	0.0158	0.0231	0.0113	0.0296	0.0296	0.0237
Standard deviation	0.0666	0.0124	0.0131	0.0204	0.0106	0.0230	0.0157	0.0311
Percentage error	4.9454	1.8304	1.5837	2.3102	1.1272	2.9642	2.0033	2.3735
Standard deviation	6.6618	1.2427	1.3150	2.0397	1.0633	2.2999	1.5718	3.1129

Figure 4.25 illustrates the measured and predicted pH values, derived from L*a*b* color values, through the use of the SVR (radial basis kernel). The R^2 value was 0.819, which was higher than linear regression.

มหาวิทยาลัยรังสิต Rangsit University

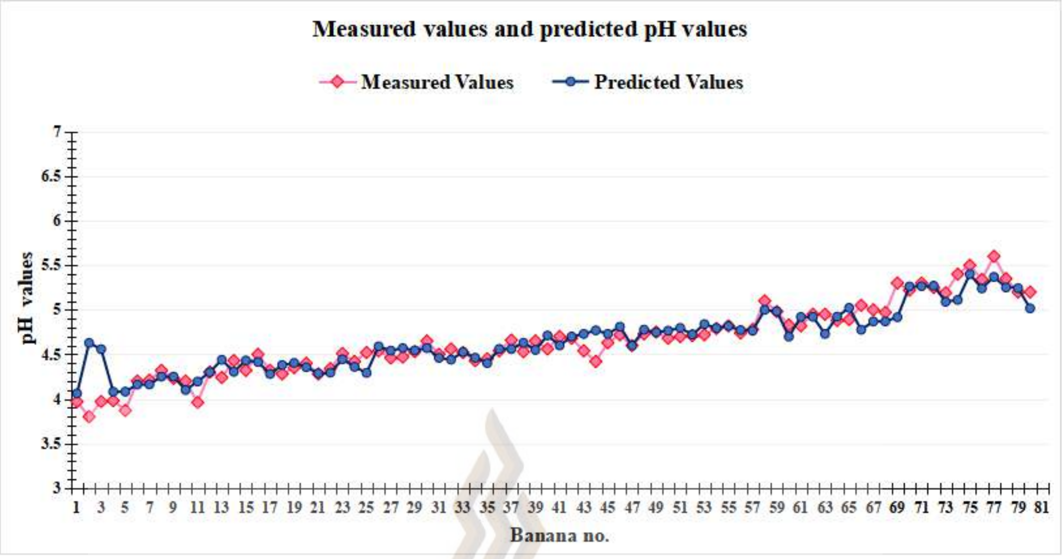

Figure 4.25 Graphs of measured and predicted pH values when using SVR (radial basis kernel)

4.3.4.3 Use KNN (k=3) to Predict pH Based on L*a*b* Values

Table 4.33 shows the error in predicting pH values based on L*a*b* color values using KNN (k=3). The KNN (k=3) exhibited the best overall performance among the three methods. The average absolute error for all classes was 0.1011, with class 2 having the lowest error (0.0511) and class 5 having the highest error (0.2159). The standard deviation of absolute error was 0.1156, indicating that the prediction performance was quite consistent among all banana classes.

มหาวิทยาลัยรังสิต Rangsit University

Table 4.33 Errors when using KNN (k=3) to predict pH values from L*a*b* color values measured from one point

	class 0	class 1	class 2	class 3	class 4	class 5	class 6	All classes
Absolute error	0.1664	0.0691	0.0511	0.0641	0.0736	0.2159	0.0988	0.1011
Standard deviation	0.1647	0.0448	0.0423	0.0847	0.0573	0.1869	0.0162	0.1156
Relative error	0.0420	0.0158	0.0113	0.0142	0.0153	0.0425	0.0425	0.0220

Table 4.33 Errors when using KNN (k=3) to predict pH values from L*a*b* color values measured from one point (continued)

	class 0	class 1	class 2	class 3	class 4	class 5	class 6	All classes
Standard deviation	0.0432	0.0103	0.0093	0.0191	0.0118	0.0354	0.0162	0.0259
Percentage error	4.2024	1.5849	1.1336	1.4157	1.5261	4.2528	1.8219	2.2025
Standard deviation	4.3193	1.0255	0.9345	1.9113	1.1799	3.5422	1.6234	2.5881

Figure 4.26 shows the measured and predicted pH values obtained from L*a*b* color values using KNN (k=3). The R^2 value was 0.844, which was higher than SVR and linear regression but lower than using RGB to predict pH value. The graphs showed a high degree of matching between the predicted values and the measured values, with only the banana numbers 2, 3, and 78 showing significant errors.

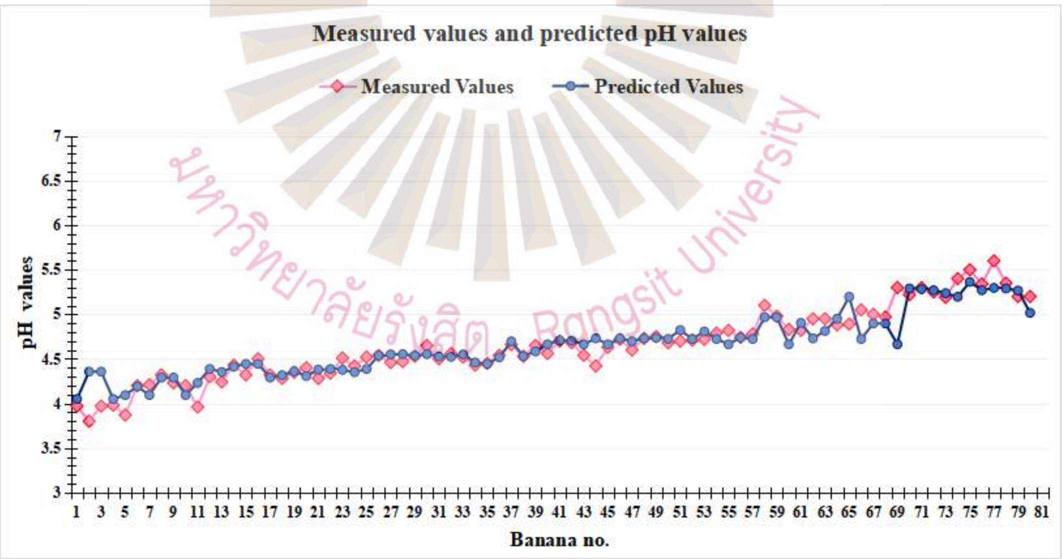

Figure 4.26 Graphs of measured and predicted pH values when using KNN (k=3)

มหาวิทยาลัยรังสิต Rangsit University

4.4 Predicting the Internal Properties of Bananas using RGB and L*a*b* Color Values Measured from One Points

This section further examined the relationships between the RGB and L*a*b* color values of bananas and their Brix and pH measurements. RGB and L*a*b* color values served as feature variables to predict Brix and pH values utilizing linear regression, SVR, and KNN. The Brix and pH values were measured for 12, 11, 13, 11, 13, 10, and 10 bananas of class 0 to class 6, respectively, for the Brix and pH prediction.

4.4.1 Comparison of Different Methods for Predicting Brix Values Using RGB and L*a*b* Color Features

Table 4.34 compares the R² values of different methods for predicting Brix values using RGB and L*a*b* color features. Among the evaluated methods, KNN (k=3) demonstrated the highest predictive performance, achieving an R² value of 0.947, indicating its effectiveness in predicting Brix values. Linear regression and KNN (k=5) showed R² values of 0.873 and 0.869, respectively. In contrast, the SVR models exhibited varied performance. While SVR with a radial basis function kernel achieved a moderate R² value of 0.739, SVR with a linear kernel performed similarly at 0.739. SVR with a polynomial kernel, however, had the lowest predictive performance, with an R² value of 0.571.

Based on these results, subsequent analysis will focus on the prediction errors related to KNN (k=3), linear regression, and SVR (radial basis function kernel).

Table 4.34 R2 values of different methods for predicting brix values using RGB and L*a*b* color features

Features	Methods	R^2
RGB and L*a*b* values	**Linear regression**	**0.873**
RGB and L*a*b* values	SVR (linear)	0.739
RGB and L*a*b* values	SVR (polynomial)	0.571
RGB,L*a*b* values	**SVR (radial basis function)**	**0.739**

มหาวิทยาลัยรังสิต Rangsit University

Table 4.34 R2 values of different methods for predicting brix values using RGB and L*a*b* color features (continued)

Features	Methods	R2
RGB, L*a*b* values	**KNN (k=3)**	**0.947**
RGB,L*a*b* values	**KNN (k=5)**	**0.869**
RGB,L*a*b* values	**KNN (k=7)**	**0.847**

4.4.1.1 Use Linear Regression to Predict Brix Values from RGB and L*a*b* Color Values

The following equation is the result of applying linear regression to predict Brix values:

$$\text{PredictedBrixvalue}=(R*0.362)+(G*-0.363)+(B*0.125)+(L*0.336)+(a*0.155)+(b*0.285)+7.772 \quad (4\text{-}7)$$

The Brix prediction using RGB and L*a*b* color values yielded an R^2 of 0.873. Table 4.35 displays the prediction errors of the linear regression that predicts Brix values based on RGB and L*a*b* color values. The absolute error, relative error, percentage error, and their corresponding standard deviations were calculated from Class 0 to Class 6. The absolute errors of the classes ranged from 1.2062 to 2.5345, and the overall average absolute error of all classes was 2.0588, showing a certain gap between the predicted and actual values.

Table 4.35 Errors when using linear regression to predict Brix values from RGB and L*a*b* color values

	class 0	class 1	class 2	class 3	class 4	class 5	class 6	All classes
Absolute error	1.8553	2.4430	2.4803	2.5345	1.2062	1.7287	2.1612	2.0588
Standard deviation	1.0916	1.9878	1.3091	1.2969	0.9829	1.5366	0.0800	1.4351
Relative error	0.5564	0.5001	0.2250	0.1503	0.0586	0.0767	0.0767	0.2423

Table 4.35 Errors when using linear regression to predict Brix values from RGB and L*a*b* color values (continued)

	class 0	class 1	class 2	class 3	class 4	class 5	class 6	All classes
Standard deviation	0.3339	0.4282	0.1531	0.0817	0.0461	0.0651	0.0800	0.2847
Percentage error	55.6365	50.0060	22.5026	15.0276	5.8625	7.6651	11.0390	24.2335
Standard deviation	33.3913	42.8183	15.3111	8.1740	4.6074	6.5089	7.9959	28.4683

Figure 4.27 illustrates the outcomes of applying linear regression to predict values based on RGB and L*a*b* color values. The obtained R^2 value of 0.873 indicated a certain relationship between measured and predicted values. Linear regression can reflect the overall trend in predicting Brix values, but its accuracy is limited, and some predicted values deviate significantly from measured values.

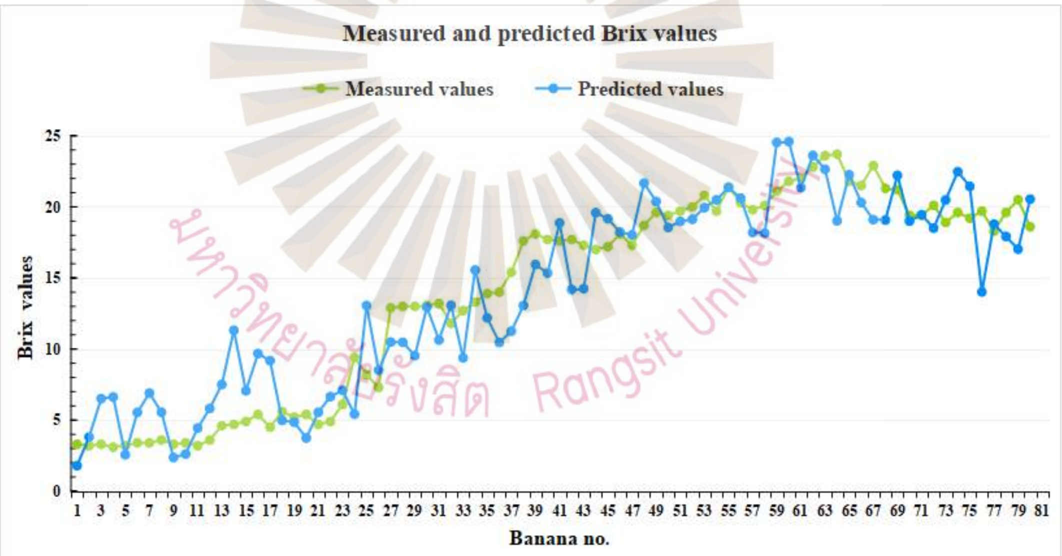

Figure 4.27 Graphs of measured and predicted Brix values from RGB and L*a*b* color values when using linear regression

มหาวิทยาลัยรังสิต Rangsit University

4.4.1.2 Use SVR (radial basis function) to Predict Brix Values from RGB and L*a*b* Color Values

Table 4.36 shows that SVR with an RBF kernel achieved moderate overall error but exhibited high absolute error in certain classes, such as Class 0 (5.4431) and Class 1 (3.7961)

Table 4.36 Brix prediction errors when using SVR (radial basis kernel)

	class 0	class 1	class 2	class 3	class 4	class 5	class 6	All classes
Absolute error	5.4431	3.7961	2.1510	1.3806	0.8562	2.1798	1.2062	2.4206
Standard deviation	4.1375	2.7370	1.5682	1.1798	0.8891	1.2561	0.0596	2.5995
Relative error	1.6270	0.7647	0.1974	0.0810	0.0397	0.0981	0.0981	0.4171
Standard deviation	1.3297	0.6002	0.1697	0.0723	0.0398	0.0538	0.0596	0.7834
Percentage error	162.704	76.4659	19.7353	8.0994	3.9657	9.8072	6.1593	41.7138
Standard deviation	132.969	60.0169	16.9729	7.2291	3.9786	5.3808	5.9570	78.3378

Figure 4.28 shows the effectiveness of using the SVR (radial basis kernel) model to predict Brix values. The R^2 value was 0.739. When the Brix values were low, the deviation between the predicted value and the measured value was very high. The predictive performance of this model was relatively poor in a low Brix value region.

มหาวิทยาลัยรังสิต Rangsit University

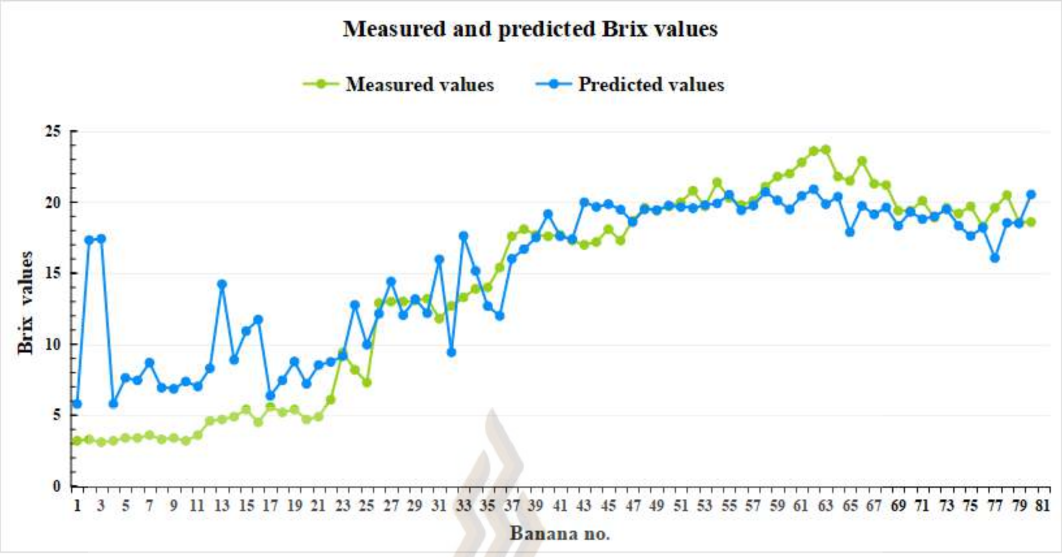

Figure 4.28 Graphs of measured and predicted Brix values when using SVR (radial basis kernel)

4.4.1.3 Use KNN (k=3) to Predict Brix Values from RGB and L*a*b* Color Values

Table 4.37 displays the errors when using the KNN (k=3) for Brix prediction. The average absolute error for all classes was 1.0944, and the percentage error was 12.810. The standard deviation of class 6 was extremely low compared to those of other classes. Overall, the KNN (k=3) exhibite smaller errors and higher stability in predicting Brix values, with lower errors and better prediction performance than other methods.

มหาวิทยาลัยรังสิต Rangsit University

Table 4.37 Errors when using KNN (k=3) to predict Brix values from RGB color values

	class 0	class 1	class 2	class 3	class 4	class 5	class 6	All classes
Absolute error	0.8511	0.9739	1.2839	1.2413	0.7362	1.4185	0.6746	1.0944
Standard deviation	1.1191	1.0486	1.2300	0.6216	0.9195	1.3087	0.0284	1.1779
Relative error	0.2406	0.1678	0.1104	0.0714	0.0346	0.0625	0.0625	0.1281
Standard deviation	0.3193	0.1815	0.0984	0.0365	0.0426	0.0547	0.0284	0.2757
Percentage error	24.061	16.780	11.035	7.1358	3.4584	6.2516	3.5460	12.810

Table 4.37 Errors when using KNN (k=3) to predict Brix values from RGB color values (continued)

	class 0	class 1	class 2	class 3	class 4	class 5	class 6	All classes
Standard deviation	31.927	18.146	9.8393	3.6470	4.2593	5.4743	2.8398	27.573

Figure 4.29 shows the results of employing the KNN (k=3) to forecast the Brix value based on RGB and L*a*b* values. The figure illustrates that the model closely adheres to the trend of the measured values. This indicated that the KNN could provide high accuracy in predicting the Brix values. The attained R^2 value was 0.947, indicating robust fitting capability.

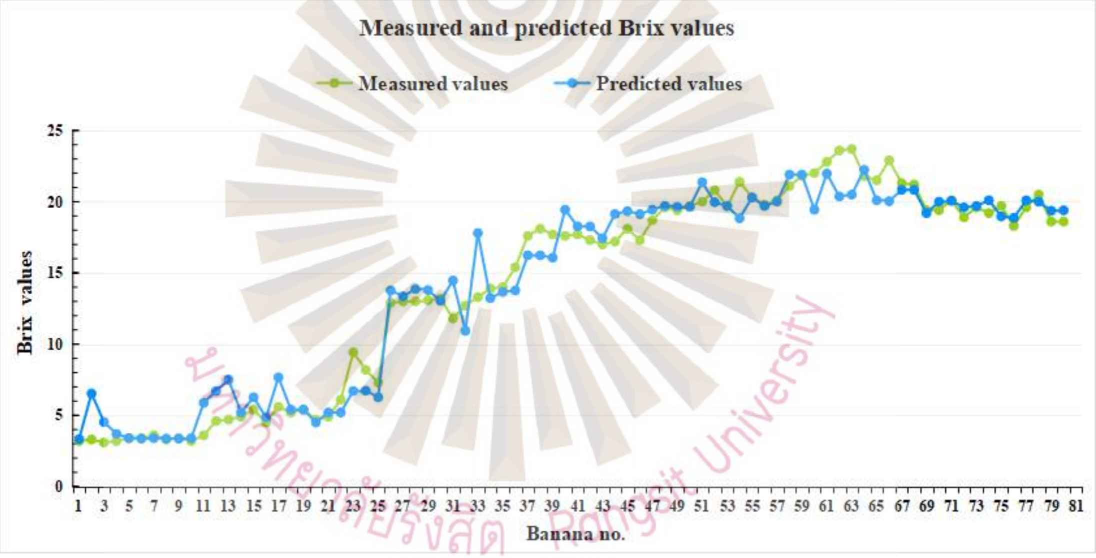

Figure 4.29 Graphs of measured and predicted Brix values when using KNN (k=3)

4.4.2 Comparison of Different Methods for Predicting pH Values Using RGB and L*a*b* Color Features

Table 4.38 compares the R^2 values of various methods for predicting pH values using RGB and L*a*b* color features. Among the methods evaluated, SVR with a radial basis function kernel achieved the highest R^2 value of 0.873, demonstrating its superior performance in pH prediction. KNN (k=3) also performed well, with an R^2 value of 0.860. Linear regression and SVR with linear and polynomial kernels showed R^2 values

มหาวิทยาลัยรังสิต Rangsit University

of 0.776, 0.743, and 0.729, respectively. However, KNN with higher k values (k = 5 and k = 7) performed less effectively, with R² values of 0.608 and 0.658, respectively.

Based on these results, further analysis will focus on the prediction errors associated with SVR (radial basis function kernel), KNN (k=3), and linear regression to better understand their predictive capabilities for pH values.

Table 4.38 R^2 values of different methods for predicting pH values using RGB and L*a*b* color features

Features	Methods	R^2
RGB,L*a*b* values	**Linear regression**	**0.776**
RGB,L*a*b* values	**SVR (linear)**	**0.743**
RGB,L*a*b* values	**SVR (polynomial)**	**0.729**
RGB,L*a*b* values	**SVR (radial basis function)**	**0.873**
RGB,L*a*b* values	**KNN (k=3)**	**0.860**
RGB,L*a*b* values	**KNN (k=5)**	**0.608**
RGB,L*a*b* values	**KNN (k=7)**	**0.658**

4.4.2.1 Use Linear Regression to Predict pH Values from RGB and L*a*b* Color Values

The equation derived from the application of linear regression to predict Brix values is as follows:

$$\text{pH value}=(R*0.21)+(G*-0.27)+(B*0.009)+(L*-0.22)+(a*-.001)+(b*0.009)+5.377 \quad (4\text{-}8)$$

Table 4.39 shows that linear regression achieved small and stable errors in predicting pH values, with the absolute error ranging from 0.0664 (Class 4) to 0.2173 (Class 6) and a moderate overall standard deviation of 2.5795%.

Table 4.39 pH prediction errors when using linear regression

	class 0	class 1	class 2	class 3	class 4	class 5	class 6	All classes
Absolute error	0.2036	0.1330	0.1717	0.1630	0.0664	0.1402	0.2173	0.1548
Standard deviation	0.1193	0.0852	0.1076	0.0833	0.0534	0.1176	0.0368	0.1205
Relative error	0.0509	0.0305	0.0380	0.0356	0.0137	0.0280	0.0280	0.0337
Standard deviation	0.0314	0.0194	0.0236	0.0183	0.0108	0.0234	0.0368	0.0258
Percentage error	5.0943	3.0497	3.7971	3.5577	1.3716	2.7994	3.9994	3.3689
Standard deviation	3.1402	1.9382	2.3608	1.8349	1.0825	2.3426	3.6768	2.5795

Figure 4.30 shows the use of a linear regression model to predict the pH values based on RGB and L*a*b* color values. The red dots represented the measured pH value, while the blue dots represented the predicted value. The R^2 was 0.776, indicating a high correlation between the predicted and actual values.

มหาวิทยาลัยรังสิต Rangsit University

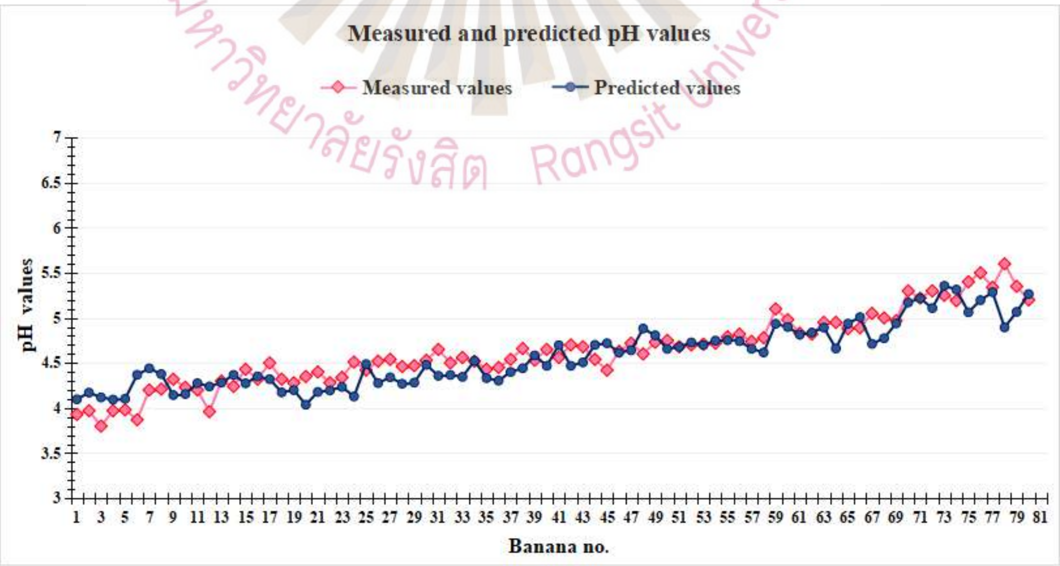

Figure 4.30 Graphs of measured and predicted pH values from RGB and L*a*b* color values when using linear regression

4.4.2.2 Use SVR (radial basis function) to Predict pH Values from RGB and L*a*b* Color Values

Table 4.40 shows the errors in predicting pH values using the SVR (radial basis kernel). The absolute errors ranged from 0.0541 to 0.1569 for different banana classes, and an overall average absolute error was 0.1012. The error when applying the SVR (radial basis kernel) found in each class was quite small. The overall performance of the model in pH prediction was better than those of SVR (linear kernel) and SVR (polynomial kernel).

Table 4.40 pH prediction errors when using SVR (radial basis kernel)

	class 0	class 1	class 2	class 3	class 4	class 5	class 6	All classes
Absolute error	0.1569	0.0877	0.0541	0.1025	0.0628	0.1262	0.1317	0.1012
Standard deviation	0.1473	0.0708	0.0390	0.0920	0.0401	0.0713	0.0228	0.0951
Relative error	0.0396	0.0202	0.0119	0.0225	0.0130	0.0251	0.0251	0.0222
Standard deviation	0.0388	0.0167	0.0086	0.0208	0.0082	0.0142	0.0228	0.0221
Percentage error	3.9635	2.0201	1.1950	2.2507	1.3033	2.5123	2.4293	2.2153
Standard deviation	3.8751	1.6659	0.8553	2.0821	0.8204	1.4212	2.2755	2.2090

มหาวิทยาลัยรังสิต Rangsit University

Figure 4.31 shows the measurement and prediction results of pH using SVR (radial basis kernel). The model's R^2 value, which reaches 0.873, indicated that the predicted and measured values agreed quite well. Even so, there were minor variations between the measured and predicted values.

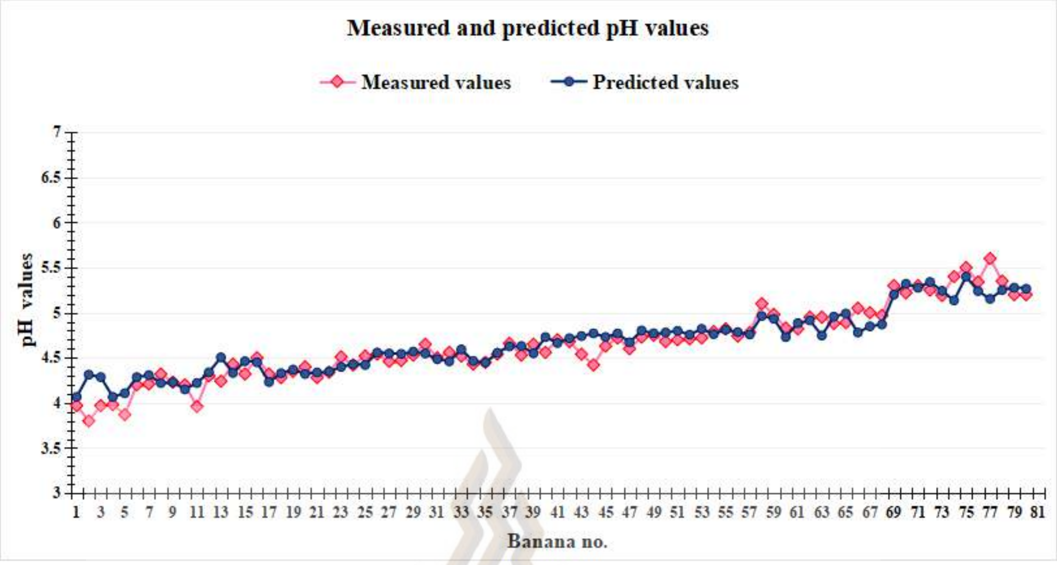

Figure 4.31 Graphs of measured and predicted pH values when using SVR (RBF kernel)

4.4.2.3 Use KNN (k=3) to Predict pH Values from RGB and L*a*b* Color Values

Table 4.41 shows the errors when using the KNN (k=3) for pH prediction. The absolute error was relatively small in all banana classes, with an overall average absolute error of 0.0440. KNN (k=3) achieved a low relative and percentage error of 0.0218 and 2.1771, respectively. The results revealed that KNN was efficient for predicting pH values based on RGB and L*a*b* color features.

มหาวิทยาลัยรังสิต Rangsit University

Table 4.41 pH prediction errors when using KNN (k=3)

	class 0	class 1	class 2	class 3	class 4	class 5	class 6	All classes
Absolute error	0.1669	0.0915	0.0553	0.0672	0.0708	0.1715	0.0895	0.0988
Standard deviation	0.1841	0.0576	0.0462	0.0831	0.0690	0.1259	0.0146	0.1072
Relative error	0.0423	0.0209	0.0122	0.0148	0.0147	0.0344	0.0344	0.0218
Standard deviation	0.0481	0.0132	0.0102	0.0187	0.0144	0.0256	0.0146	0.0255

Table 4.41 pH prediction errors when using KNN (k=3) (continued)

	class 0	class 1	class 2	class 3	class 4	class 5	class 6	All classes
Percentage error	4.2268	2.0921	1.2220	1.4775	1.4690	3.4413	1.6494	2.1771
Standard deviation	4.8083	1.3166	1.0171	1.8728	1.4388	2.5646	1.4639	2.5491

Figure 4.32 shows the results of using the KNN (k=3) to predict the pH value based on RGB and L*a*b* values. The obtained R2 value was 0.860, indicating that the model explains 85.97% of the data changes. Compared with the previous linear regression and SVR, it is only lower than that of the SVR (radial basis function) model.

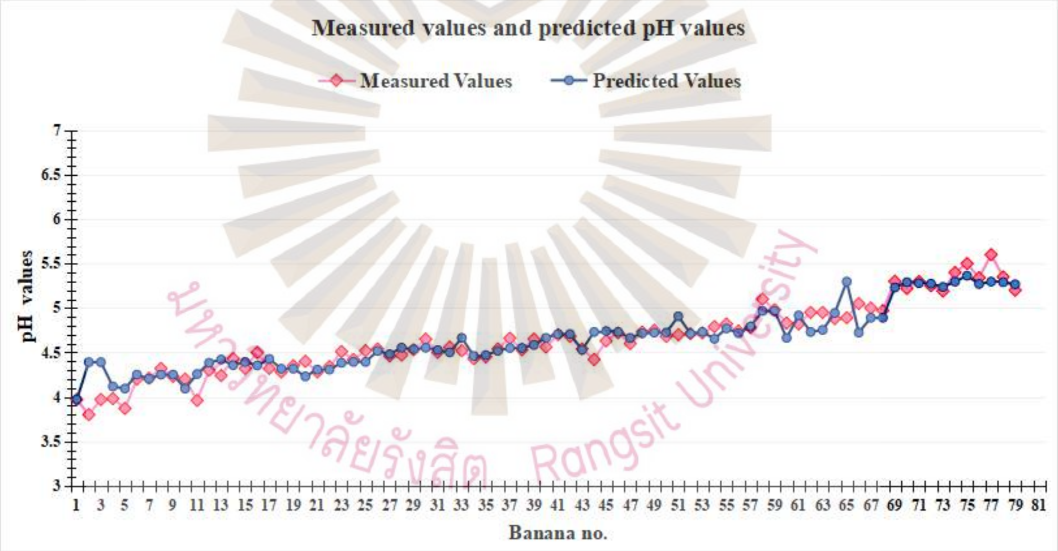

Figure 4.32 Graphs of measured and predicted Brix values when using KNN (k=3)

มหาวิทยาลัยรังสิต Rangsit University

Chapter 5

Conclusion and Recommendations

5.1 Conclusion

This study investigated the use of various machine learning models for banana ripeness classification, Brix (sweetness), and pH prediction. The research background indicated that the increasing global demand for fruit quality has rendered traditional manual detection and classification methods unsuitable for large-scale production due to their time-consuming, subjective, and ineffective nature. Therefore, the study concentrated on machine learning-based classification and prediction systems to achieve high accuracy in banana ripeness classification and to predict internal fruit quality, such as Brix and pH values. The work was divided into two main parts.

The first part studied and compared the performance of four machine learning classifiers—MobileNet, ResNet50, a simple CNN, and VGG16—in banana ripeness classification tasks and concludes that MobileNet performed the best among all models, achieving an accuracy of 98.45%, demonstrating its superiority in banana ripeness classification. Although VGG16 and CNN also demonstrated strong classification capabilities, achieving accuracies of 96.82% and 95.70%, respectively, they were slightly inferior to MobileNet in terms of efficiency and performance. In contrast, ResNet50 performs relatively poorly, with an accuracy rate of only 92.43%.

The second part used a variety of machine learning algorithms to predict Brix and pH, including linear regression, SVR, and KNN. The first method predicted Brix and pH values based on the softmax features extracted by MobileNet. The results revealed that KNN performed the best at predicting Brix values, with an R^2 value of 0.984. It did better than linear regression ($R^2 = 0.958$) and SVR (R^2 values for different kernel functions ranging from 0.925 to 0.952). KNN also performed the best in pH

มหาวิทยาลัยรังสิต Rangsit University

prediction, with an R² value of 0.972. This indicated that KNN can more accurately predict Brix and pH values in prediction tasks based on softmax features.

This study evaluated machine learning models for predicting Brix and pH values using RGB, L*a*b*, and combined RGB and L*a*b* color features measured from one point on a banana. The results indicated that there were significant differences in the performance of different methods when predicting pH and Brix values. For pH prediction, when using L*a*b* features, KNN (k=3) performed the best. SVR with a radial basis kernel obtained a rather high R² of 0.819. When using RGB and L*a*b* features, the SVR (radial basis kernel) achieved the best performance at 0.873. For Brix value prediction, KNN performed well with an R² value of 0.941. Overall, KNN performs outstandingly in Brix prediction. In contrast, the performance of linear regression, SVR using a linear kernel, and SVR using a polynomial kernel was poorer. These results emphasized the superior predictive ability of the KNN when using the combined RGB and L*a*b* features.

5.2 Recommendations

5.2.1 Limitations

Due to the limited amount of image data in certain ripeness stages, the performance of the model may decrease when dealing with imbalanced data. This study predicts Brix and pH values based solely on the RGB and L*a*b* color values of a single location on bananas. Although these color features can, to some extent, reflect the internal quality of bananas, they may not be sufficient to capture more complex nonlinear relationships.

This study only focused on the detection and analysis of individual bananas, while in practical applications, bananas are usually transported and sold in whole bundles. Due to the possibility of individuals with different maturity levels in whole bundles of bananas, the predicted results of individual bananas may not accurately

มหาวิทยาลัยรังสิต Rangsit University

reflect the average maturity level of the whole bundle of bananas. The object of this study was only Musa acuminata bananas.

5.2.2 Future Outlook

In the future, more banana images at different ripeness stages should be collected to ensure a more balanced distribution of various types of data. At the same time, data on different varieties of bananas and other fruits can be added to improve the generalization ability of the model. To enhance the adaptability of the model in practical environments, data should be collected under various lighting conditions, backgrounds, and shooting angles. Future research should further expand on existing work by introducing predictions of mineral composition, in addition to predicting Brix and pH values. This will help to more comprehensively evaluate the nutritional quality of fruits and improve accurate prediction of fruit ripeness and internal nutritional components.

Although different banana varieties may have differences in appearance and maturation process, this study suggested that color features such as RGB and L*a*b* have high sensitivity in predicting the internal quality of bananas, such as Brix and pH value. This discovery showed that these color features could serve as reliable indicators for predicting internal quality across varieties, and this method can be extended to other similar banana varieties.

มหาวิทยาลัยรังสิต Rangsit University

References

Al-Azzwi, Z. H. N. (2024). Medical image Classification using Transfer Learning: Convolutional Neural Network Models approach. *Journal of Electrical Systems, 20*(6s), 2561-2569. https://doi.org/10.52783/jes.3243

Albawi, S., Mohammed, T. A., & Al-Zawi, S. (2017). Understanding of a convolutional neural network. In *2017 International Conference on Engineering and Technology (ICET)* (pp. 1-6). https://doi.org/10.1109/ICEngTechnol.2017.8308186

Ballester, C., Bugeau, A., Carrillo, H., Clément, M., Giraud, R., Raad, L., & Vitoria, P. (2022). *Influence of Color Spaces for Deep Learning Image Colorization*. Retrieved from https://arxiv.org/pdf/2204.02850

Borenstain, S., Bar-Haim, G., Goldshtein, K., & Cohen-Taguri, G. (2020). Optimization of quinacridone magenta, Cu-phthalocyanine cyan, and arylide yellow ink films formulated for maximum color gamut. *Color Research & Application*, *45*(6), 1153-1169. https://doi.org/10.1002/col.22552

Braun, M. R., Altan, H., & Beck, S. B. M. (2014). Using regression analysis to predict the future energy consumption of a supermarket in the UK. *Applied Energy*, *130*, 305-313. https://doi.org/10.1016/j.apenergy.2014.05.062

Burt, R., Thigpen, N. N., Keil, A., & Principe, J. C. (2021). Unsupervised foveal vision neural architecture with top-down attention. *Neural Networks*, *141*, 145-159. https://doi.org/10.1016/j.neunet.2021.03.003

Castro, W., Oblitas, J., De-La-Torre, M., Cotrina, C., Bazán, K., & Avila-George, H. (2019). Classification of Cape Gooseberry Fruit According to its Level of Ripeness Using Machine Learning Techniques and Different Color Spaces. *IEEE Access*, *7*, 27389-27400. https://doi.org/10.1109/ACCESS.2019.2898223

Chen, H., & Phoophuangpairoj, R. (2024). Determining Banana Ripeness Using MobileNet. In *2024 12th International Electrical Engineering Congress (iEECON)* (pp. 1-6). https://doi.org/10.1109/iEECON60677.2024.10537906

มหาวิทยาลัยรังสิต Rangsit University

References (continued)

Darapaneni, N., Krishnamurthy, B., & Paduri, A. R. (2020). Convolution Neural Networks: A Comparative Study for Image Classification. In *2020 IEEE 15th International Conference on Industrial and Information Systems (ICIIS)* (pp. 327-332). https://doi.org/10.1109/ICIIS51140.2020.9342667

Eyarkai Nambi, V., Thangavel, K., Shahir, S., & Geetha, V. (2015). Evaluation of colour behavior during ripening of Banganapalli mango using CIE-Lab and RGB colour coordinates. *Journal of Applied Horticulture*, *17*(03), 205-209. https://doi.org/10.37855/jah.2015.v17i03.38

El-Sharkawy, M. A. (2004). Cassava biology and physiology. *Plant Molecular Biology*, *56*, 481-501. https://doi.org/10.1007/s11103-005-2270-7

Gulzar, Y. (2023). Fruit Image Classification Model Based on MobileNetV2 with Deep Transfer Learning Technique. *Sustainability*, *15*(3), Article 3. https://doi.org/10.3390/su15031906

He, K., Gkioxari, G., Dollár, P., & Girshick, R. (2017). Mask R-CNN. In *2017 IEEE International Conference on Computer Vision (ICCV)* (pp. 2980-2988). https://doi.org/10.1109/ICCV.2017.322

Hirose, H., Soejima, Y., & Hirose, K. (2012). NNRMLR: A Combined Method of Nearest Neighbor Regression and Multiple Linear Regression. In *2012 IIAI International Conference on Advanced Applied Informatics* (pp. 351-356). https://doi.org/10.1109/IIAI-AAI.2012.76

Howard, A. G., Zhu, M., Chen, B., Kalenichenko, D., Wang, W., Weyand, T., . . . Adam, H. (2017). *MobileNets: Efficient Convolutional Neural Networks for Mobile Vision Applications*. Retrieved from https://arxiv.org/pdf/1704.04861

Imsabai, W., Ketsa, S., & van Doorn, W. G. (2006). Physiological and biochemical changes during banana ripening and finger drop. *Postharvest Biology and Technology*, *39*(2), 211-216. https://doi.org/10.1016/j.postharvbio.2005.10.001

Jiang, Z. -P., Liu, Y. -Y., Shao, Z. -E., & Huang, K. -W. (2021). An Improved VGG16 Model for Pneumonia Image Classification. *Applied Sciences*, *11*(23), Article 11185. https://doi.org/10.3390/app112311185

มหาวิทยาลัยรังสิต Rangsit University

References (continued)

Khaing, Z. M., Naung, Y., & Htut, P. H. (2018). Development of control system for fruit classification based on convolutional neural network. In *2018 IEEE Conference of Russian Young Researchers in Electrical and Electronic Engineering (EIConRus)* (pp. 1805-1807). https://doi.org/10.1109/EIConRus.2018.8317456

Kong, G., Tian, H., Duan, X., & Long, H. (2021). Adversarial Edge-Aware Image Colorization With Semantic Segmentation. *IEEE Access*, *9*, 28194-28203. https://doi.org/10.1109/ACCESS.2021.3056144

Kumar, S., & Kumar, H. (2024). Efficient-VGG16: A Novel Ensemble Method for the Classification of COVID-19 X-ray Images in Contrast to Machine and Transfer Learning. *Procedia Computer Science*, *235*, 1289-1299. https://doi.org/10.1016/j.procs.2024.04.122

Luo, M. R., Cui, G., & Rigg, B. (2001). The development of the CIE 2000 colour-difference formula: CIEDE2000. *Color Research & Application*, *26*(5), 340-350. https://doi.org/10.1002/col.1049

Minitab Blog Editor. (2013, May 30). Regression analysis: How do I interpret R-squared and assess the goodness-of-fit? [Web log message]. Retrieved from https://blog.minitab.com/en/adventures-in-statistics-2/regression-analysis-how-do-i-interpret-r-squared-and-assess-the-goodness-of-fit

Moreno, J. L., Tran, T., Cantero-Tubilla, B., López-López, K., Becerra Lopez Lavalle, L. A., & Dufour, D. (2021). Physicochemical and physiological changes during the ripening of Banana (Musaceae) fruit grown in Colombia. *International Journal of Food Science & Technology*, *56*(3), 1171-1183. https://doi.org/10.1111/ijfs.14851

Munkhdalai, L., Munkhdalai, T., & Ryu, K. H. (2022). *A Locally Adaptive Interpretable Regression*. Retrieved from https://arxiv.org/pdf/2005.03350

Phiphiphatphaisit, S., & Surinta, O. (2020). Food Image Classification with Improved MobileNet Architecture and Data Augmentation. In *Proceedings of the 3rd International Conference on Information Science and Systems* (pp. 51-56). https://doi.org/10.1145/3388176.3388179

มหาวิทยาลัยรังสิต Rangsit University

References (continued)

Poynton, C. A. (2012). *Digital video and HDTV: Algorithms and interfaces*. San Francisco, CA: Morgan Kaufmann.

Phoophuangpairoj, R., Ngoenrungrueang, T., & Audomsin, S. (2023). Ripeness Classification of a Bunch of Bananas Using a CNN. In *2023 International Electrical Engineering Congress (iEECON)* (pp. 180-183). https://doi.org/10.1109/iEECON56657.2023.10126585.

Rahman, Md. M., Basar, Md. A., Shinti, T. S., Khan, Md. S. I., Babu, H. Md. H., & Uddin, K. M. M. (2023). A deep CNN approach to detect and classify local fruits through a web interface. *Smart Agricultural Technology*, *5*, 100321. https://doi.org/10.1016/j.atech.2023.100321

Sahoo, D., Hoi, S. C. H., & Li, B. (2019). Large Scale Online Multiple Kernel Regression with Application to Time-Series Prediction. *ACM Transactions on Knowledge Discovery from Data, 13*(1), 1-33. https://doi.org/10.1145/3299875

Sandler, M., Howard, A., Zhu, M., Zhmoginov, A., & Chen, L. -C. (2018). MobileNetV2: Inverted Residuals and Linear Bottlenecks. In *2018 IEEE/CVF Conference on Computer Vision and Pattern Recognition* (pp. 4510-4520). https://doi.org/10.1109/CVPR.2018.00474

Saputro, A. H., Juansyah, S. D., & Handayani, W. (2018). Banana (Musa sp.) maturity prediction system based on chlorophyll content using visible-NIR imaging. In *2018 International Conference on Signals and Systems (ICSigSys)* (pp. 64-68). https://doi.org/10.1109/ICSIGSYS.2018.8373569

Saragih, R. E., & Emanuel, A. W. R. (2021). Banana Ripeness Classification Based on Deep Learning using Convolutional Neural Network. In *2021 3rd East Indonesia Conference on Computer and Information Technology (EIConCIT)* (pp. 85-89). https://doi.org/10.1109/EIConCIT50028.2021.9431928

Sarkar, T., Das, S., Prakash, P., Mishra, B., & Singh, D. (2022). Edge detection aided geometrical shape analysis of Indian gooseberry (Phyllanthus emblica) for freshness classification. *Food Analytical Methods, 15*(6), 1490-1507. https://doi.org/10.1007/s12161-021-02206-x

มหาวิทยาลัยรังสิต Rangsit University

References (continued)

Sharma, V., & Singh, N. (2021). Deep Convolutional Neural Network with ResNet-50 Learning algorithm for Copy-Move Forgery Detection. In *2021 7th International Conference on Signal Processing and Communication (ICSC)* (pp. 146-150). https://doi.org/10.1109/ICSC53193.2021.9673422

Simonyan, K., & Zisserman, A. (2015). *Very Deep Convolutional Networks for Large-Scale Image Recognition*. Retrieved from https://arxiv.org/pdf/1409.1556

Symmank, C., Zahn, S., & Rohm, H. (2018). Visually suboptimal bananas: How ripeness affects consumer expectation and perception. *Appetite, 120*, 472-481. https://doi.org/10.1016/j.appet.2017.10.002

Tun, N. L., Gavrilov, A., Tun, N. M., Trieu, D. M., & Aung, H. (2021). Remote Sensing Data Classification Using A Hybrid Pre-Trained VGG16 CNN-SVM Classifier. In *2021 IEEE Conference of Russian Young Researchers in Electrical and Electronic Engineering (ElConRus)* (pp. 2171-2175). https://doi.org/10.1109/ElConRus51938.2021.9396706

Ukey, N., Yang, Z., Li, B., Zhang, G., Hu, Y., & Zhang, W. (2023). Survey on Exact kNN Queries over High-Dimensional Data Space. *Sensors, 23*(2), 629. https://doi.org/10.3390/s23020629

Wang, S., Han, K., & Jin, J. (2019). Review of image low-level feature extraction methods for content-based image retrieval. *Sensor Review, 39*(6), 783-809. https://doi.org/10.1108/SR-04-2019-0092

Xie, T., Chen, L., Yi, B., Li, S., Leng, Z., Gan, X., & Mei, Z. (2024). Application of the Improved K-Nearest Neighbor-Based Multi-Model Ensemble Method for Runoff Prediction. *Water, 16*(1), 69. https://doi.org/10.3390/w16010069

Yuan, P., Lin, S., Cui, C., Du, Y., Guo, R., He, D., . . . Han, S. (2020). *HS-ResNet: Hierarchical-Split Block on Convolutional Neural Network*. Retrieved from https://arxiv.org/pdf/2010.07621

Zhan, Y., Zhang, H., & Liu, Y. (2021). Forecast of Meteorological and Hydrological Features Based on SVR Model. In *2021 4th International Conference on Advanced Electronic Materials, Computers and Software Engineering (AEMCSE)* (pp. 579-583). https://doi.org/10.1109/AEMCSE51986.2021.00123

มหาวิทยาลัยรังสิต Rangsit University

References (continued)

Zhang, Y., Lian, J., Fan, M., & Zheng, Y. (2018). Deep indicator for fine-grained classification of banana’s ripening stages. *EURASIP Journal on Image and Video Processing, 2018*(1), 46. https://doi.org/10.1186/s13640-018-0284-8

มหาวิทยาลัยรังสิต Rangsit University

Biography

Name	Hong Chen
Date of birth	December 8, 2000
Place of birth	Anhui, China
Education background	Chiang Mai University, Thailand Bachelor of Modern Management and Information Technology, 2022 Rangsit University, Thailand Master of Engineering in Electrical and Computer Engineering, 2024
Address	Helen International Community, Guandu District, Kunming, Yunnan Province, China
Email Address	hong.c65@rsu.ac.th

มหาวิทยาลัยรังสิต Rangsit University